AD-A260 890

NAVAL POSTGRADUATE SCHOOL
Monterey, California

MAR 0 1 1993

THESIS

EXPERIMENTAL STUDY OF THE EFFECT
OF HELICAL GROOVES
ON AN INFINITE CYLINDER

by

Thomas Dean Stuart

December, 1992

Thesis Advisor: Louis V. Schmidt

Approved for public release; distribution is unlimited.

REPORT DOCUMENTATION PAGE

1a Report Security Classification: Unclassified	1b Restrictive Markings

2a Security Classification Authority	3 Distribution/Availability of Report
2b Declassification/Downgrading Schedule	Approved for public release; distribution is unlimited.

4 Performing Organization Report Number(s)	5 Monitoring Organization Report Number(s)

6a Name of Performing Organization Naval Postgraduate School	6b Office Symbol (if applicable) 31	7a Name of Monitoring Organization Naval Postgraduate School

6c Address (city, state, and ZIP code) Monterey CA 93943-5000	7b Address (city, state, and ZIP code) Monterey CA 93943-5000

8a Name of Funding/Sponsoring Organization	6b Office Symbol (if applicable)	9 Procurement Instrument Identification Number

Address (city, state, and ZIP code)	10 Source of Funding Numbers			
	Program Element No	Project No	Task No	Work Unit Accession No

11 Title (Unclass) EXPERIMENTAL STUDY OF THE EFFECT OF HELICAL GROOVES ON AN INFINITE CYLINDER

12 Personal Author(s) Thomas Dean Stuart

13a Type of Report Engineer's Thesis	13b Time Covered From To	14 Date of Report (year, month, day) December, 1992	15 Page Count 125

16 Supplementary Notation The views expressed in this thesis are those of the author and do not reflect the official policy or position of the Department of Defense or the U.S. Government.

17 Cosati Codes			18 Subject Terms (continue on reverse if necessary and identify by block number)
Field	Group	Subgroup	Inclined wire, inclined cylinder, infinite wire, infinite cylinder, normal force, axial force, side force, drogue, circulation

19 Abstract (continue on reverse if necessary and identify by block number)
   A series of low-speed wind-tunnel investigations were conducted to determine the aerodynamic behavior of a grooved inclined cylinder representing a long trailing wire antenna towed from an orbiting airplane. The large angle-of-attack range of the trailing wire required two different model configurations. The first configuration, using full-scale wire lengths suspended between steel stanchions, was mounted on a flush four-degree-of-freedom wall balance. The second configuration used a 15-scale grooved cylinder model with an ogive nose mounted on a six-degree-of-freedom sting balance. Wall balance wire data, valid for higher angles of attack, were integrated with low angle-of-attack sting balance data. Empirical relationships for the normal and axial force coefficients were verified with historical references for tested clean circular cylinders and extended for the grooved configurations. Existence of a side force coefficient due to circulation caused by the helical grooves was discovered, expressed analytically, and verified with flow-visualization techniques. Finally, the experimental coefficients were used to improve an existing simulation model describing the static equilibrium conditions of a cable towed by an airplane in a circular orbit. Inclusion of the side force influence in the static model proved consistent with the lateral skew angle and direction observed during flight test.

20 Distribution/Availability of Abstract XX unclassified/unlimited XX same as report __ DTIC users	21 Abstract Security Classification Unclassified

22a Name of Responsible Individual Louis V. Schmidt	22b Telephone (include Area Code) (408) 646-2972	22c Office Symbol AA/Sc

DD FORM 1473,84 MAR   83 APR edition may be used until exhausted   security classification of this page
All other editions are obsolete   Unclassified

Experimental Study of the Effect
of Helical Grooves
on an Infinite Cylinder

by

Thomas Dean Stuart
Lieutenant Commander, United States Navy
B.S., U.S. Naval Academy, 1983
M.S., University of Tennessee, 1990
M.S., Naval Postgraduate School, 1992

Submitted in partial fulfillment
of the requirements for the degree of

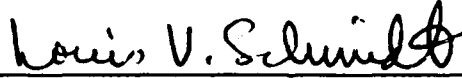AERONAUTICAL AND ASTRONAUTICAL ENGINEER

from the

NAVAL POSTGRADUATE SCHOOL
December 1992

Author: _____
Thomas Dean Stuart

Approved by: _____
Louis V. Schmidt, Thesis Advisor

_____
Richard M. Howard, Second Reader

_____
Daniel J. Collins, Chairman
Department of Aeronautics and Astronautics

_____
Richard S. Elster, Dean of Instruction

ABSTRACT

A series of low-speed wind-tunnel investigations were conducted to determine the aerodynamic behavior of a grooved inclined cylinder representing a long trailing wire antenna towed from an orbiting airplane. The large angle-of-attack range of the trailing wire required two different model configurations. The first configuration, using full-scale wire lengths suspended between steel stanchions, was mounted on a flush four-degree-of-freedom wall balance. The second configuration used a 15-scale grooved cylinder model with an ogive nose mounted on a six-degree-of-freedom sting balance. Wall balance wire data, valid for higher angles of attack, were integrated with low angle-of-attack sting balance data. Empirical relationships for the normal and axial force coefficients were verified with historical references for tested clean circular cylinders and extended for the grooved configurations. Existence of a side force coefficient due to circulation caused by the helical grooves was discovered, expressed analytically, and verified with flow-visualization techniques. Finally, the experimental coefficients were used to improve an existing simulation model describing the static equilibrium conditions of a cable towed by an airplane in a circular orbit. Inclusion of the side force influence in the static model proved consistent with the lateral skew angle and direction observed during flight test.

iii

TABLE OF CONTENTS

vi

ACKNOWLEDGEMENTS

I. INTRODUCTION

The use of wires in the field of aeronautics started well before the Wright Flyer took to the air. Initially, wires were used as structural support for bi-wing gliders, and their use extended to powered biplanes. With their use came experimental studies and tests, and the flow over an infinite cylinder became the baseline for many disciplines in classical aerodynamics and fluid mechanics.

With the rapid advance of aircraft design, and the development of the monoplane with wing spars, metal skins, and monocoque fuselages, the use of wires and cables became restricted to internal flight control systems, and a new purpose, as instruments to tow other aircraft. Interest in towing cable form and stability manifested as early as 1934 with a study by Glauert [Ref. 1].

With the advent of radio and the use of a long trailing wire as an antenna, concern for wire stability and form increased. The Navy EC-130, circa 1970, was the first of two airplanes designed to trail 15,000 to 25,000 feet of wire in a circular orbit for use as a very low frequency (VLF) antenna. The wire, with a cone-shaped drogue at the end, exhibited extreme oscillations in shape and tension. These oscillatory problems continued with the 1987 replacement airplane, the E-6A. The trailing wire came in two configurations: a 19-strand wire wrapped by a flattened copper sheath (1x19), and three 7-strand bundles twisted in a triple thread helical groove of 15° (3x7).

Three major discrepancies were documented during E-6A flight test of the 3x7 wire. The first discrepancy from the oscillatory behavior was contact between the wire and towplane's horizontal tail. The conical motion of the first 50 feet of wire and subsequent airplane contact has potential to entangle horizontal flight control surfaces. The second discrepancy stemmed from wire failure due to oscillatory tension forces exceeding the ultimate strength of the wire. The third discrepancy was the mission degradation displayed by the reduced transmissivity of the wire during oscillations. Also discovered during flight test was an exhibited trait of the 3x7 wire to trail approximately 10° to 15° right of centerline (looking aft) while in level flight and zero degrees bank angle.

Limited simulation studies and expensive flight test experimentation were conducted over the past 20 years to model and control trailing wire oscillations. Recent studies by Clifton [Ref. 2] currently provide the best system model and viable solutions to the nonlinear oscillatory dynamics presented by the 3x7 wire. Clifton's model commenced with the establishment of no-wind static equilibrium conditions of the 3x7 wire, towplane, drogue system while in a circular orbit. The simulation model was extended to include dynamic conditions and a wind forcing function. Accuracy of the Clifton model was only limited by the use of approximate force coefficients for the 3x7 trailing wire and drogue.

The purpose of this research was to:

- experimentally determine all aerodynamic traits of the E-6A trailing wire and drogue configurations,

- discover, determine, and explain the existence of a side force induced from the helical grooves of the 3x7 wire at low angles of attack, and

- establish the amplitude of the side force, and by refining the Clifton static simulation model, determine its effect on the E-6A antenna system.

II. BACKGROUND

A. BASIC AERODYNAMIC THEORY

The study of the infinite cylinder has become the foundation of aerodynamic analysis. From classical fluid mechanics, stream functions of two elementary flows, a doublet and a uniform flow field, can be superimposed to produce a streamline describing flow about the surface of a circular cylinder. Pressure fields can then be calculated for two-dimensional, invisid flow with analytical solutions determined. Integration of the pressure field in an invisid, irrotational flow about a cylinder results in forces in the direction of flow, drag, and orthogonal to the flow, lift, equal to zero. By adding circulation to the flow fields, the force orthogonal to the flow (lift) acting per unit length was nonzero and expressed by Kutta-Joukowski as

$$F = \rho_\infty * (V_\infty x \Gamma) \qquad (2.1)$$

Where:
F ≡ force vector
ρ_∞ ≡ freestream density
V_∞ ≡ freestream velocity vector
Γ ≡ circulation vector

A circular cylinder in viscous flow acts as a bluff body producing drag primarily due to flow separation over the downstream part of the cylinder. The drag about a cylinder, due to separation-induced pressure drag, results in a drag coefficient dependent on the nondimensional Reynolds number, Re, defined as

4

II. BACKGROUND

A. BASIC AERODYNAMIC THEORY

The study of the infinite cylinder has become the foundation of aerodynamic analysis. From classical fluid mechanics, stream functions of two elementary flows, a doublet and a uniform flow field, can be superimposed to produce a streamline describing flow about the surface of a circular cylinder. Pressure fields can then be calculated for two-dimensional, invisid flow with analytical solutions determined. Integration of the pressure field in an invisid, irrotational flow about a cylinder results in forces in the direction of flow, drag, and orthogonal to the flow, lift, equal to zero. By adding circulation to the flow fields, the force orthogonal to the flow (lift) acting per unit length was nonzero and expressed by Kutta-Joukowski as

$$F = \rho_\infty *(V_\infty \, x \, \Gamma) \qquad\qquad (2.1)$$

Where: $F \equiv$ force vector
$\rho_\infty \equiv$ freestream density
$V_\infty \equiv$ freestream velocity vector
$\Gamma \equiv$ circulation vector

A circular cylinder in viscous flow acts as a bluff body producing drag primarily due to flow separation over the downstream part of the cylinder. The drag about a cylinder, due to separation-induced pressure drag, results in a drag coefficient dependent on the nondimensional Reynolds number, Re, defined as

4

$$Re = \frac{\rho_\infty * V_\infty * d}{\mu_\infty} \qquad (2.2)$$

Where:

ρ_∞ = freestream density (slugs/ft^3)

V_∞ = freestream velocity (ft/s)

d = diameter of cylinder (ft)

μ_∞ = freestream viscosity (slug/ft*s)

The relationship between C_D of a circular cylinder and Reynolds number is presented in Figure 2.1. [Ref. 3]
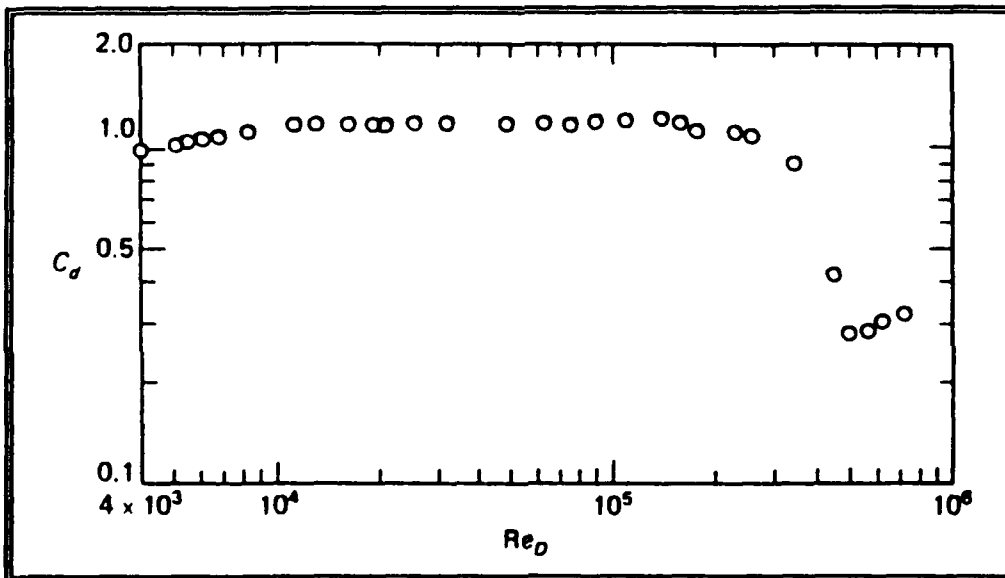
Figure 2.1 Circular Cylinder C_D vs Reynolds Number

In the subcritical Reynolds number range, from 4×10^3 to 3×10^5, the C_D of the cylinder is an approximately constant value of 1.2. Subcritical flow over a cylinder is characterized by laminar conditions until separation around the $\pm90°$ from stagnation. The wake is characterized by an asymmetric "vortex street" first analyzed by von Kármán. The flow reaches critical Reynolds number around 3×10^5 as transition from laminar to turbulent conditions occur. Supercritical flow is

5

characterized by a lower value of C_D due to turbulent layer separation past $\pm 100°$ producing a smaller wake and less form drag. [Ref. 4]

An experimental study of smooth and stranded wires was conducted as early as 1917 by Relf and Powell [Ref. 5]. In 1951 Hoerner published <u>Aerodynamic Drag</u> followed in 1958 by <u>Fluid Dynamic Drag</u>. His works presented empirical relationships for the lift and drag coefficient of inclined wires, cables and cylinders at subcritical Reynolds numbers. In a body axis system for an inclined wire as shown in Figure 2.2, the normal force coefficient, C_N, is determined from the force perpendicular to the wire, and the axial force coefficient, C_A, from the force parallel to the wire. Stability axis lift and drag coefficients can be resolved by transforming C_N and C_A using

$$\begin{Bmatrix} C_L \\ C_D \end{Bmatrix} = \begin{bmatrix} \cos\alpha & -\sin\alpha \\ \sin\alpha & \cos\alpha \end{bmatrix} * \begin{Bmatrix} C_N \\ C_A \end{Bmatrix} \qquad (2.3)$$

Hoerner produced an analytic expression from empirical results based on C_N only. Summarized:

$$C_D = C_{D,Basic} * \sin^3\alpha$$
$$C_L = C_{D,Basic} * \sin^2\alpha * \cos\alpha \qquad (2.4)$$
$$C_{D,Basic} = \frac{C_N}{\sin^2\alpha}$$

6

Where: C_N = N/(Q*S)
           N ≡ normal force (lb$_f$)
           Q ≡ dynamic pressure = $0.5 * \rho_\infty * V_\infty^2$ (lb$_f$/ft^2)
           S ≡ reference area (ft^2)

Setting $C_{D,Basic}$ = 1.1, Hoerner's closed-form solutions are presented in Figure 2.3.

Hoerner did not consider an axial force but added a frictional term $\Delta C_D = \pi C_f = 0.02$.

[Ref. 6]
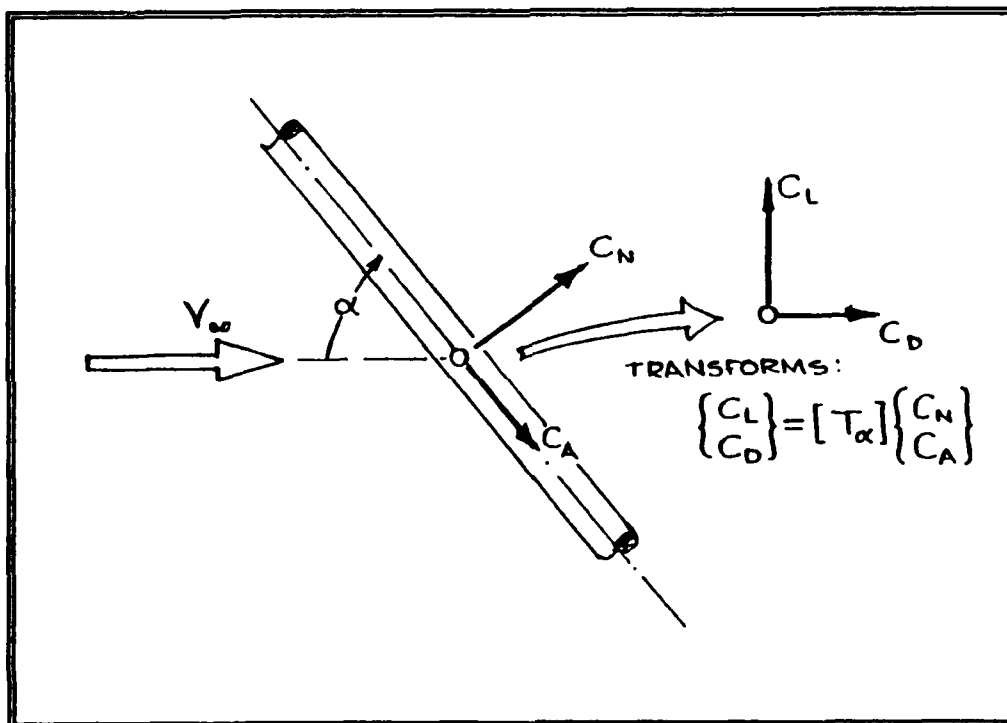
Figure 2.2 Inclined Wire Coordinate System
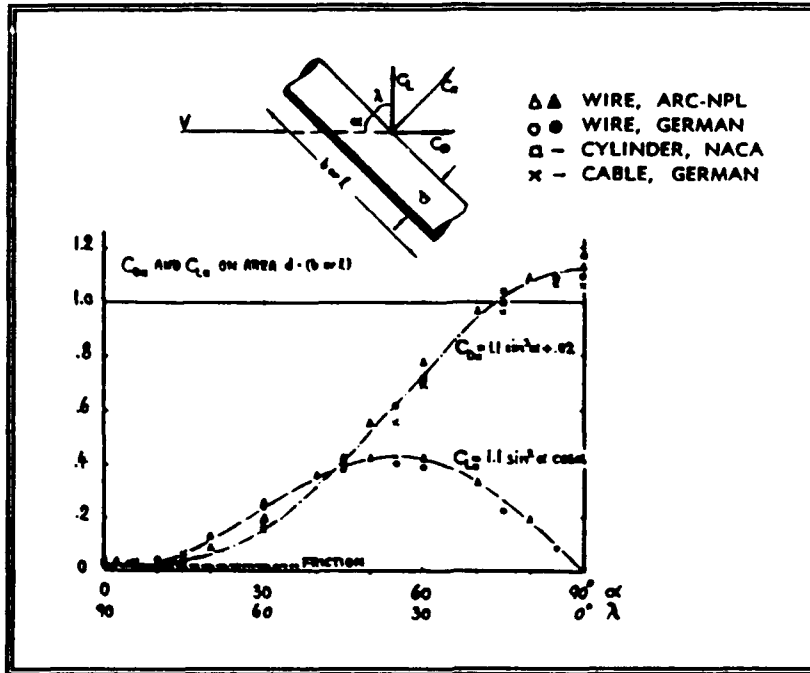
Figure 2.3 Hoerner's Empirical Relationships [Ref. 6]

In 1970, Bootle [Ref. 7] extended Hoerner's expressions to supercritical Reynolds numbers at low Mach numbers. Further studies concentrated on critical and supercritical flow over slender, axisymmetric, finite-length bodies in response to interest in missile related aerodynamics. Studies by Alnosnino and Rom using a sting balance cone-cylinder model discussed the magnitude of side force coefficient C_Y at higher angles of attack, and the effect of symmetric blowing on alleviation of side force [Ref. 8]. Vortex-induced side force investigations continued with high-angle-of-attack studies by Reding and Ericsson [Ref. 9]. Their experiments postulated that the maximum side force occurred at critical Reynolds numbers on an order of magnitude equal to the ogive cylinder normal force. Other studies have addressed vortex separation points by the measurement of skin friction coefficient [Ref. 10].

Currently, research only addresses vortex induced separation and side forces, as applied to missiles, at high angles of attack and high Reynolds numbers.

This paper addresses the side forces generated by helical grooves on an infinite cylinder, representative of ai wrapped inclined wire, at low angles of attack and subcritical Reynolds numbers.

B. 3 x 7 WIRE

One towed cable used for long trailing antenna applications is the 3x7 wire. Constructed of three sets of six symmetrically placed steel wires around a seventh strand, the 0.158-inch-diameter wire was wrapped in a triple helix with a 1.87-inch pitch. The forming process of the three wire groupings yielded a helical indentation or groove with an approximate helix angle of 15°. Shown in Figure 2.4 and 2.5, the 3x7 wire exhibited failure at a 3000 lb$_f$ load. With a length up to 25,000 feet, the 3x7 wire flew in an aerodynamic environment with altitudes from 3000 to 20,000 feet, airspeeds from 36 knots (60 ft/s) to more than 225 knots (375 ft/s), and angles of attack ranging from 10° to 90°.
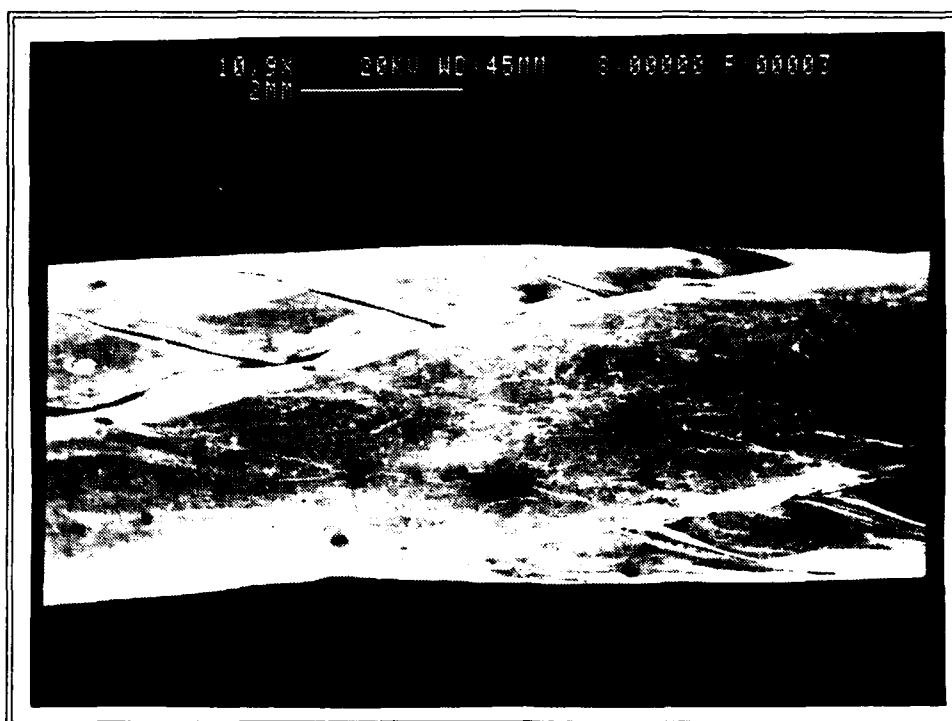
Figure 2.4 3x7 Wire

Figure 2.5 3x7 Wire (End View)

C. DROGUE

The antenna system drogue was designed to provide aerodynamic stability and adequate tension during reel-in and reel-out operations. The 31.7-inch-long drogue has a base diameter of 24 inches and a weight of 87 lb_f. The center of gravity was measured 13.0 inches aft of the 22.5° apex. In actual operation, the wire is attached to the forward end of the hollow-cone, weighted-nose drogue.

D. STATIC CONDITIONS SIMULATION COMPUTER MODEL

The static conditions simulation program, TAC17, was the foundation for the dynamic, nonlinear system simulation model by Clifton [Ref. 2]. The static model simulated an airplane in circular orbit at a specified altitude towing a trailing wire in no-wind conditions. Although the program allowed freedom of choice for airplane altitude, velocity, and bank angle, as well as wire length, baseline airplane operational conditions were 18,325 feet of altitude, 156 KEAS (knots, equivalent airspeed), and 34° bank angle towing 20,290 feet of wire. The baseline conditions corresponded to a particular set of flight data used by Clifton for correlation purposes. Program design for an orbiting airplane required a minimum bank angle of 3° (left) to preclude an infinite orbit radius. Wire and drogue aerodynamic coefficients were defined values, and the model used central difference numerical methods with the wire represented by 200 equi-length segments. Program operation commenced from an initial guess position of the drogue, and calculated up the 200 grid points to the towplane position. Calculations were iterated until towplane

boundary conditions (inputed) were satisfied to a specified error. Outputs from the program included radial, theta, and z position, tension, angle of attack, true velocity, and Reynolds number for each wire grid point. A detailed discussion of the static conditions simulation model genesis and operation is presented in Reference 2.

III. EXPERIMENTAL SETUP

A. WIND TUNNEL

Experimentation was conducted in the Naval Postgraduate School (NPS) horizontal low-speed wind tunnel. Presented in Figure 3.1, the Aerolab single-return, closed-circuit tunnel was powered by a 100 hp electric motor driving a three-blade, variable-pitch fan. A four-gear transmission and a 10:1 contraction ratio allowed for test section speeds to 200 miles per hour. Low test section turbulence intensity of 0.2% was attributed to stator blades immediately aft of the fan, and two fine wire mesh screens six inches apart in the settling chamber, in addition to turning vanes in each corner. The 8.75 ft^2 test section, 45 inches wide by 28 inches in height, was slightly divergent to counter the effective contraction caused by boundary layer growth. A 5/100 tunnel diameter breather slot, immediately downstream of the test section, helped maintain approximate atmospheric static pressure conditions. Swing windows on either side of the test section and frosted glass corner fillet fluorescent lights provided adequate illumination, visualization, and access to the test models.

Test section dynamic pressure, Q, was determined by measuring the static pressure difference, Δp, between four manifold-flush taps in the test section and a similar set of four taps in the settling chamber. Connected via a common manifold, the Δp was presented on a micromanometer and digital display. The Δp was

13
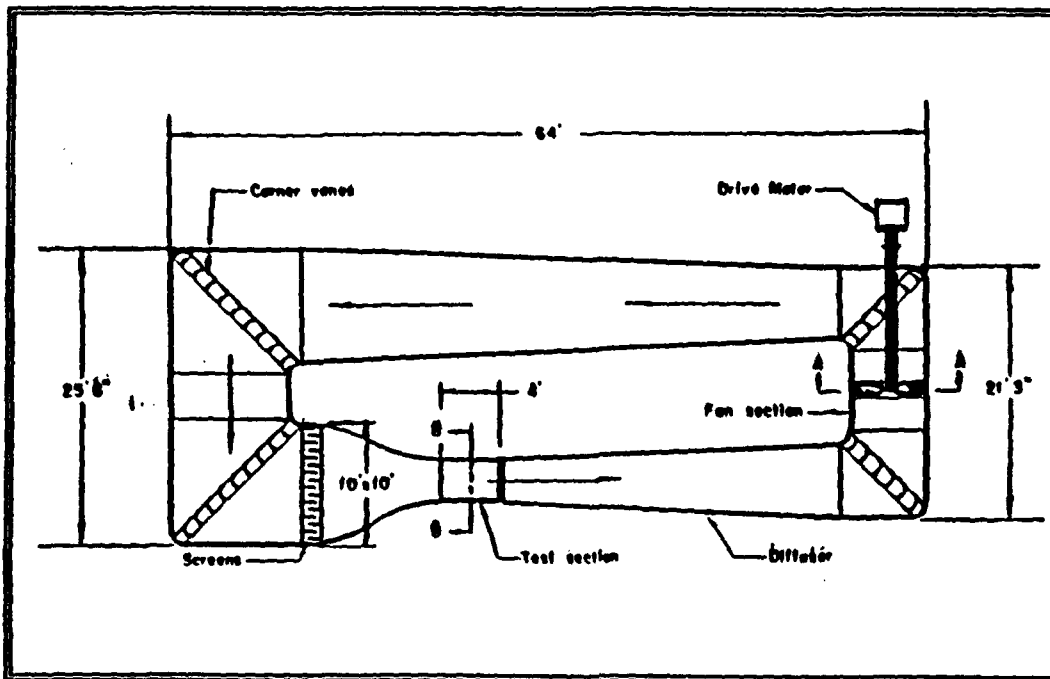
Figure 3.1 NPS Horizontal Low Speed Wind Tunnel

converted into dynamic pressure using the relationship in equation (3.1) calculated

from a previous tunnel calibration.

$$Q = \frac{1}{2} * V_\infty^2 = 2.046 * K * \Delta p \qquad (3.1)$$

Where: Q ≡ dynamic pressure (lb_f/ft^2)
          V_∞ ≡ freestream velocity (ft/s)
          Δp ≡ static pressure difference (cm of H_2O)
          K ≡ tunnel calibration constant = $1/0.93$

Tunnel air temperature was measured using a dial thermometer extending into the

settling chamber. A more detailed description of the wind tunnel is presented in

Reference 11.

14

B. BALANCES

1. Wall Balance

An external, cylindrical, reflection-plane (wall) balance, shown in Figure 3.2, was used to measure forces and moments of the wire at the higher angles of attack. Flush mounted in the test section, the wall balance was designed to measure normal and axial forces to 150 lb_f and their respective moments. Built by NPS personnel in 1974, the four degree of freedom balance was designed with two pairs of strain gage bridges orthogonally mounted on flexure links separated vertically by 26.5 inches. Each bridge circuit had four active legs for automatic temperature compensation. The lower bridge A, and the upper bridge B, each output an axial and normal voltage (E_{aa}, E_{ba}, E_{an}, E_{bn}) which were converted into forces and moments using the results of a balance calibration described in Appendix A. Electrical schematics of the bridges and pin connections are presented in Reference 12.

The balance column was rigidly mounted on an electrically-controlled turntable capable of rotating -18° to +200° from the centerline orientation shown in Figure 3.3. A 15.625-inch-diameter aluminum plate was mounted with eight screws atop the reflective plane and flush with the floor of the test section. A 0.125 inch gap existed between the plate and reflective plane to prevent contact and ensure accurate measurements when under load. Models were mounted on the aluminum plate for tests.
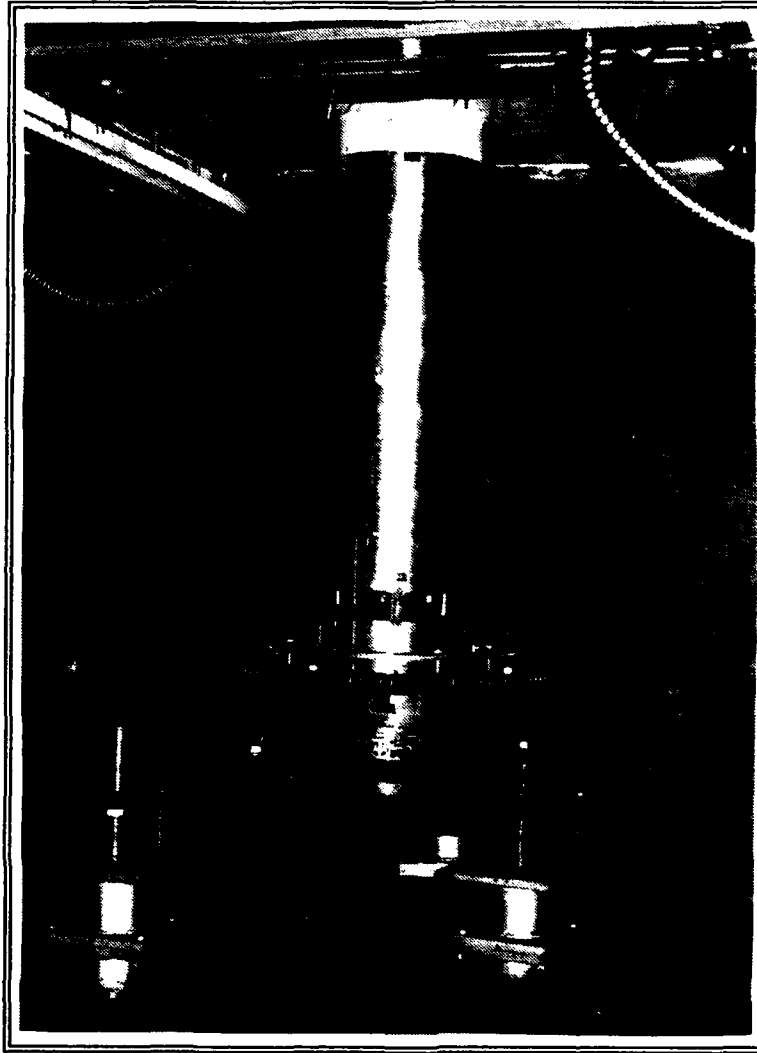
Figure 3.2 NPS Wall Balance

2. Sting Balance

A six-degree-of-freedom, one-inch-diameter, Mark XIV, internal Task[*] balance was used to measure forces and moments for models representing lower angles of attack of the wire, and for the drogue. The 4.9-inch-long balance had eight 350Ω wheatstone bridges: two normal force (N1, N2), two side force (S1, S2), two axial force (A1, A2), and two rolling moment (l1, l2). The two axial force and two rolling moment bridges were each connected in parallel to produce 175Ω circuits,
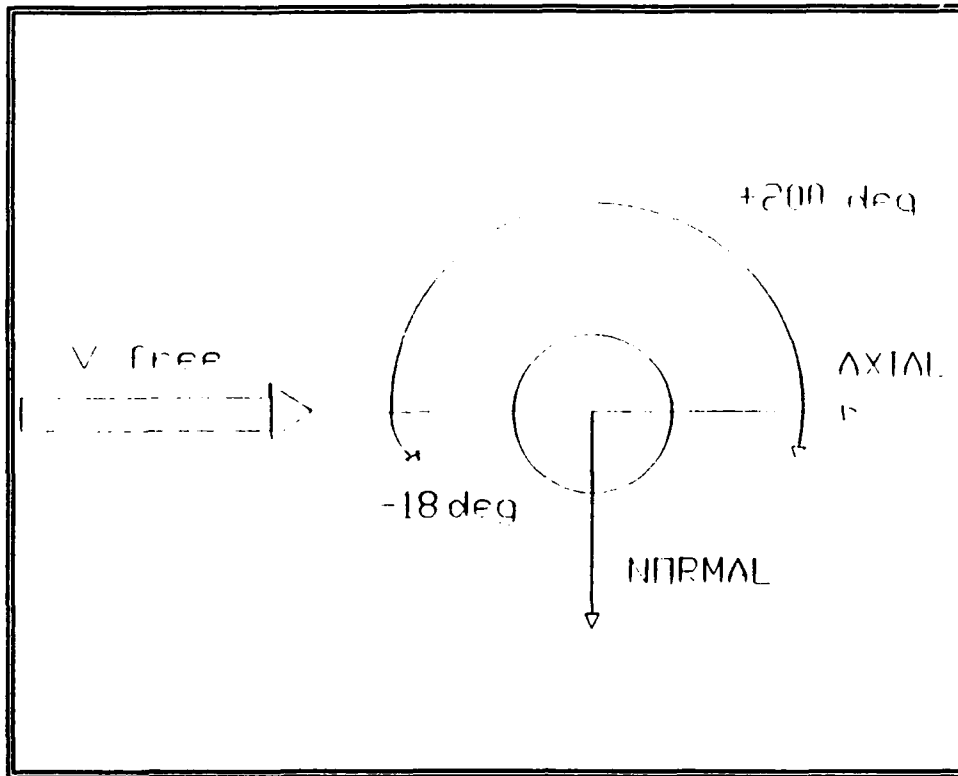
Figure 3.3 Wall Balance Coordinate System

and therefore six electrical outputs: N1, N2, S1, S2, A, l. Maximum balance loads were 400 lb$_f$ in the normal channels, 200 lb$_f$ in the side force channels, 100 lb$_f$ axially, and 250 inlb$_f$ of rolling moment. On loan from NASA-Ames Research Center through the Navy-NASA Joint Institute of Aeronautics, the balance was calibrated to a 5 V$_{DC}$ bridge excitation voltage by NASA-Ames personnel. Additional calibration, presented in Appendix B, was required to ensure proper force measurement, and moment focal point position prior to testing. Calibration constants and their accuracies are presented in Appendix B, Tab I.

The balance was mounted into a 6.75-inch sleeve extender and locked with set screws onto a "U" frame as shown in Figure 3.4. The twenty-four 36-gage

17
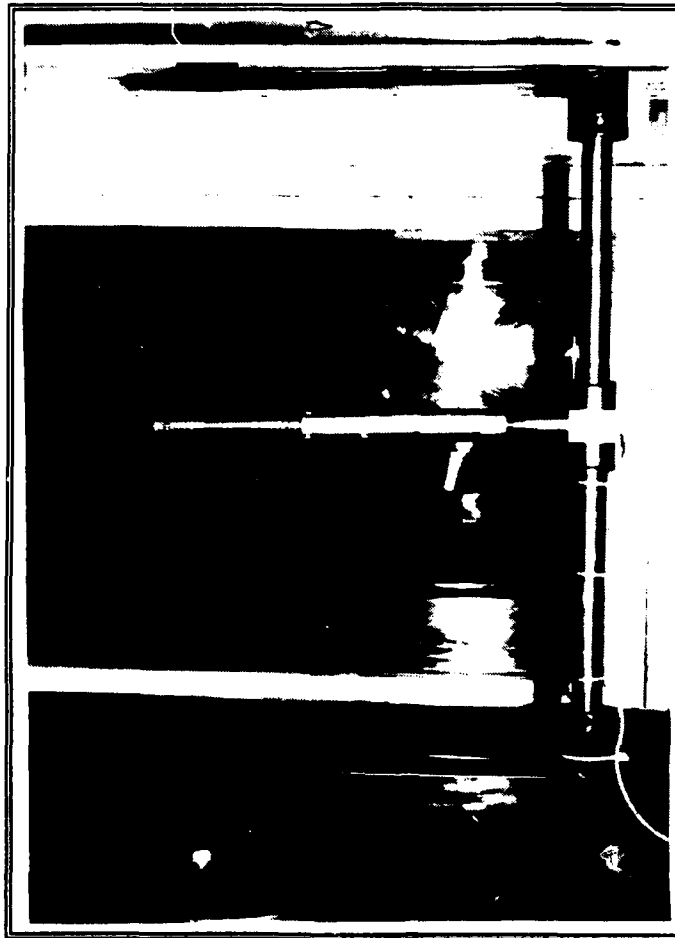
Figure 3.4 MK XIV 1" Task (Sting) Balance

wires were fed through the sleeve and frame, and out the tunnel. Wire slack was

provided to allow $\pm 65°$ of angle of attack (AOA). Balance orientation is presented

in Figure 3.5. The balance had four pairs of pin recesses orthogonally positioned for

model mounting.
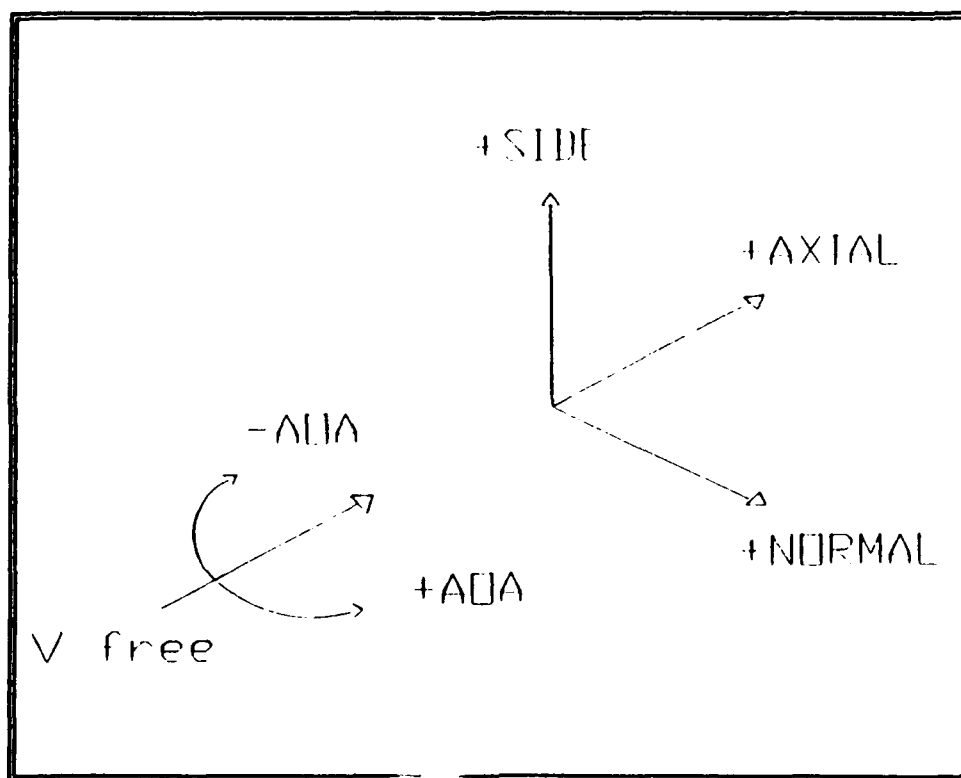
Figure 3.5 Sting Balance Coordinate System

C. ACQUISITION SYSTEM

1. Signal Conditioners / Pacific® Amplifiers

The electrical bridge outputs from the wall and sting balances were connected to individual signal conditioners that controlled bridge excitation. The excitation voltages were 10 V_{DC} for the four wall balance channels and a precalibrated 5 V_{DC} for the six sting balance channels. Sting balance channels were connected to the cannon plugs on the signal conditioners as shown in Figure 3.6. The conditioned signals were amplified with a gain of 1000 by individual Pacific® 8255/6 amplifiers and routed to a National Instrument MC-MIO-16L-9, 50 pin input/output (I/O) connector presented in Figure 3.7. Wall balance channels E$_{aa}$,

BLACK

COLOR

BLANK

COLOR

RED

GREEN

N1 - blue
N2 - white
S1 - gray
S2 - yellow
A - purple
I - orange
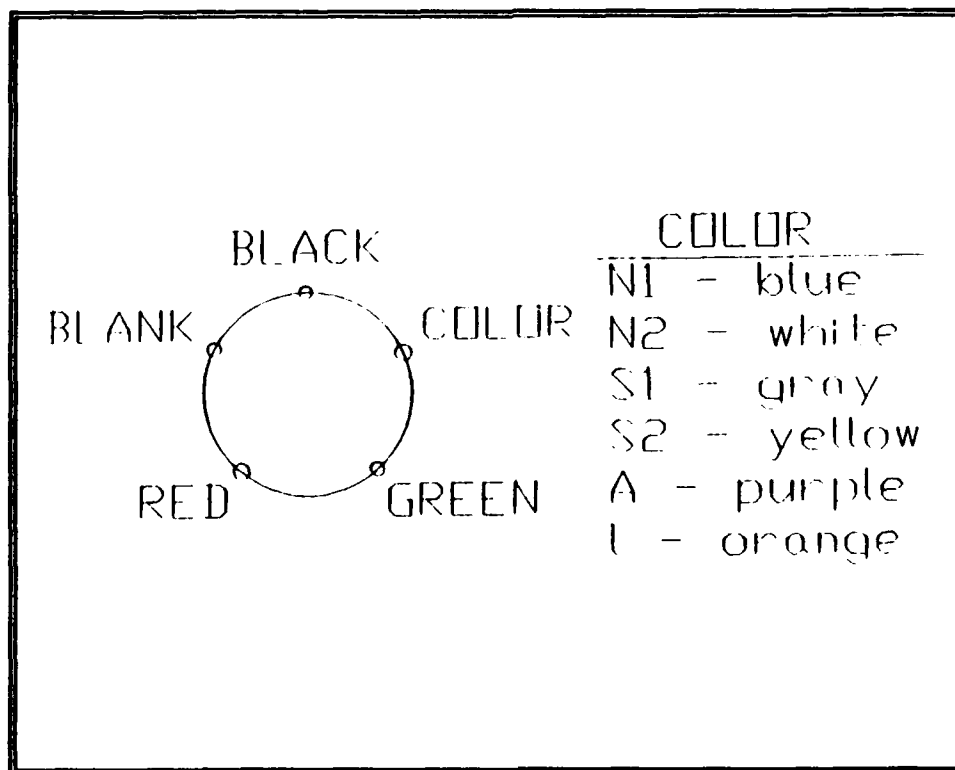
Figure 3.6 Sting Lead/Cannon Plug Connections

E_{ba}, E_m, E_{bn} were connected to pins 4/3 (lead/ground), 8/7, 12/11, 16/15, respectively. Sting balance channels N1, N2, A, S1, S2, 1 were connected to pins 4/3, 6/5, 8/7, 10/9, 12/11, and 14/13 respectively.

2. **Data Sampling / Computer System**

The MC-MIO-16L-9 board has a 12 bit (i.e. 2^{12} bits) analog to digital (A/D) converter with a 9 μs conversion time and design acquisition rates up to 100 Kbytes/s [Ref. 13]. Digital resolution was 4.88 mV with bridge excitation of 10 V_{DC} (-2048 to 2047 bits) and 2.44 mV with an excitation of 5 V_{DC}. Data acquisition was controlled by programs written and complied in QuickBasic using Microsoft QuickBasic 4.5* software and run on an IBM PS/2* microcomputer. National

20

AI GND — | 1 | 2 | — AI GND
ACH0 — | 3 | 4 | — ACH8
ACH1 — | 5 | 6 | — ACH9
ACH2 — | 7 | 8 | — ACH10
ACH3 — | 9 | 10 | — ACH11
ACH4 — | 11 | 12 | — ACH12
ACH5 — | 13 | 14 | — ACH13
ACH6 — | 15 | 16 | — ACH14
ACH7 — | 17 | 18 | — ACH15
AI SENSE — | 19 | 20 | — DAC0 OUT
DAC1 OUT — | 21 | 22 | — EXTREF
AO GND — | 23 | 24 | — DIG GND
ADIO0 — | 25 | 26 | — BDIO0
ADIO1 — | 27 | 28 | — BDIO1
ADIO2 — | 29 | 30 | — BDIO2
ADIO3 — | 31 | 32 | — BDIO3
DIG GND — | 33 | 34 | — +5 V
+5 V — | 35 | 36 | — SCANCLK
EXTSTROBE* — | 37 | 38 | — START TRIG*
STOP TRIG — | 39 | 40 | — EXTCONV*
SOURCE1 — | 41 | 42 | — GATE1
OUT1 — | 43 | 44 | — SOURCE2
GATE2 — | 45 | 46 | — OUT2
SOURCE5 — | 47 | 48 | — GATE5
OUT5 — | 49 | 50 | — FOUT

Figure 3.7 MC-MIO-16L-9 I/O Board

Instruments LabWindows™ interactive software version 1.1 was utilized in the programs to command data sampling and averaging. One thousand samples per channel were taken for each data point at a rate of 1770 Hz. Time averaged sampling required 2.26 seconds for the wall balance and 3.39 seconds for the sting balance.

21

The QuickBasic programs converted the averaged voltage samples to forces and moments for output and analysis. The wall balance program multiplied the four voltage samples by the 4x4 calibration matrix, [K], to produce normal and axial forces and moments in balance coordinates.

$$[K]*\begin{Bmatrix} E_{aa} \\ E_{ba} \\ E_{an} \\ E_{bn} \end{Bmatrix} = \begin{Bmatrix} AXIAL\ FORCE \\ AXIAL\ MOMENT \\ NORMAL\ FORCE \\ NORMAL\ MOMENT \end{Bmatrix} \qquad (3.2)$$

Voltage readings, in addition to the force and moment calculations, were output to two files for analysis. The sting balance program utilized nonlinear equations derived by Yuan [Ref.14], multiplying calibration constants in Appendix B, Tab I by the six voltage readings. Additionally, nonlinear interaction equations were iterated to simultaneously solve cross channel dependence of the balance. The primary output file consisted of normal, side, and axial forces, and pitching, yawing, and rolling moments. Both wall and sting balance acquisition programs are presented in Appendix C.

D. MODELS

1. Wall Balance Models

All wall balance models were mounted on the 15.625-inch-diameter rotating aluminum plate. The baseline model, shown in Figure 3.8, consisted of six 0.3125-inch-diameter steel rods horizontally oriented between two 0.625-inch-

22
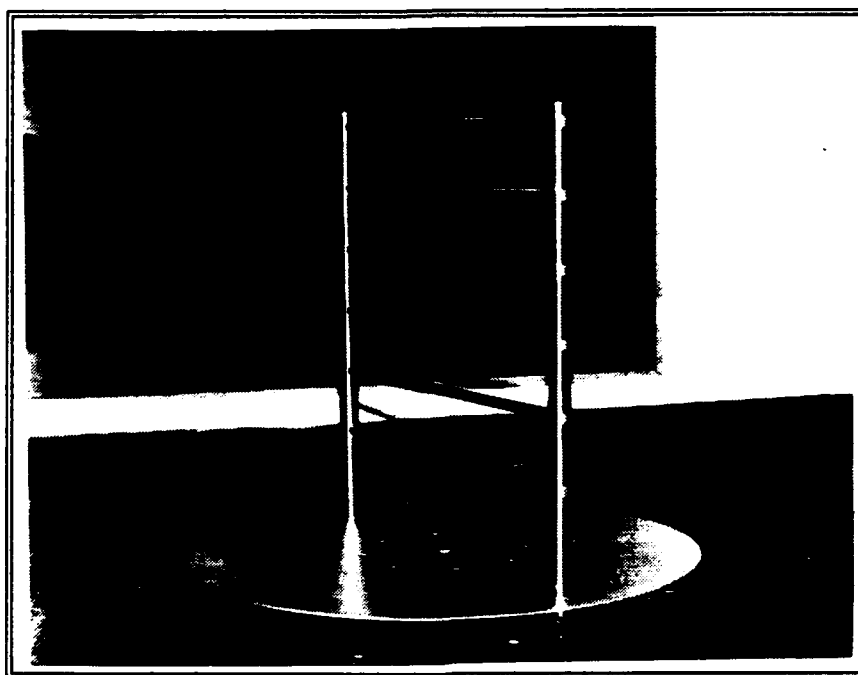
Figure 3.8 Clean Cylinder (Rod) Model (105° AOA)

diameter, 13.5-inch-tall steel stanchions. Each rod presented 12 inches of length to

tunnel flow. By vertically separating the rod by 2.0 inches, less than 1% interference

effects from an adjacent rod was calculated. The rods, representing long circular

cylinders, were used to verify experimental procedures, for analysis, and to provide

a baseline for the 3x7 wire comparison.

Six actual 3x7 wires of 0.158-inch diameter were also mounted between

the 0.625-inch-diameter stanchions. Shown in Figure 3.9 at an angle of attack 90°

to tHe flow direction, the wires presented six feet of total length at full scale

Reynolds number.   Finally, two clean 0.625-inch-diameter stanchions were

constructed for calculation of stanchion forces alone. Sketches of wall balance

models are presented in Appendix D.
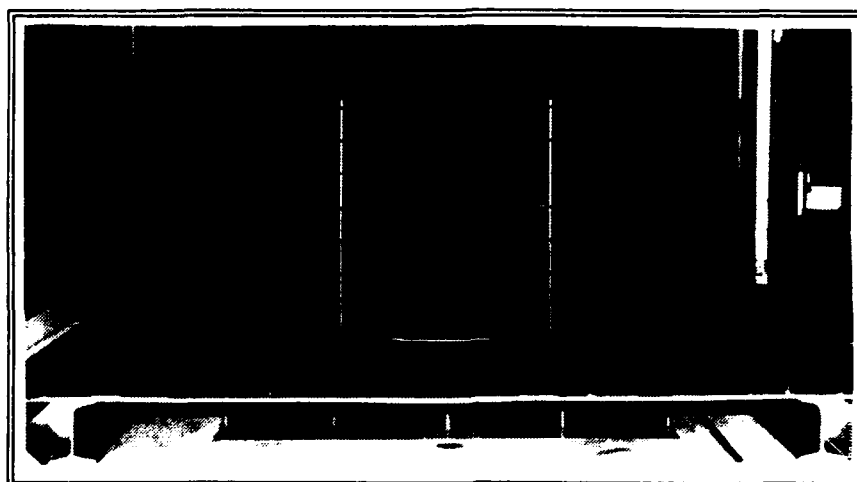
Figure 3.9 3x7 Wires (90° AOA)

2. Sting Balance Models

Sting balance models were mounted on the 1.0-inch-diameter Mark XIV internal balance. The baseline model, shown in Figure 3.10, consisted of a 21.0-inch long, 2.375-inch-diameter aluminum cylinder with a 5.35-inch long, two-caliber tangent-ogive nose with radius of 10.094 inches blunted at the nose by an 0.375 inch radius. When mounted, the nose declined 1.6° from the horizontal in the (-) side force coordinate direction. The balance focal point was 10.0 inches aft of the nose cylinder joint. Additionally, 80 and 220 grit sandpaper was mounted at the nose base to trip the boundary layer and disrupt nose-generated asymmetric flow separation and vortex shedding [Ref. 15]. The clean cylinder sting model was used to verify experimental procedures, as a baseline for integration with wall balance data, and comparison with helix sting models.

Helix models were constructed to represent the 3x7 wire. The right helix model, shown in Figure 3.11, was a 15-times scale model constructed with the same
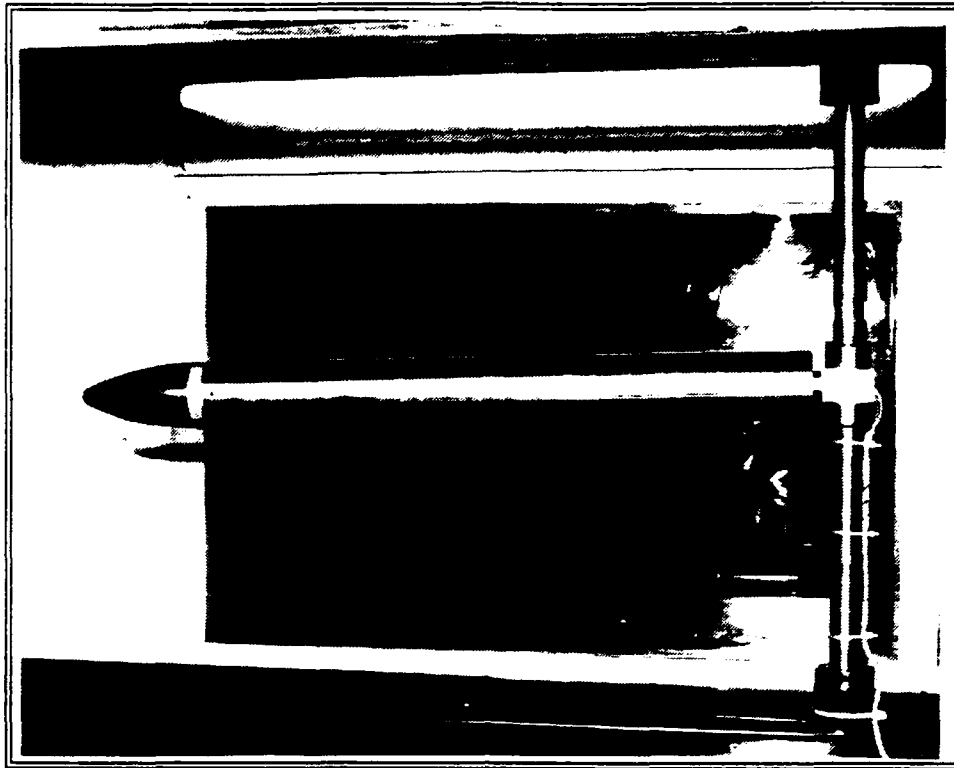
Figure 3.10 Clean Cylinder Sting Model

relative 1.87-inch helical pitch and direction of the 3x7 wire. The 21.0-inch-long,

2.375-inch-diameter grooved section was representative of 1.4 inches of 3x7 wire and

contained 0.75 revolutions. The left helix sting model, shown in Figure 3.12, was

identical in groove pitch but opposite in direction to the right model. Nose

dimensions were identical to the clean baseline cylinder. Finally, a 0.32-scale sting

model of the wire system drogue is shown in Figure 3.13. Drogue model length was

9.264 inches with a base diameter of 7.675 inches. The balance focus was 5.082

inches aft of the $22.5°$ apex. Constructed of mahogany with an aluminum core, the

drogue model did not decline from the horizontal when mounted. Sketches of the

sting balance models are presented in Appendix D.
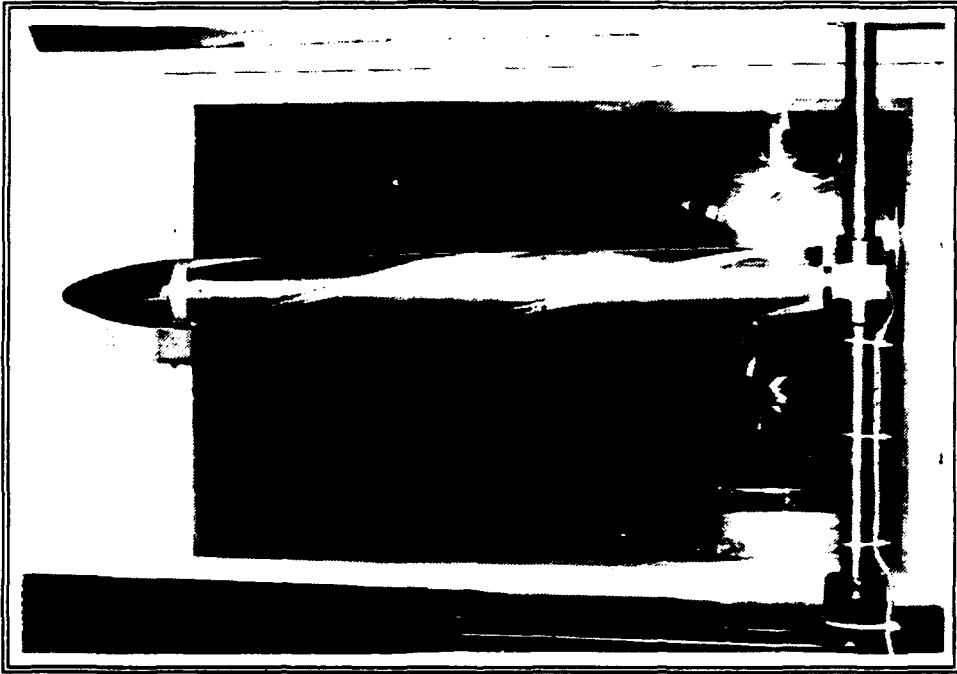
Figure 3.11 Right Helix Sting Model

Figure 3.12 Left Helix Sting Model

26
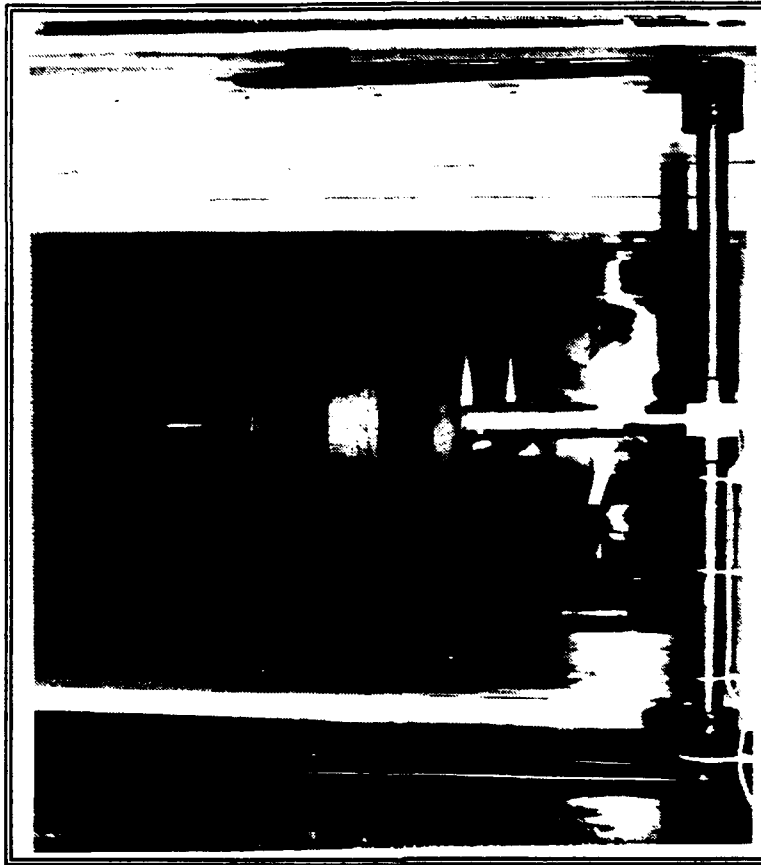
Figure 3.13 Drogue Sting Model

E. STATIC CONDITIONS SIMULATION MODEL

An existing simulation model by Clifton was used to determine the Reynolds number range for wind tunnel testing [Ref.2]. The model described the static, no wind equilibrium conditions of a cable towed by an airplane in a circular orbit for positive angles of attack to 90°. Additionally, modifications were conducted by Clifton for inclusion of experimentally derived force coefficients for improved static predictions.

27

IV. EXPERIMENTAL PROCEDURES

A. GENERAL

1. Model Preparation

Wall balance models required approximately two hours of preparation before testing. The steel cylindrical rods and support stanchions were sanded with fine grit finishing paper and soaked in an ethanol bath. After removal and drying they were coated in spray silicon and handled with latex gloves to prevent surface oxidation. The rods or wires were installed and set with two screws per piece per stanchion. The set screw and end cap holes were filled with clay to reduce aerodynamic interference. The aluminum plate with model was then mounted on the balance.

Sting balance models required less preparation. After surface cleaning with a soft cloth, the models were carefully slid over the Task balance and screws set into the locking recesses. Tape was used over the mounting holes on the drogue model and clay fill on the other sting models.

2. Signal Conditioner / Amplifier Preparation

The signal-conditioner span rheostat controlled bridge excitation voltage. For the wall balance channels, excitation was set at 10.00 V_{DC} -0.05mV (MC-MIO-16L-9 I/O board saturation was at 10 V_{DC}). For the sting balance, channels N1 and

28

N2 excitation were set to 5.15 and 5.75 V_{DC} as required from the local calibration (Appendix B). The remaining four channels set 5.00 V_{DC} with all error ±0.02mV.

The Pacific* amplifiers required input and output to be zeroed after model changes, long test periods and long off periods. With the amplifier input shorted and a gain of 1, the output set screw was adjusted to zero to ±100 μV tolerance. After increasing the gain to 1000, the input screw was zeroed to ±500 μV [Ref. 16]. Finally, the shorting plugs were pulled and the incoming signals set to zero, ±0.01 mV with the signal control on the signal-conditioner panel. Acquisition system preparation was complete.

B. W.⸱⸱⸱ BALANCE EXPERIMENTS

1. Test Matrix

Simulation software by Clifton was run to determine the Reynolds number of the 20,000-foot-long 3x7 wire for test matrix construction [Ref. 2]. Results are presented in Figure 4.1. The simulation model used a density look-up table from flight test data, and constant viscosity. Hand calculations of Reynolds number using altitude varying temperature, density, and viscosity produced a low bound value of 3500, and an upper bound Reynolds number of 17,500 [Ref. 3:p. 6-10]. After accounting for tunnel test conditions, test velocities were selected and are presented in Table 4.1.
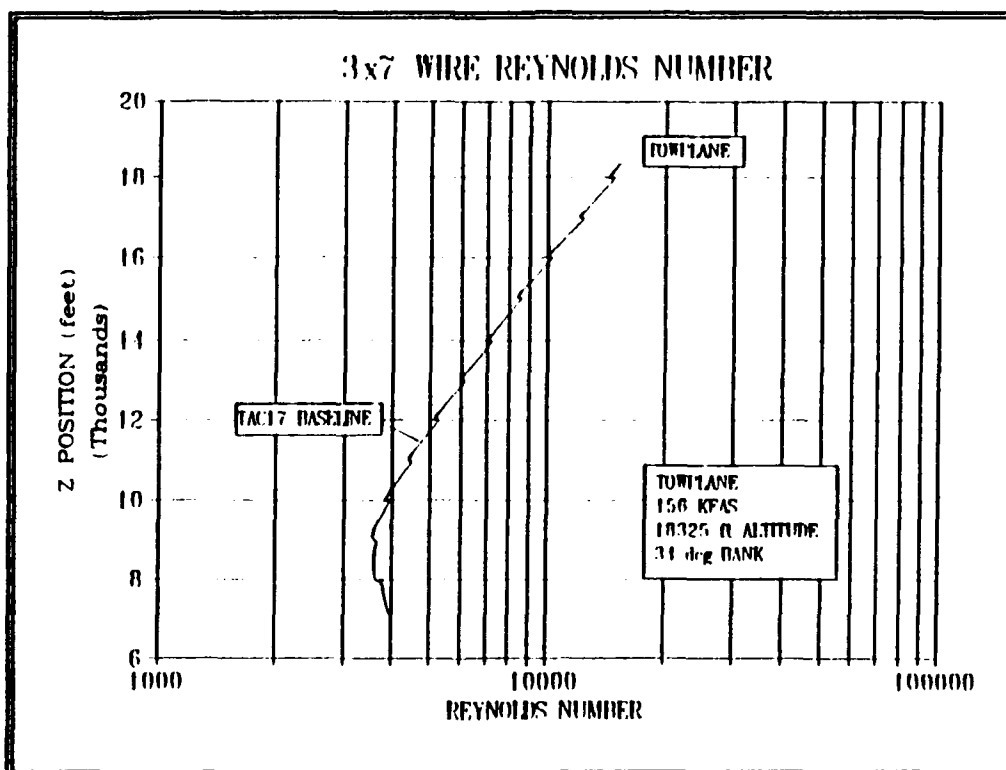
Figure 4.1 Static Simulation - Reynolds Number vs Altitude

TABLE 4.1 WALL BALANCE TEST VELOCITIES / REYNOLDS NUMBERS

Tunnel Conditions	Reynolds Number	
Q (lb_f/ft^2)	3x7 Wire (d=0.158")	Rods (d=0.3125")
10	7680	15180
20	10860	21470
30	13300	26300
40	15350	30360
50	17160	-----
60	18800	-----

The lowest dynamic pressure of 10 lb_f/ft^2 was selected due to balance resolution limitations. Velocities representative of Q = 50 lb_f/ft^2 and Q = 60 lb_f/ft^2 were not run

30

for the 0.3125-inch-diameter steel cylindrical rods to maintain Reynolds number ranges, and allow correlation of 3x7 wire data at similar dynamic pressures. All wall balance tunnel runs produced subcritical Reynolds numbers [Ref. 3:p. 106].

Wall balance tunnel experiments were started with the model at 105° to the flow (Figure 3.8) and advanced through 90° (Figure 3.9) to -15° in 5° decrements; resulting in 25 angle-of-attack settings. Four additional check points were taken per run. A total of 16 tunnel runs were completed in 11.4 tunnel operating hours. Breakdown of runs are as follows: a) clean stanchions alone - 6 runs (Q = 10-60 psf), b) 0.3125-inch-diameter rods - 4 runs (Q = 10-40 psf), c) 3x7 wires - 6 runs (Q = 10-60 psf).

2. Balance Tare Values

Wall balance channels exhibited a linear drift with respect to time requiring tare readings immediately prior and after tunnel operation. The tare difference was prorated assuming equal time between angle of attack positions by a QuickBasic program contained in Appendix C, and stored for data reduction.

3. Tunnel Operation

Wind tunnel operating procedures are summarized below:

a) After setting desired velocity (cm H_2O) in the tunnel manometer, the tunnel was started and brought up to and stabilized at desired dynamic pressure.

b) When stable, 3 data points were taken.

c) Model angle of attack was advanced to the next position.

d) Tunnel velocity was adjusted to maintain test Q.

e) Steps (b) through (d) were repeated for all test points.

f) The tunnel was shut down and elapsed time, temperature logged.

A detailed description of tunnel operating procedures is presented in Reference 10.

C. STING BALANCE EXPERIMENTS

1. Test Matrix

To maintain Reynolds number integrity with the wall balance experiments, the 15-times scale sting balance models would be required to be tested at velocities well below balance resolution. A mid-tunnel range dynamic pressure of 40 lb_f/ft^2 was selected to utilize the full calibration range, minimize turbulence, and achieve force measurements greater than 2% of balance resolution. Experimentation was also conducted at $Q = 20$ lb_f/ft^2 to determine velocity dependence. At $Q = 20$ and 40 lb_f/ft^2 the model Reynolds numbers were 1.63×10^5 and 2.31×10^5 respectively, still subcritical for a circular cylinder [Ref. 3].

Baseline model mounting position was with the two mounting screws in front, facing the front model access window. Test runs were repeated with mounting holes rotated to top, back, and bottom reference positions for each model to ensure helix representation of an infinite wire, and reveal asymmetries from nose and body construction. Additional test runs were conducted with a 0.5-inch-wide strip of 80 and 220 grit sandpaper attached to the base of the nose designed to disrupt nose

generated asymmetric flow separation and vortex shedding at the higher angles of attack [Ref. 15].

Sting balance models were tested from 0° to 20° in 4° increments and from 20° to 50° in 5° increments. The angle-of-attack positions were repeated in the negative direction. Six check points were taken for a total of 29 angle-of-attack positions per experimental run. A total of 24 data runs were conducted in 11.5 tunnel operating hours. A breakdown of runs, model and test conditions are presented in Table 4.2.

TABLE 4.2 STING BALANCE MODEL TEST CONDITIONS

Model	Q (lb_f/ft^2)	Mounting Position	Sandpaper
Clean	40	Front	None,80,220
		Top	None,80,220
		Back	None
		Bottom	None
	30	Front	None
	20	Front	None
Right Helix	40	Front	None, 220
		Top	None, 220
		Back	None
		Bottom	None
	20	Front	None
Left Helix	40	Front	None, 220
		Top	None, 220
		Back	None
		Bottom	None
Drogue	40	Top	None
	20	Top	None

2. Balance Tares

The sting balance acquisition program recorded wind-off force and moment tare values to be subtracted from wind-on data points. The sting balance exhibited no drift.

3. Tunnel Operation

Wind tunnel operating procedures for sting balance experiments were identical to wall balance operating procedures.

4. Flow Visualization

String tufts flow visualization was conducted with the right helix model, front mounted, at a $Q = 20$ lb_f/ft^2. The model, shown in Figure 4.2, had 36 1.75 inch black tufts taped in three bands positioned 4, 10, and 15.5 inches aft of the nose. Four tufts were attached on each $\frac{1}{3}$ wrap of the helix with end tufts positioned close to the groove edges. One run of 0.9 hours was conducted with photographs taken at the same angle-of-attack positions as the data runs.

D. DATA REDUCTION

1. General

Raw experimental data was transferred from the IBM PS/2* via 1.4 megabyte, 3.5 inch disk to a 486-33 MHz computer for data reduction. Any corrections to inputed angles-of-attack values were completed using Microsoft DOS 5.0 Editor prior to importing into QuattroPro 3.0 spreadsheet software. All data manipulation and graphing were conducted in QuattroPro 3.0.
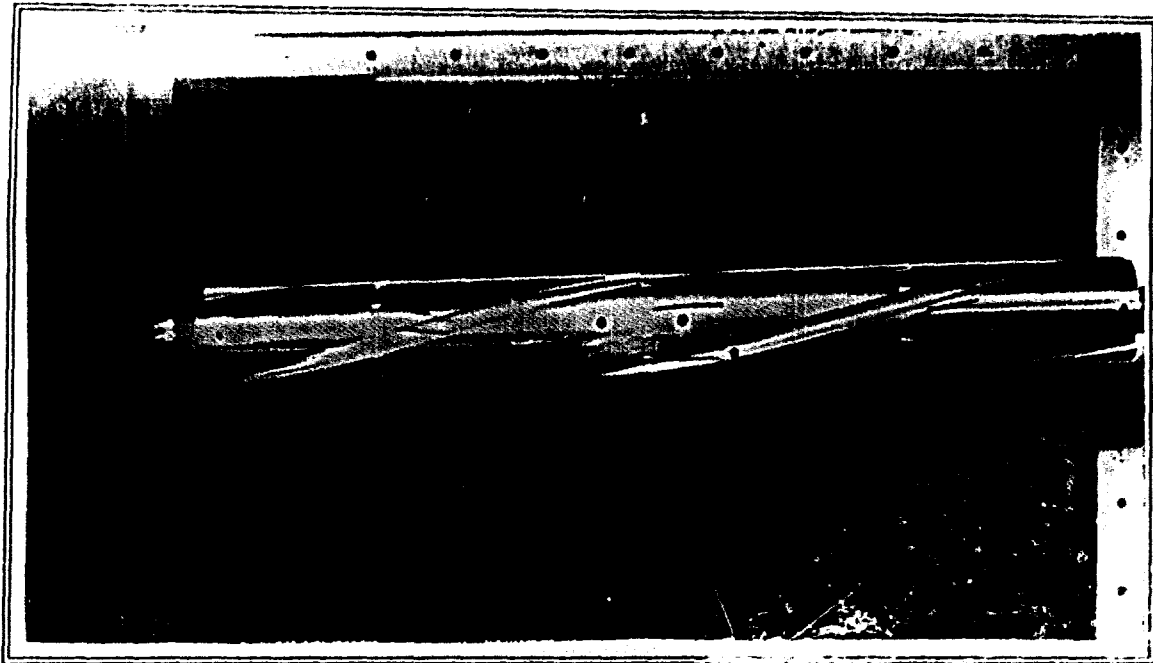
Figure 4.2 Right Helix Model - Flow Visualization (Wind Off)

2.   Wall Balance Data

Ten spreadsheets, one for each 3x7 wire and cylindrical rod velocity, were constructed for the wall balance experimentation. Each spreadsheet imported four files of 4 columns (axial force, axial moment, normal force, normal moment) by 75 rows (AOA data). The four files required per spreadsheet were: a) the clean stanchion test run, b) its calculated tare variation, c) the wire or bar test run, and d) its representative tare calculations. Resultant normal and axial forces and moments were calculated using

$$\left\{ \begin{matrix} NET\ FORCES \\ NET\ MOMENTS \end{matrix} \right\} = \left| \begin{matrix} (TEST\ FORCES/MOMENTS & MODEL\ TARE) \\ (CLEAN\ STANCHIONS & STANCHION\ TARE) \end{matrix} \right| \quad (4.1)$$

Computations were conducted in wire/cylinder vice balance coordinate system and defined as follows:

35

Normal ≡ perpendicular to wire/cylinder
Axial ≡ parallel to wire/cylinder

Nondimensional force coefficients were calculated for each angle of attack in the normal direction using

$$C_N = \frac{N}{Q*L*d} \qquad (4.2)$$

Where:
- C_N ≡ normal force coefficient
- N ≡ normal force (lb_f)
- Q ≡ test dynamic pressure (lb_f/ft^2)
- L ≡ wire/cylinder cumulative length (ft)
- d ≡ wire/cylinder diameter (ft)

Additionally, a normal force coefficient referenced to the normal velocity component was calculated using

$$C_{N,\ Vcomp} = \frac{N}{0.5*\rho*(Vn)^2*L*d} \qquad (4.3)$$

Where:
- $C_{N,\ Vcomp}$ ≡ normal force coefficient
- N ≡ normal force (lb_f)
- Vn ≡ velocity component in the normal direction (ft/s)
- ρ ≡ atmospheric density ($lb_f\ s^2/ft^4$)
- L ≡ wire/cylinder cumulative length (ft)
- d ≡ wire/cylinder diameter (ft)

Axial force coefficients, C_A, were calculated using (4.2) substituting axial force, A, for normal force, N.

3. Sting Balance Data

Four primary spreadsheets were constructed for the four sting balance models. Each test run file consisted of 6 columns (3 forces, 3 moments) and 84 rows (AOA data). The clean cylinder, right, and left helix model spreadsheets contained the four different mounting positions and different dynamic pressure data runs as

36

applicable. One spreadsheet contained all drogue data runs, and three separate spreadsheets were opened to reduce sandpaper modified model test data.

For the clean cylinder and helix models, normal, axial, and side force coefficients (C_N, C_A, C_Y) were calculated using the respective form of (4.2) with normal, axial, and side forces (N, A, S), L = cylinder reference length, and d = cylinder diameter. Additionally, nondimensional pitching and yawing moment coefficients were calculated using

$$Cm_{N,Y} = \frac{PITCHING/YAWING\ MOMENT\ (ftlb_f)}{Q*L^2*d} \qquad (4.4)$$

Where: $Cm_{N,Y}$ ≡ pitching, yawing moment coefficient
    Q ≡ dynamic pressure (lb_f/ft^2)
    L ≡ length of cylinder section (ft)
    d ≡ diameter of cylinder (ft)

For the drogue, force and moment coefficients were calculated in (4.5) and (4.6) referenced to the base area and drogue length. Graphs of coefficients versus angle of attack were plotted.

$$C_{N,A} = \frac{N,\ A}{Q*(\pi/4)*d^2} \qquad (4.5)$$

$$Cm_N = \frac{PITCHING\ MOMENT\ (ft\ lb_f)}{Q*(\pi/4)*d^2*L} \qquad (4.6)$$

Where: $C_{N,A}$ ≡ normal, axial force coefficient
    Cm_N ≡ normal moment coefficient
    N,A ≡ normal, axial force
    Q ≡ dynamic pressure (lb_f/ft^2)
    d ≡ drogue base diameter (ft)
    L ≡ drogue length (ft)

E.   STATIC CONDITIONS SIMULATION MODEL

An existing simulation model by Clifton [Ref.2] was modified with the experimentally derived normal, axial, and side force coefficients of the 3x7 wire. Drag and lift coefficients for the drogue and moment modifications were also included. The FORTRAN program, TAC17, was renamed TAC17A and is contained in Appendix E. Eight test runs using Microsoft FORTRAN 5.1 and TAC17 and TAC17A programs were conducted on a 486-33 MHz computer with conditions described in Tables 4.3 and 4.4.

TABLE 4.3   STATIC SIMULATION TEST CONDITIONS

Condition	Program	KEAS	Altitude (ft)	Bank Angle	Name of Condition
A	TAC17	156	18,325	34°	Operational
B	TAC17	156	18,325	34°	Level
C	TAC17A	156	18,325	34°	Operational
D	TAC17A	156	18,325	34°	Level

TABLE 4.4   SIMULATION TEST RUNS

Run	Condition	C_Y	Notes
1	A	NO	Previous Baseline
2	C	NO	Comparison
3	C	YES	Compare (C_Y on)
4	C	YES (3^*C_Y)	Operational
5	B	NO	Previous Baseline
6	D	NO	Comparison
7	D	YES	Compare (C_Y on)
8	D	YES (3^*C_Y)	Observed Trail Angle

Outputs from these programs included radial, theta, and z position, tension, angle of attack, true velocity, and Reynolds number for each grid point of the wire. The 64 output files were imported into one QuattroPro 3.0 spreadsheet for plotting and analysis.

V. RESULTS AND DISCUSSION

A. HOERNER MODEL VERIFICATION

Hoerner presented an empirical relationship for lift and drag coefficients of inclined cylinders at subcritical Reynolds numbers. His relationship was based on the premise that the "fluid-dynamic pressure forces of such bodies only correspond to the velocity component in the direction normal to their axis." [Ref. 6] From that relationship, for a circular cylinder,

$$C_D = C_{D,Basic} * \sin^3 \alpha$$

$$C_L = C_{D,Basic} * \sin^2 \alpha * \cos \alpha \qquad (2.4)$$

$$C_{D,Basic} = \frac{C_N}{\sin^2 \alpha}$$

Where:
- C_D ≡ drag force coefficient
- C_L ≡ lift force coefficient
- C_N ≡ normal force coefficient (equation (4.2))
- α ≡ angle of attack

Hoerner's relationships are presented in Figure 2.3. Instead of defining an axial force coefficient, C_A, Hoerner added a $\pi C_f = 0.02$ skin friction term. By transforming a body axis system of C_N and C_A into C_D and C_L, Hoerner's relationships can be written as equation (5.1) with $C_A = 0$.

$$\left\{\begin{matrix} C_L \\ C_D \end{matrix}\right\} = \left[\begin{matrix} \cos\alpha & -\sin\alpha \\ \sin\alpha & \cos\alpha \end{matrix}\right] * \left\{\begin{matrix} C_N \\ C_A \end{matrix}\right\} + \left\{\begin{matrix} 0 \\ 1 \end{matrix}\right\} * \pi C_f \qquad (5.1)$$

Using wall balance data for the 0.3125-inch-diameter clean cylinder and the relationships presented by Hoerner in (2.4) and (5.1), lift and drag coefficients were calculated. Plotted against Hoerner's empirical findings, the C_D and C_L of the clean cylinders are presented in Figure 5.1. C_D of the cylinders showed agreement with Hoerner except in the region of 90° angle of attack. The difference was attributed to Hoerner using $C_{D,Basic} = 1.1$ while the $C_{N,90°}$, which is equal to $C_{D,Basic}$, was calculated from (4.2) as 1.193. The C_L of the experimental cylinders showed close agreement with Hoerner's closed form relationships.

Similar analysis was conducted using 3x7 wire wall balance data and is presented in Figure 5.2. $C_{N,90°}$ of the wire, calculated from (4.2), was 1.09. Wire C_L and C_D showed fairly good agreement with Hoerner's closed form-equations with the maximum deviations found in the middle range angles of attack. With verification of experimental data on the circular rods in accord with historical empirical relationships, definition of force coefficients in all three axes commenced.

B. NORMAL FORCE COEFFICIENT

1. Wall Balance Data

Normal force coefficients for the wall balance data at each velocity were calculated using the appropriate form of (4.2). $C_{N,90°}$ values for the clean cylinders and 3x7 wires plotted versus test dynamic pressure are presented in Figure 5.3. A

41
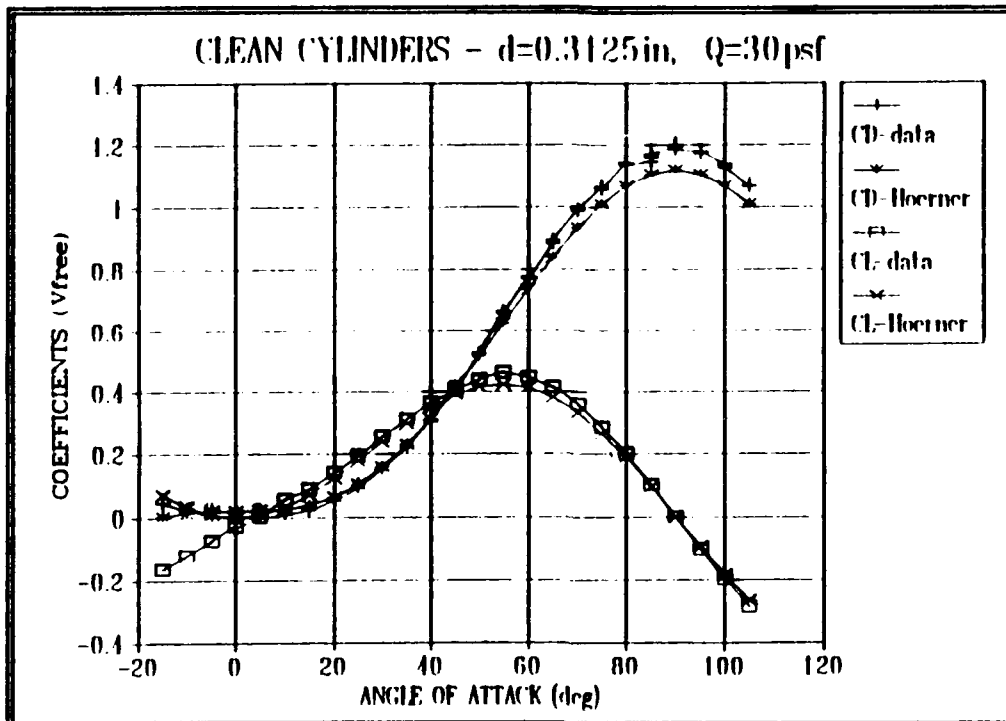
Figure 5.1 C_D, C_L, Hoerner vs AOA
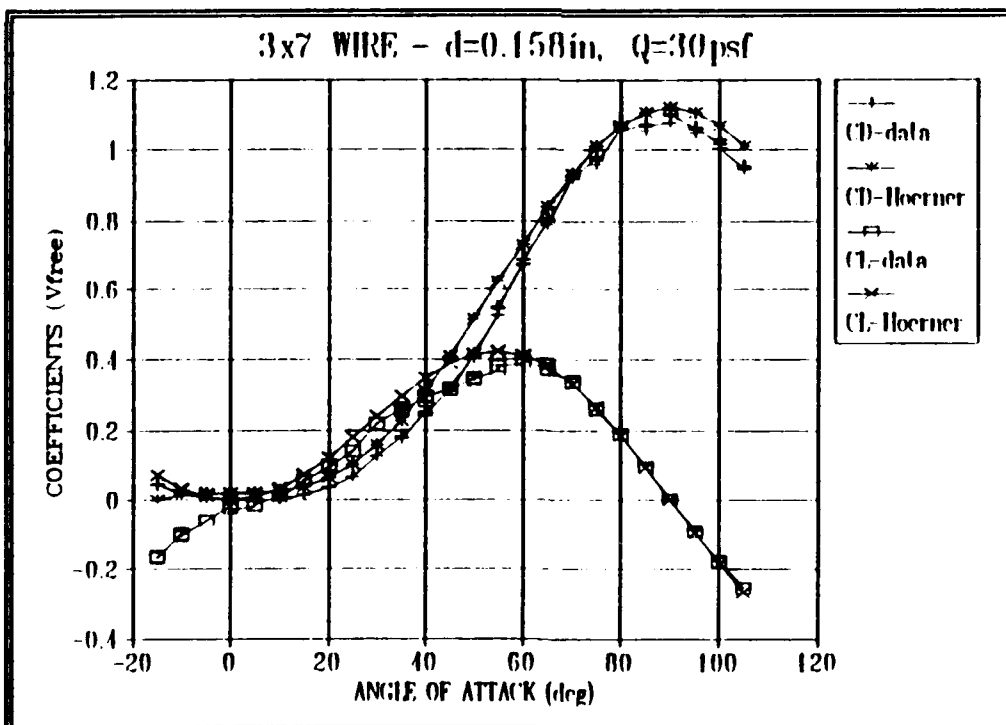
Figure 5.2 C_D, C_L, Hoerner vs AOA

42
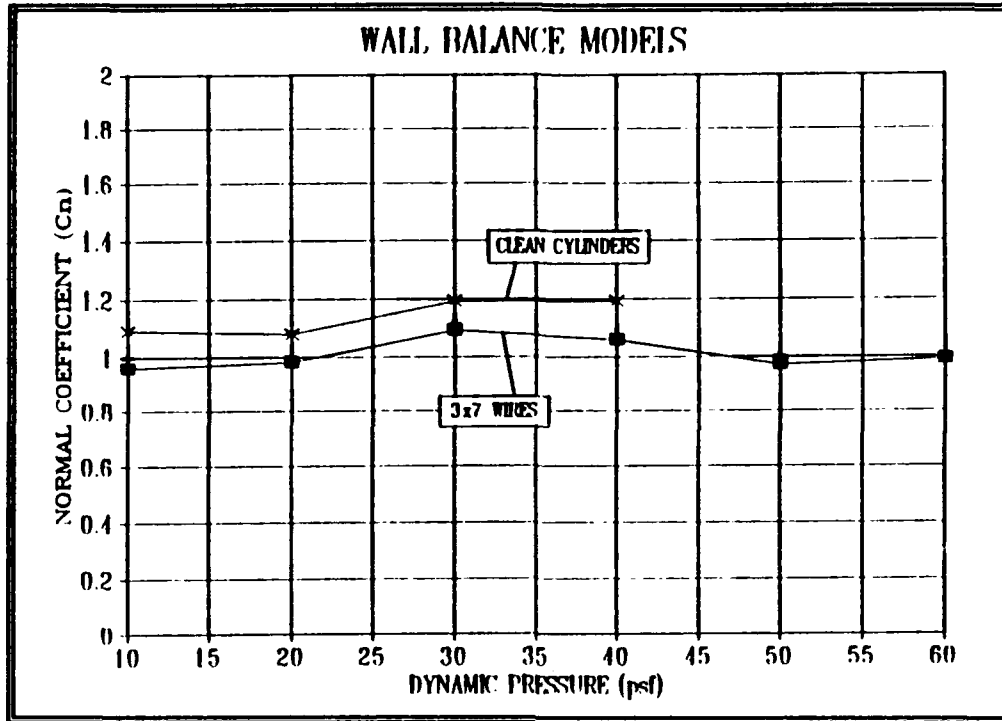
Figure 5.3 Wall Balance C_N vs Q

slight variation of C_N with respect to Q was observed. The highest values of C_N, at

Q=30 lb_f/ft^2, were selected for further calculation with the following justifications:

1) the force coefficient of a circular cylinder of finite length is less than that for a

cylinder of infinite length [Ref.17], and 2) higher C_N values produce higher wire

tension (worse case condition) in the Clifton simulation model [Ref. 2].

Normal force coefficients calculated with respect to their normal velocity

components using equation (4.3) are presented in Figures 5.4 and 5.5. The figures

confirmed the dependence of C_N on the velocity component as presented by Hoerner

[Ref. 6]. Additionally, C_N values were constant for angles of attack above 50° for the

clean cylinder data and above 60° for the 3x7 wire data. Breakdown of correlation
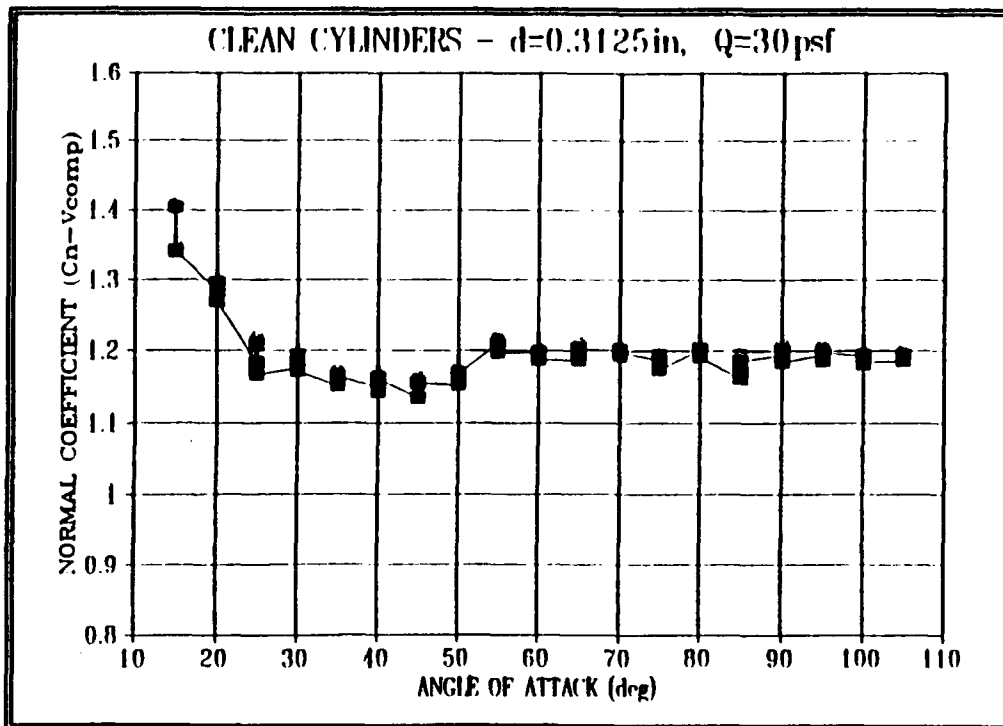
Figure 5.4 Clean Cylinders $C_{N,Vcomp}$ vs AOA
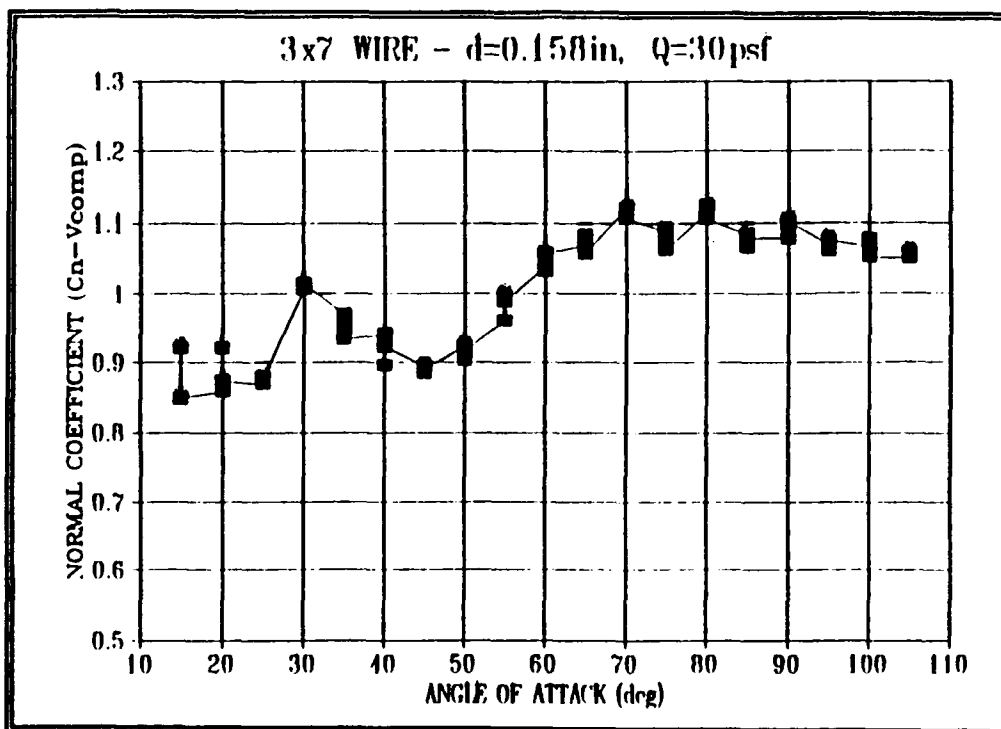
Figure 5.5 3x7 Wires $C_{N,Vcomp}$ vs AOA

44

increased as AOA decreased due to wake influences from the model stanchions. Wall balance data was considered unreliable below 20° AOA.

Analytical fit of C_N data was accomplished with emphasis on the 45° to 105° AOA range. The clean cylinder normal coefficient data was expressed by

$$C_N(\alpha) = C_{N,90°} * \sin^2\alpha \; ; \quad C_{N,90°} = 1.193 \qquad (5.2)$$

The curve fit is presented in Figure 5.6. The 3x7 wire data fit a $\sin^2\alpha$ relation at the higher AOAs but deviated low in the midrange angles of attack. After much study, the 3x7 wire data was fit by the following relationship:

$$C_N(\alpha) = C_{N,90°} * \sin^2\alpha - K * \sin^2(2\alpha) \qquad (5.3)$$

Where: $C_{N,90°} \equiv 1.09$
 $K \equiv 0.08$

Presented in Figure 5.7, correlation between data and equation (5.3) extended to AOAs from 105° down well below 45°.

2. Sting Balance Data

Normal force and moment coefficients for all runs of the clean cylinder, right, and left helix models were calculated using (4.2) and (4.4). C_N showed no variation between test runs with different mounting positions for all three models as seen in Figures 5.8, 5.9, and 5.10. The C_N versus AOA curves for the right and left helix models were identical, again indicating the dominance of normal force on long slender bodies [Ref. 18] regardless of groove direction. The use of sandpaper to trip and disrupt the flow had no influence on C_N values. Most importantly, C_N showed

45
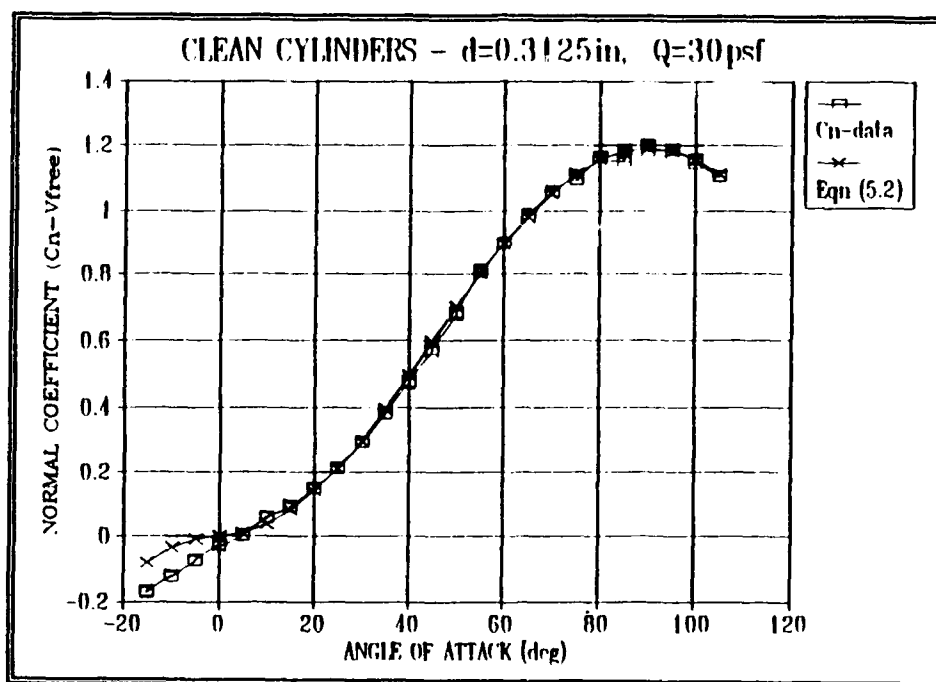
Figure 5.6   Clean Cylinders C_N vs AOA
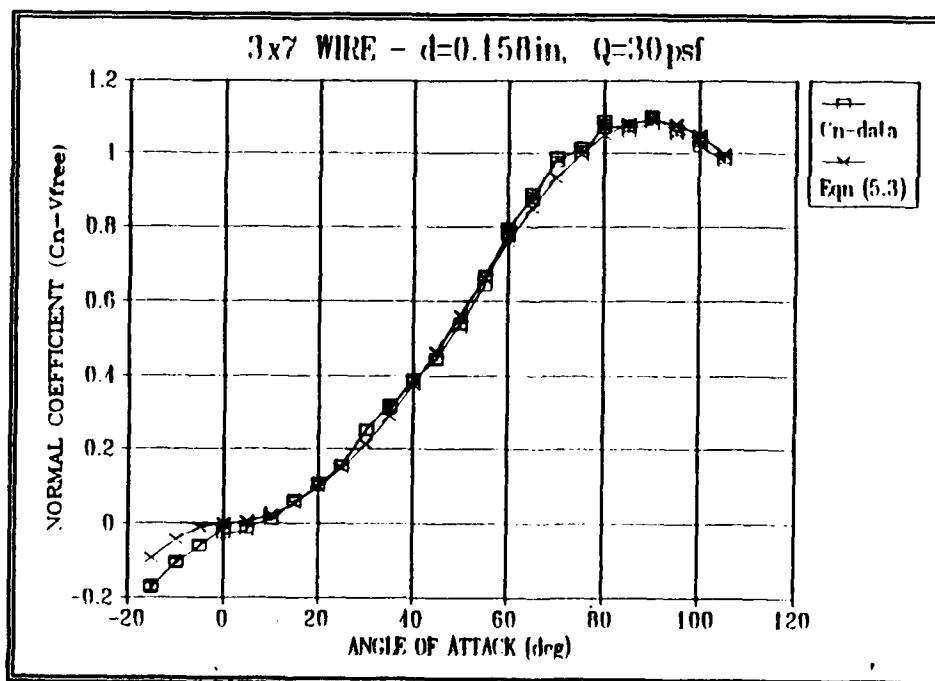
Figure 5.7   3x7 Wire C_N vs AOA

46
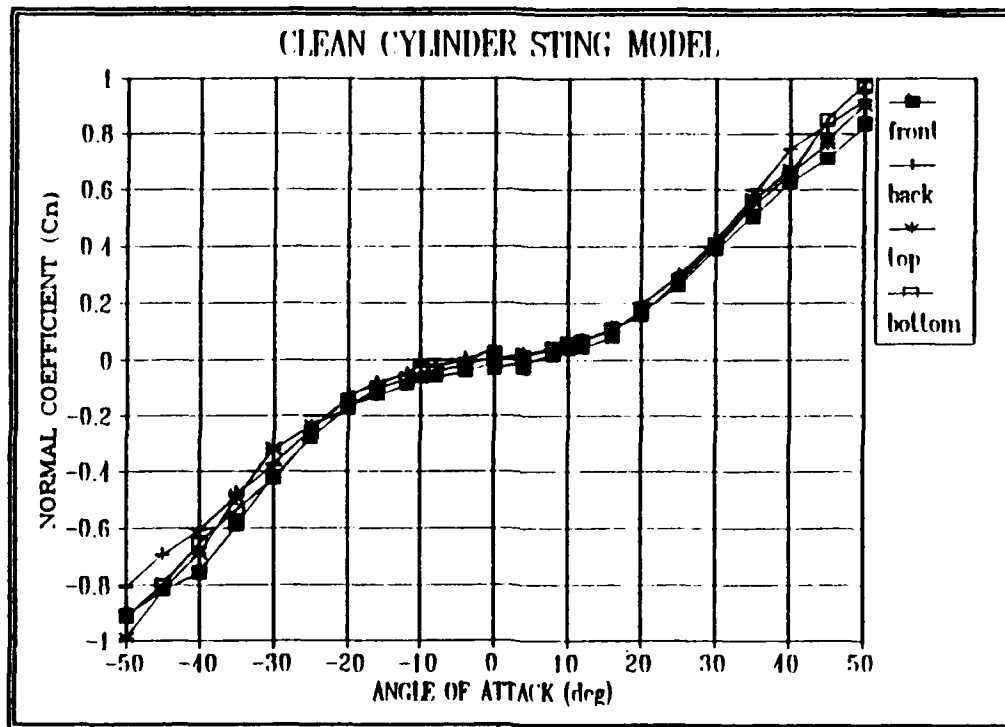
Figure 5.8 Clean Cylinder Sting Model C_N vs AOA
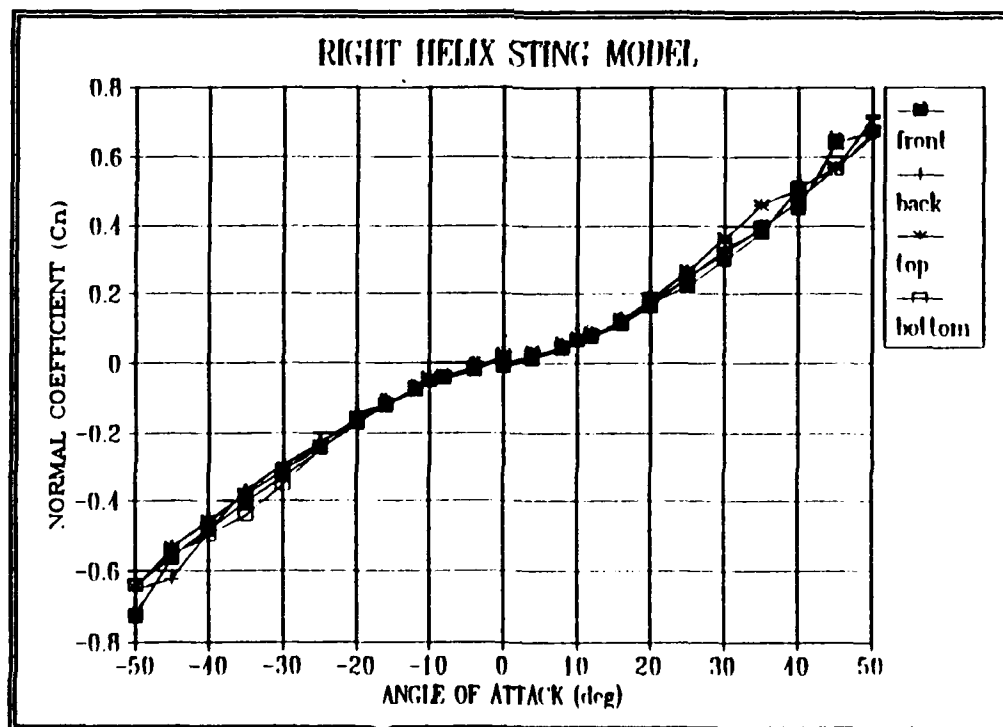
Figure 5.9 Right Helix Sting Model C_N vs AOA

47
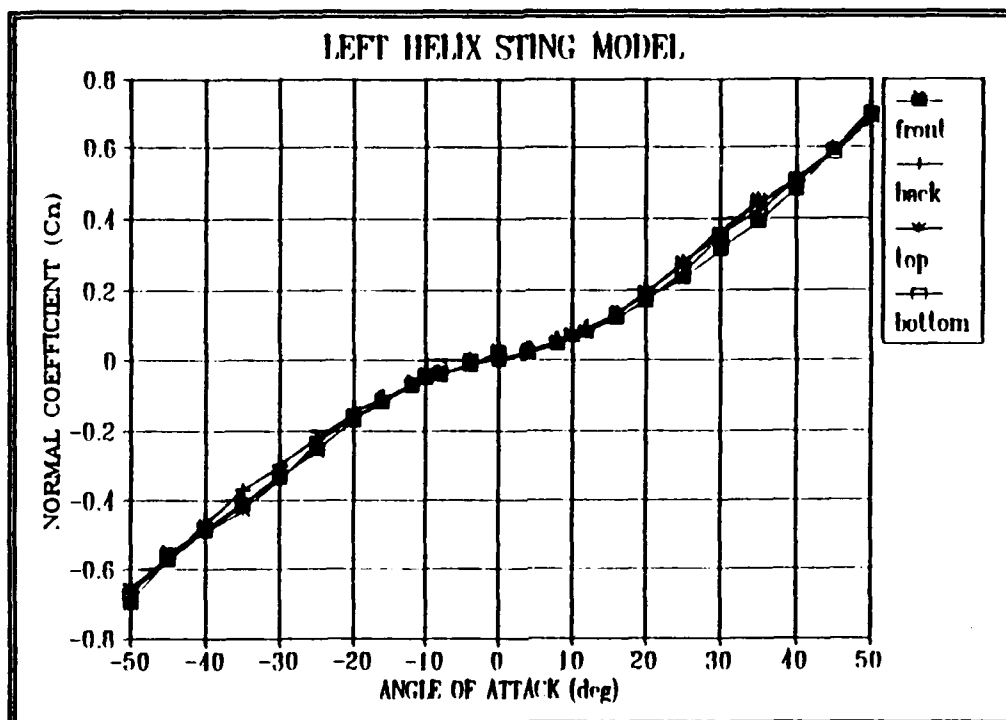
Figure 5.10 Left Helix Sting Model C_N vs AOA

no dependence on dynamic pressure at the subcritical test Reynolds numbers as presented in Figures 5.11 and 5.12 for the clean cylinder and right helix models respectively. Q independence allowed for accurate integration of the sting and wall balance data.

Integration of normal force data from the two dissimilar balance tests started by using relationships (5.2) and (5.3) generated from wall balance data. As revealed in Figure 5.13, equation (5.2) only agreed with the clean cylinder sting model in the $\pm20°$ AOA range. Sting C_N values were significantly higher at higher AOAs. Analysis of sting Cm_α and $dC_N/d\alpha$ data revealed the pitching moment center forward of the balance focal point suggesting ogive-nose influence on the normal force. C_N for sting balance models was calculated using a reference length, L, equal

48
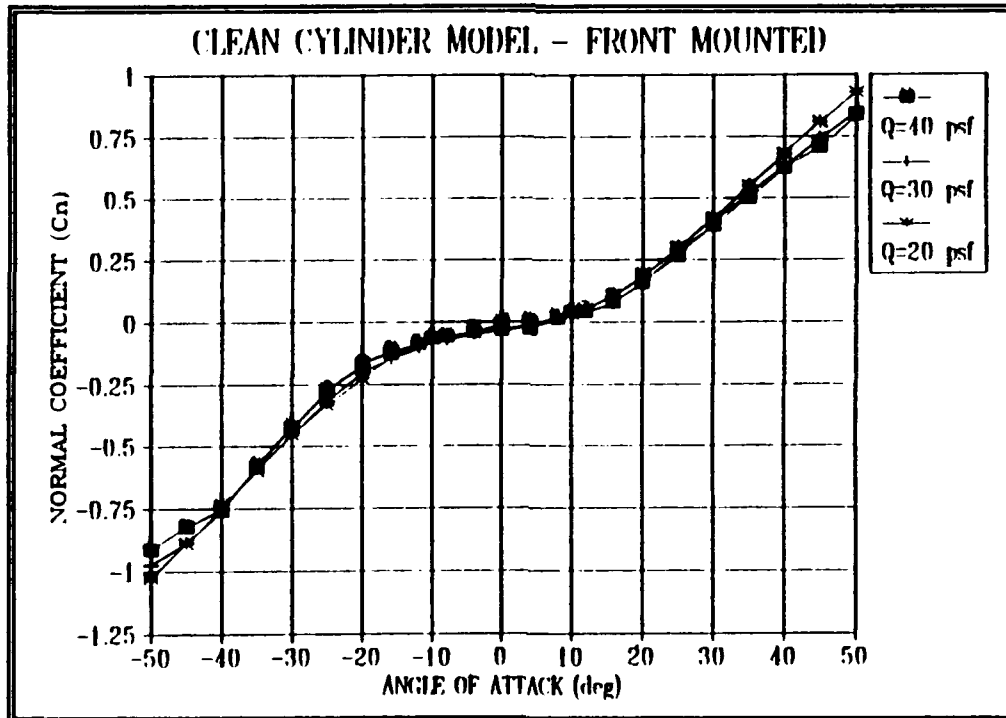
Figure 5.11 Clean Cylinder Sting Model, Q Influence on C_N
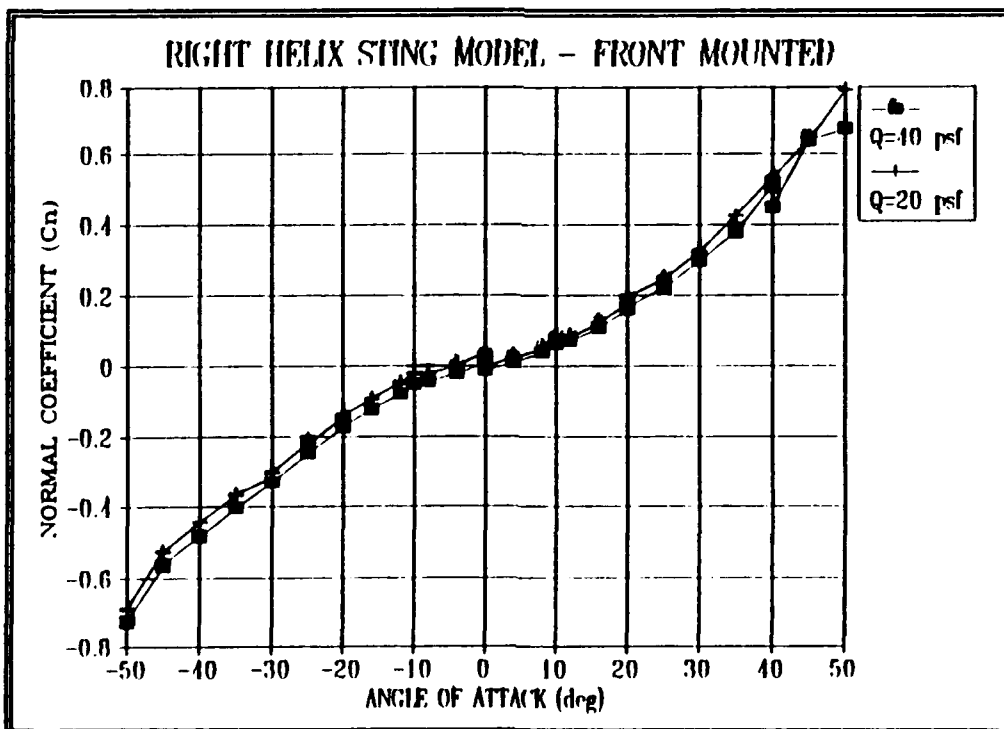
Figure 5.12 Right Helix Sting Model, Q Influence on C_N

49
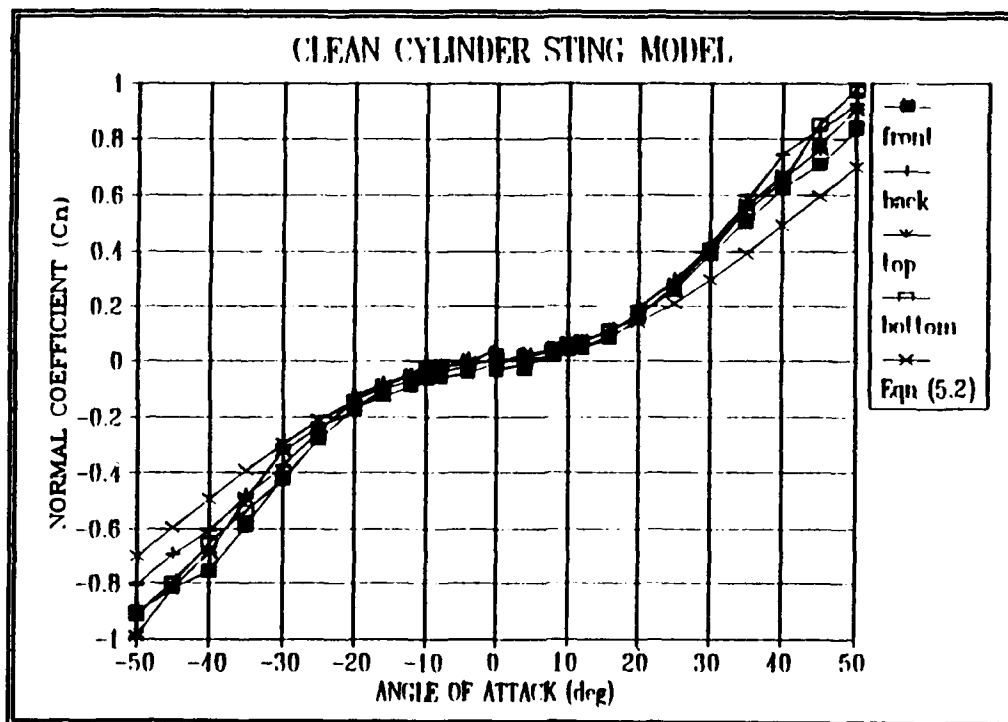
Figure 5.13 Clean Cylinder Sting Model C_N Analytical Fit Attempt

to the cylinder length and did not account for nose reference area. A change in reference area would produce just a scaling constant application to (5.2). By noting the $C_{N,45^\circ}$ value of the sting balance was 25% larger than the correct value[1] of $C_{N,45^\circ}$ from equation (5.2), a scaling constant of 1.25 was applied to (5.2) to produce

$$C_N(\alpha)_{STING} = 1.25*(1.193*\sin^2\alpha) \tag{5.4}$$

Equation (5.4) agreed with C_N data for the clean cylinder as presented in Figure 5.14. The scaling constant was extended to the right helix tests, and applied to (5.3) to yield

---

[1] From the wall balance (5.2): $C_{N,45^\circ} = 1.193*\sin^2(45^\circ) = 0.5965$

$$C_N(\alpha)_{STING} = 1.25*[1.09*\sin^2\alpha - 0.08*\sin^2(2\alpha)] \qquad (5.5)$$

Agreement of (5.5) with C_N data for the right helix model was confirmed in Figure 5.15.
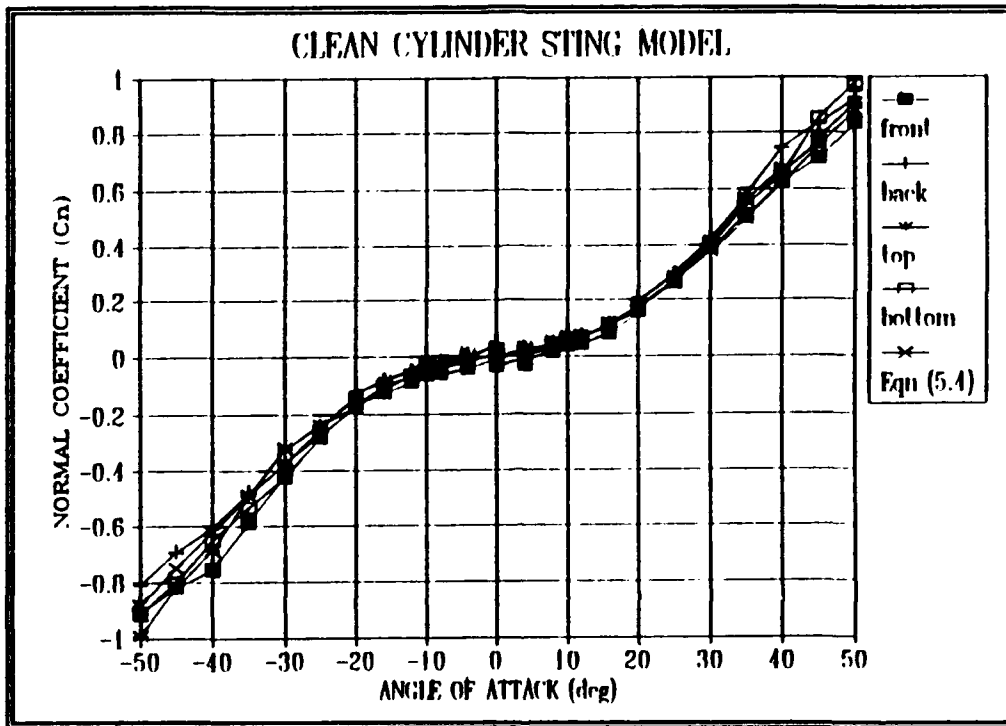
Figure 5.14 Clean Cylinder Sting Model C_N Analytical Fit

C. AXIAL FORCE COEFFICIENTS

Axial force coefficients were calculated using the appropriate form of (4.2) and axial force data from the sting balance data. Shown in Figure 5.16, C_A remained constant for low angles of attack. Over the test AOAs, C_A can be summarized by

$$C_A(\alpha) = \begin{cases} 0.017 & |\alpha| \leq 45° \\ 0.0 & |\alpha| > 45° \end{cases} \qquad (5.6)$$

The magnitude of C_A and range of AOAs was consistent with Hoerner [Ref. 6].

51
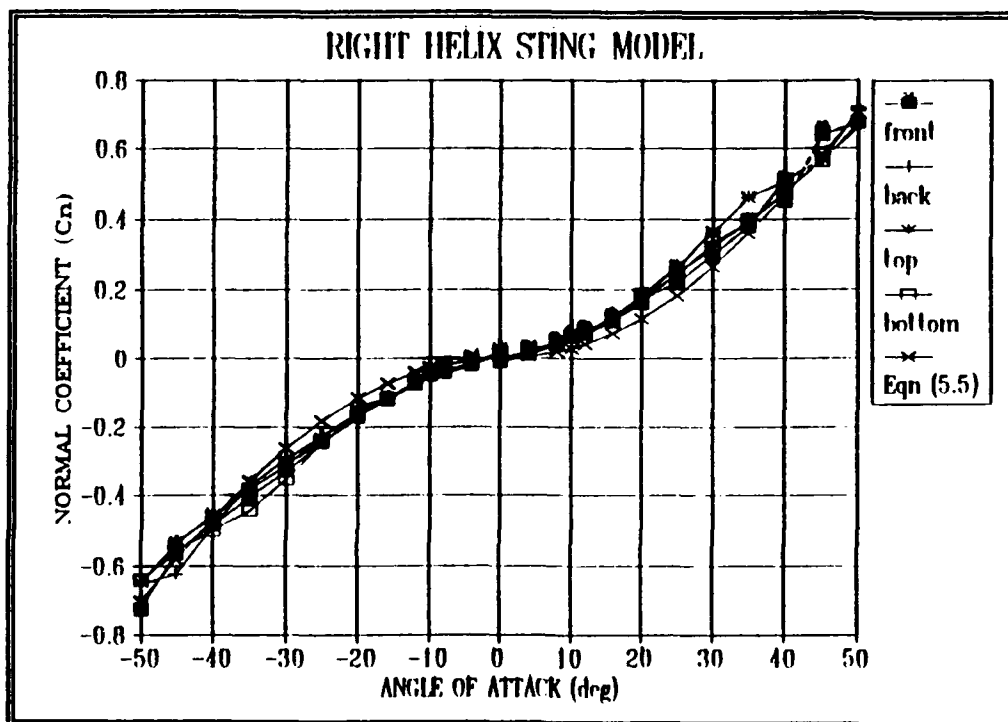
Figure 5.15 Right Helix Sting Model C_N Analytical Fit
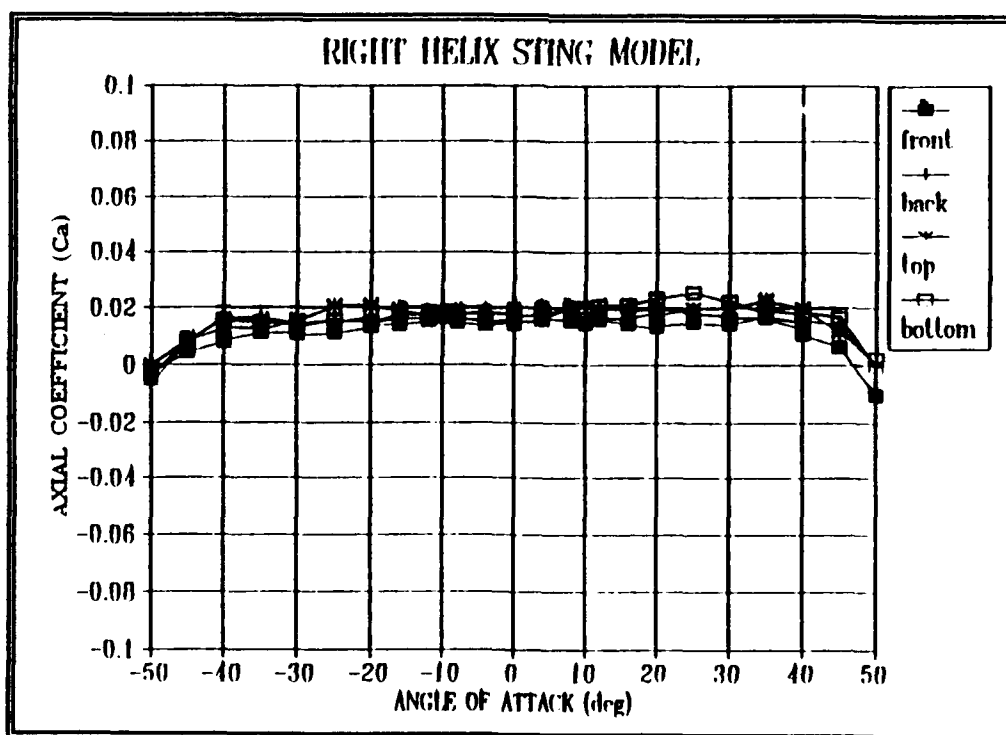
Figure 5.16 Right Helix Sting Model C_A vs AOA

52

Axial force coefficients calculated from the wall balance experiments were considered erroneous. The tare procedure did not consider the aerodynamic interference at the stanchion/wire juncture. Experimental results by Roshko [Ref. 19] revealed alterations in drag and vortex shedding frequency caused by a splitter plate in the wake of a cylinder. The wall balance models were assumed to have similar effects with stanchion/wire axial force actually less than forces from the stanchions alone. The consistent and expected value of C_A from the sting balance experiments provided added justification for neglecting wall balance C_A values.

D.   SIDE FORCE COEFFICIENTS

Side force coefficients were calculated using the appropriate form of equation (4.2) for the clean cylinder, right, and left helix sting balance models. Presented in Figures 5.17, 5.18, and 5.19, C_Y showed agreement between $\pm 20°$ for the clean cylinder model, and $\pm 12°$ for the helix models with respect to screw mounting positions. Although the 220 grit sandpaper tended to "settle" the higher C_Y values at higher AOAs for the clean cylinder, it displayed no effect on C_Y values for the helix models. This independence highlighted the strong aerodynamic influence of the helical grooves over possible asymmetric vortex shedding of the nose. As with normal force coefficients, C_Y values were independent of test dynamic pressure. Additionally, resolution of yawing moment center, within 0.5 inches of balance focus, supports using cylinder length as reference for coefficient calculations.
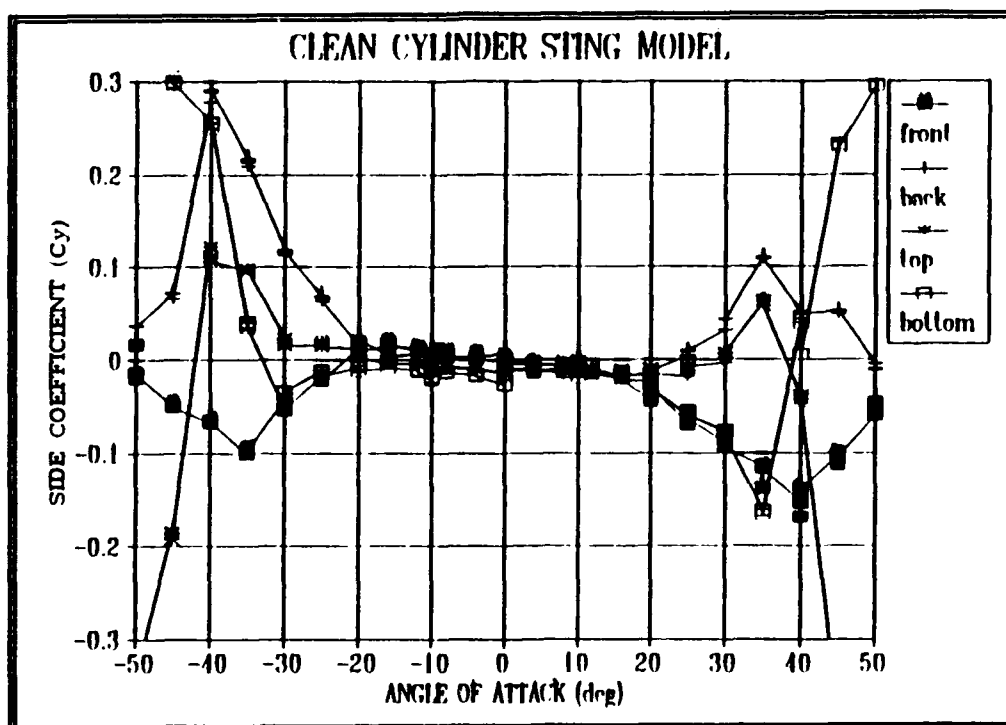
Figure 5.17 Clean Cylinder Sting Model C_Y vs AOA
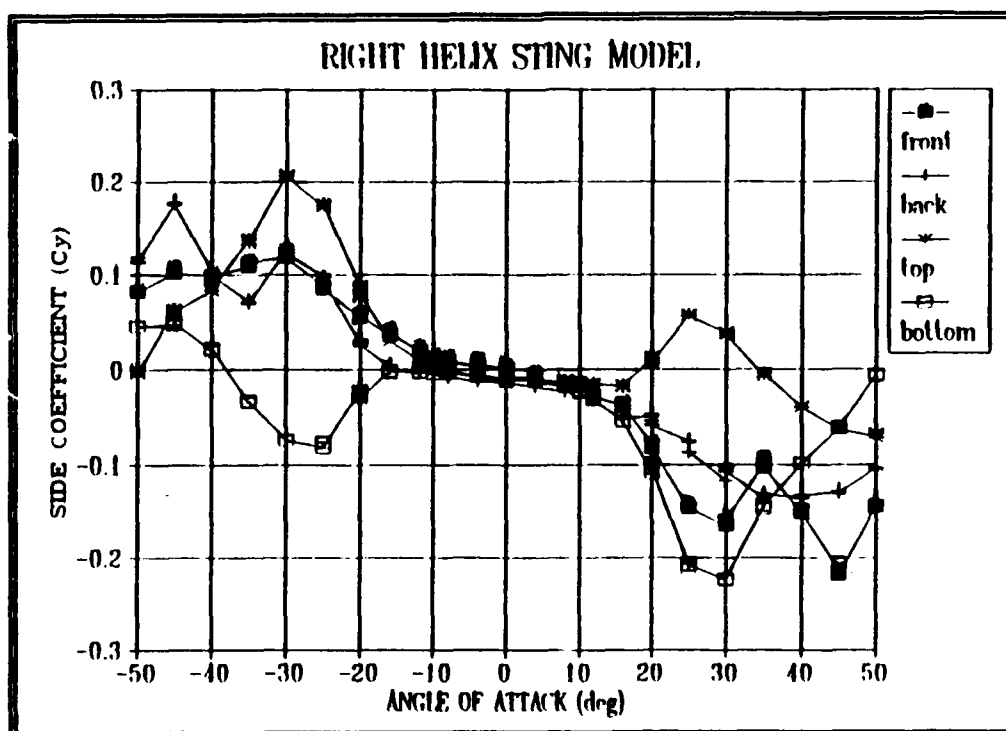
Figure 5.18 Right Helix Sting Model C_Y vs AOA

54
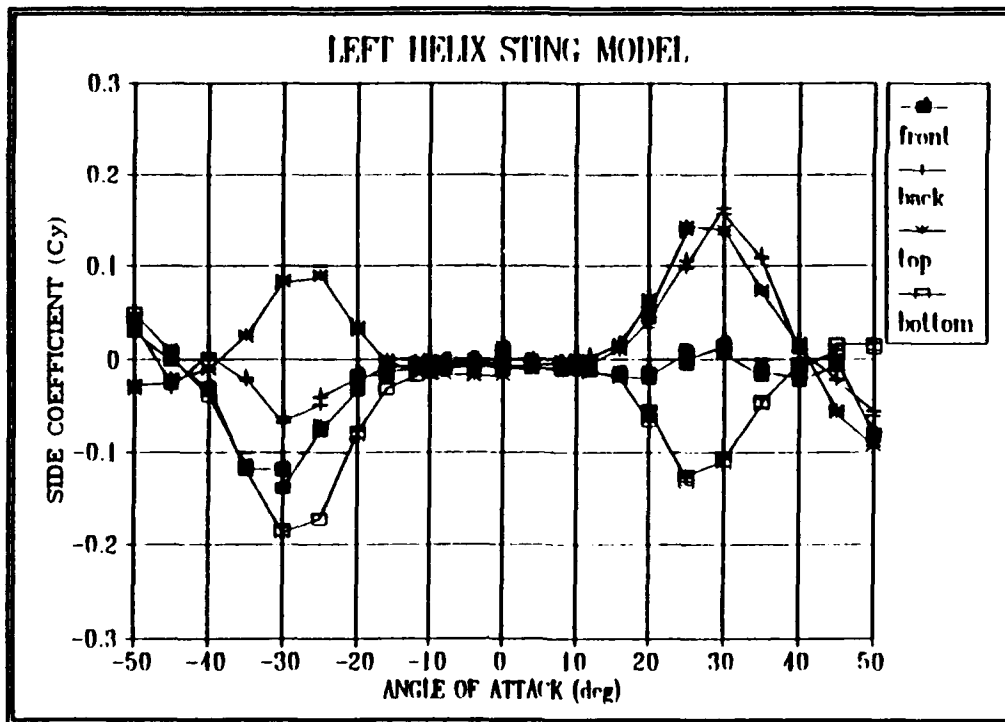
Figure 5.19 Left Helix Sting Model C_Y vs AOA

Determination of a side force relationship with respect to angle of attack for the helix model began with the baseline clean cylinder model. From Figure 5.17 for the clean cylinder,

$$\left(\frac{dC_Y}{d\alpha}\right)_{CYL} = -7.68x10^{-4} \ degs^{-1} = -0.044 \ rad^{-1} \qquad (5.7)$$

The negative bias was caused by the model mounted -1.6° nose down (-S coordinate direction). The right helix model produced a larger negative slope, and the left helix a slight positive slope as presented in Figures 5.18 and 5.19 respectively. Subtracting $(dC_Y/d\alpha)_{CYL}$ produced a net slope for each helix model.

55

$$\left(\frac{dC_Y}{d\alpha}\right)_{RT} = -0.0444 \ rad^{-1} \qquad (5.8)$$

$$\left(\frac{dC_Y}{d\alpha}\right)_{LT} = 0.0619 \ rad^{-1} \qquad (5.9)$$

Therefore, a side force, small in magnitude, was directly dependent on the helical groove direction. An analytical expression for C_Y was determined from Figure 5.18 and (5.8). Selection of a $sin(3\alpha)$ relation resulted from an observed C_Y peak around $\pm 30°$ AOA and a tendency of C_Y toward zero at $\pm 50°$ AOA. By multiplying (5.8) by $cos(3\alpha)$ and integrating, C_Y became

$$C_Y(\alpha) = \begin{cases} -0.0148*sin(3\alpha) & |\alpha| \le 60° \\ 0.0 & |\alpha| > 60° \end{cases} \qquad (5.10)$$

Equation (5.10) produced a good fit with experimental data in the $\pm 12°$ AOA range.

The model side force was hypothesized to be attributed to circulation caused by the helical grooves. Figure 5.20 shows the right helix model at 20° AOA to the flow. Orientation of the grooves would direct the flow down and around the bottom of the model inducing circulation to create a negative side force, a result supported by data. Figure 5.21 shows the opposite effect with the left helix model at 20° AOA. The circulation theory was supported with flow-visualization tests. Figure 5.22, showing the backside of the right helix model at 20° AOA, clearly showed alignment of adjacent tufts to the grooves during tunnel operation. The alignment was

56

observed at lower angles of attack only, and tuft position was dominated by direct flow at higher angles of attack.
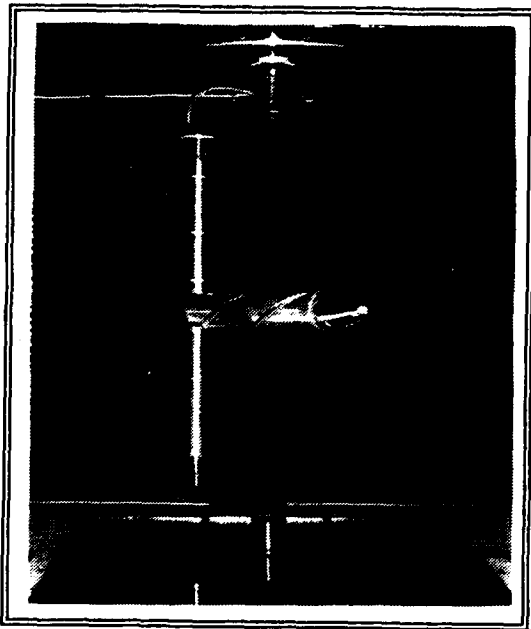
Figure 5.20 Right Helix 20° AOA
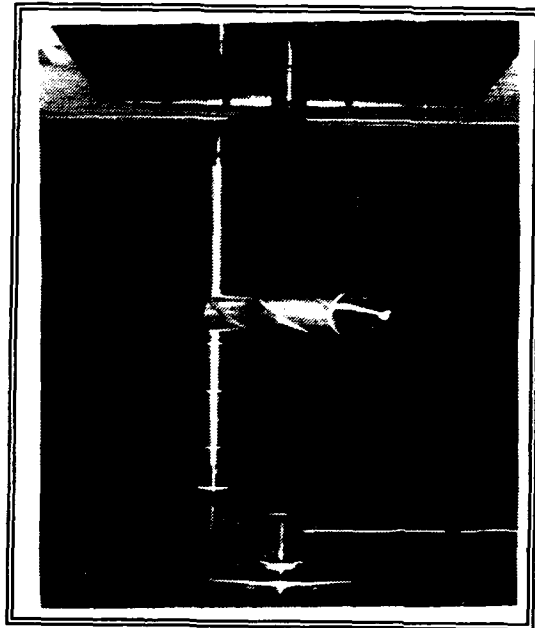
Figure 5.21 Left Helix 20° AOA
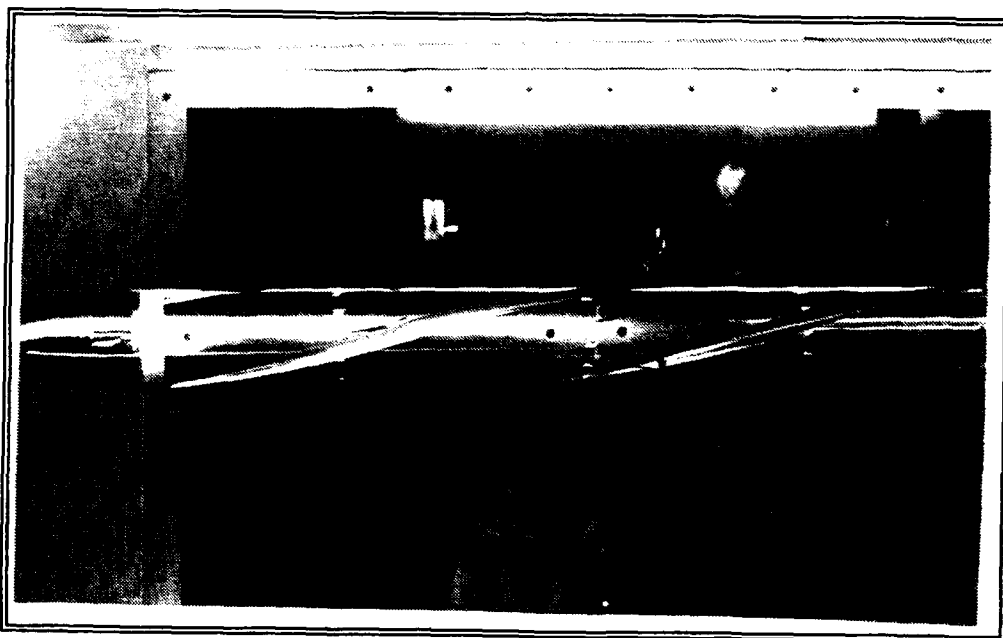
Figure 5.22 Right Helix Model in Flow Visualization, 20° AOA, Back Side

E. DROGUE MODEL DATA ANALYSIS

Force and moment coefficients were calculated for the drogue sting balance model using equations (4.5) and (4.6). Again, data showed no variation with change in dynamic pressure. C_N and C_A were transformed into C_L and C_D using

$$\begin{Bmatrix} C_L \\ C_D \end{Bmatrix}_{DROGUE} = \begin{bmatrix} \cos\alpha & -\sin\alpha \\ \sin\alpha & \cos\alpha \end{bmatrix} * \begin{Bmatrix} C_N \\ C_A \end{Bmatrix}_{DROGUE} \tag{5.11}$$

Shown in Figure 5.23, the drag coefficient showed little variation over the tested range of angles of attack. By noting $C_N = C_D$ at $\alpha = 0$,

$$C_{D_o} = 0.53 \tag{5.12}$$

Resolution of pitching moment data produced an aerodynamic center referenced to the apex at

$$\left(\frac{X}{L}\right)_{AC} = 0.7558 \tag{5.13}$$

The aerodynamic center was invariant with angle of attack. The lift coefficient, shown in Figure 5.24, was expressed by

$$C_{L,DROGUE} = 0.61 * \alpha \; (rad) \qquad |\alpha| < 45° \; (0.785 \; rad) \tag{5.14}$$

with $C_{L,\,max} = 0.42$ at $\alpha = 45°$. The drogue model displayed stall conditions at angles of attack greater than 60°.
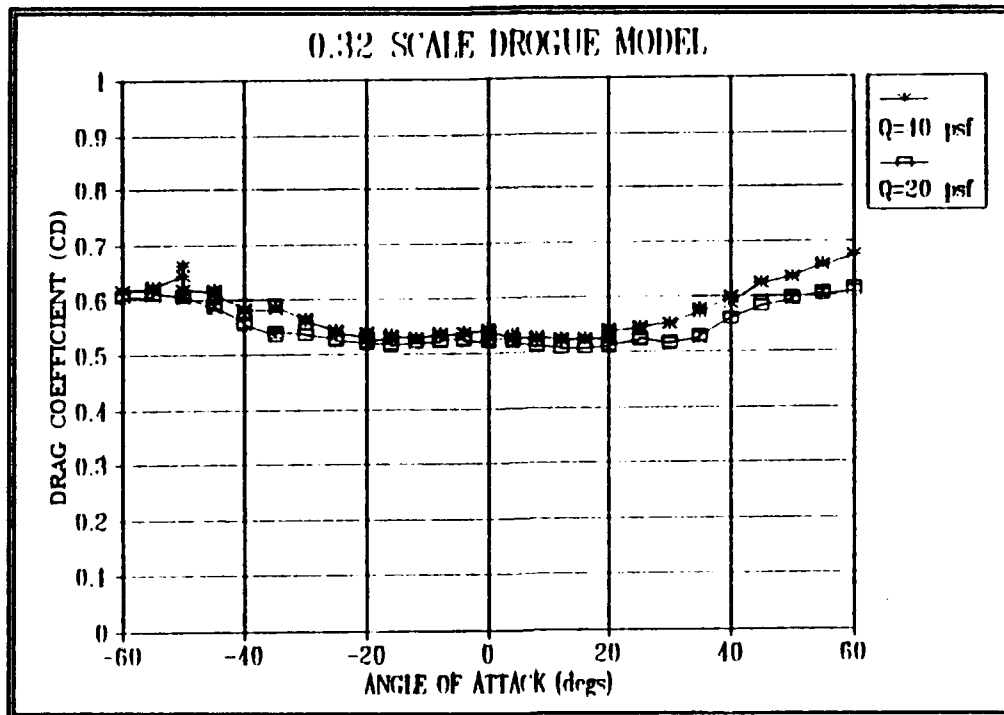
Figure 5.23   Drogue C_D vs AOA
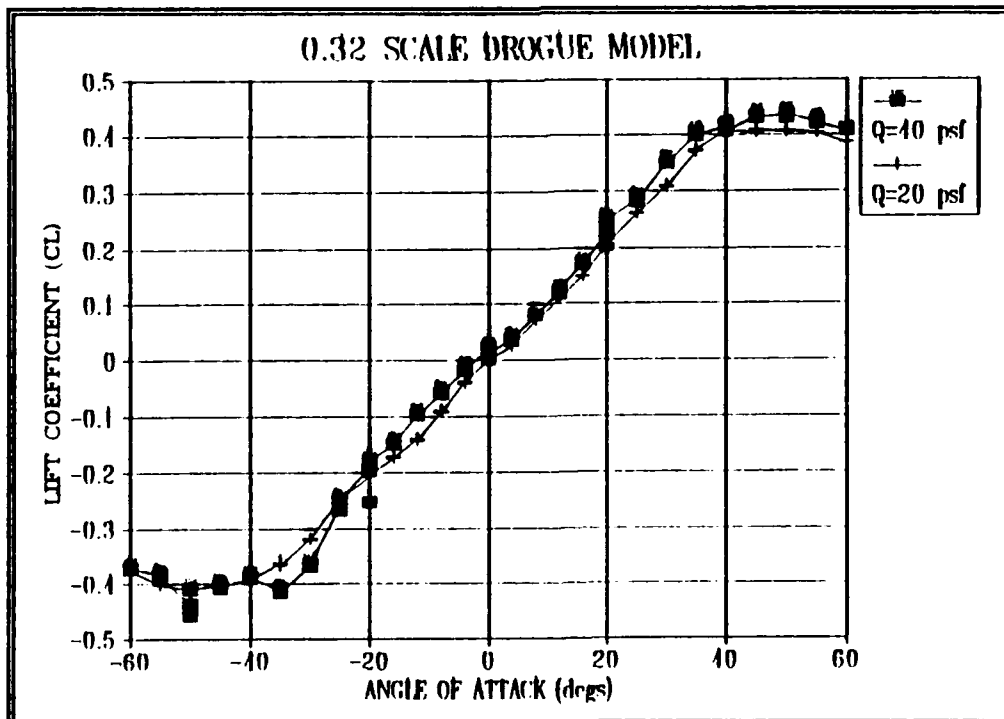
Figure 5.24   Drogue C_L vs AOA

59

F. STATIC CONDITIONS SIMULATION MODEL

1. Program Modifications

The TAC17 static equilibrium program by Clifton [Ref. 2] was modified into TAC17A using experimentally derived coefficients for the wire and drogue. Specifically, C_D and C_f of the wire were rewritten as

$$C_N(\alpha) = 1.09*\sin^2\alpha - 0.08*\sin^2(2\alpha) \qquad 0 \leq \alpha \leq 90° \qquad (5.3)$$

$$C_A(\alpha) = \begin{cases} 0.017 & 0° \leq \alpha \leq 45° \\ 0.0 & 45° < \alpha \leq 90° \end{cases} \qquad (5.6)$$

and C_Y was added with

$$C_Y(\alpha) = \begin{cases} -0.0148*\sin(3\alpha) & 0° \leq \alpha \leq 60° \\ 0.0 & 60° < \alpha \leq 90° \end{cases} \qquad (5.10)$$

For the drogue, C_{Do} was increased from 0.41 to 0.53. Previously used $dC_L/d\alpha = 2.0$ was replaced by the expression

$$C_L(\alpha) = \begin{cases} 0.61 * \alpha \ (rad) & 0.0 \leq \alpha \leq 0.785 \ rad \quad (0° \leq \alpha \leq 45°) \\ 0.42 & 0.785 < \alpha \leq 1.05 \ rad \quad (45° < \alpha \leq 60°) \\ 0.20 & 1.05 < \alpha \leq 1.57 \ rad \quad (60° < \alpha \leq 90°) \end{cases} \qquad (5.14)$$

Additionally, the aerodynamic center was moved from X/L = 0.7411 to X/L = 0.7558.

60

2. Simulation Tests

Simulations test runs were conducted to verify and validate an approximate -15° (to the right looking aft) wire trail angle observed in flight test. The conditions of observation were 18,325 feet of altitude, 156 KEAS, and 0° bank angle, into the wind. Simulation was conducted at recorded altitude and airspeed, but 3° left bank angle due to convergence constraints in the numeric model. Running TAC17A with $C_Y=0$ produced a wire trail angle = -2°, calculated from the change in radial positions of the first 100 feet of wire from the airplane. With C_Y activated, the trail angle increased to -7.6° or Δangle = -5.6° in the observed direction. TAC17A was run using $3*C_Y$, i.e. 3 * equation (5.10), with a Δangle = -14.2°. A $3*C_Y$ simulation was considered accurate because of the following conditions: a) the flight-test-observed trail angle was quantified visually, not measured from instrumentation, b) the experimental model represented only 1.4 inches and 0.75 revolutions of a 20,290 foot wire with 130,200 revolutions, and c) a finite-length circular cylinder produces a smaller force coefficient than one of infinite length [Ref. 17].

Comparison of simulation conditions at 3° bank angle was conducted with the TAC17A improvement showing some large differences with its TAC17 predecessor. Of significant interest were the variation of wire radial position, angle of attack, and tension, presented in Figures 5.25, 5.26, and 5.27 respectively. The large influence of C_Y on radial position was dramatically evident, even with small amplitudes of C_Y. The changes in wire and drogue force coefficients doubled the

wire angle of attack increasing all force coefficients due to their sine relationships. The increase in coefficients increased the wire tension at the towplane approximately 25%. The predicted static tension at the towplane was well within safety margins for avoiding wire failure [Ref. 2].

Simulation tests were also conducted in the operational conditions of 18,325 feet altitude, 156 KEAS, and 34° bank angle. Comparison of simulation conditions again produced significant differences between the TAC17A and TAC17 models. The experimental coefficients for the drogue, and C_N for the wire, produced the greatest changes as shown by wire radial in Figure 5.28 and angle of attack in Figure 5.29. Inclusion of C_Y and $3*C_Y$ showed little variation from the NO C_Y TAC17A simulation. The influence of C_N has doubled the wire length displayed to AOAs greater than 60° increasing the C_N force. The increase in forces again increased the wire tension at the towplane, from 800 lb_f to 980 lb_f (22.5%). The major improvement from TAC17A's changes came from the increased altitude range of the wire as shown in Figure 5.30. The increased z coordinate range increased the verticality from 55% to 73%. Verticality is defined as "the altitude of the towplane less the altitude of the drogue divided by the length of the wire" [Ref. 2]. The increased static verticality directly translates into increased antenna capability. Preliminary evaluation of experimental coefficients in the Clifton dynamic simulation model showed a decrease of deviation from flight test data from approximately 10% low to 5% high.

3x7 WIRE RADIAL POSITIONS
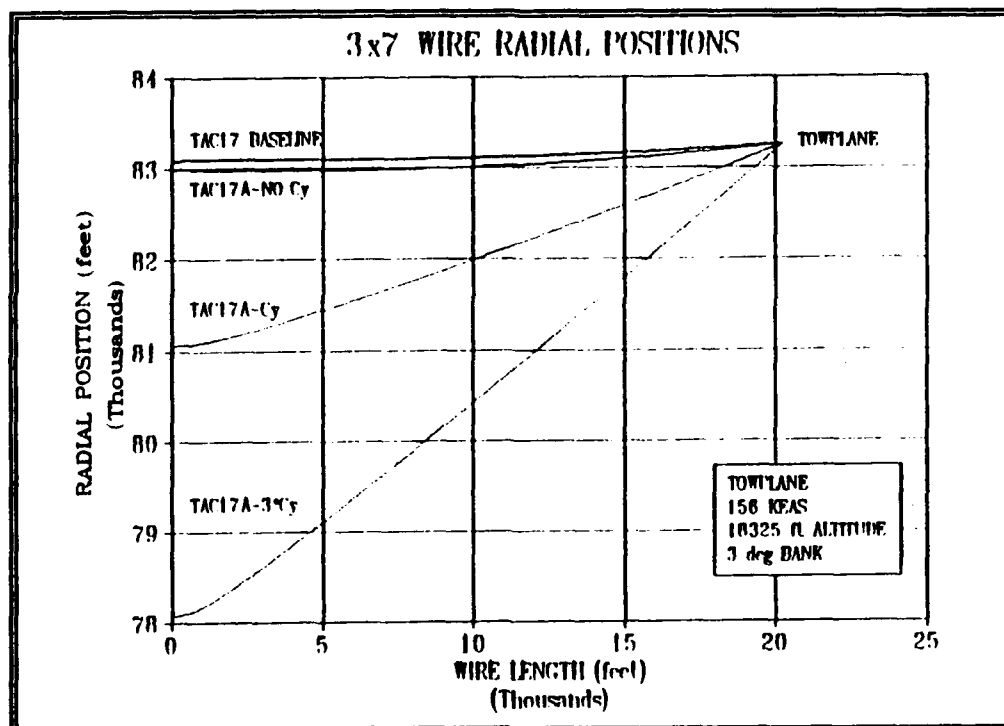
Figure 5.25 C_Y Influence on Radial Position

3x7 WIRE ANGLE OF ATTACK
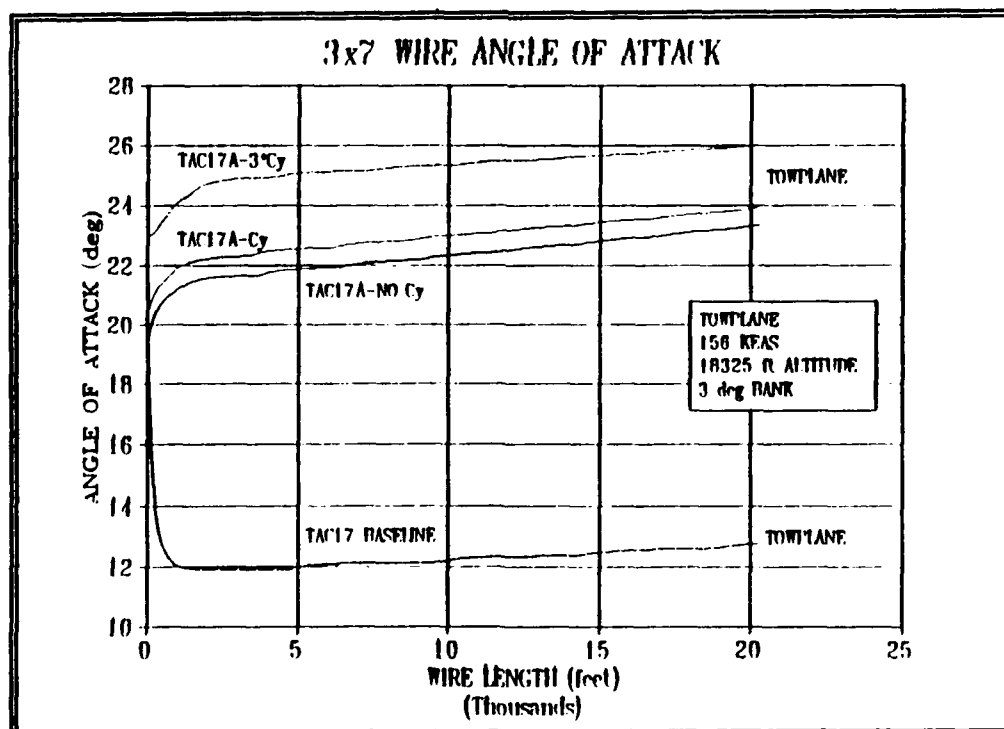
Figure 5.26 C_Y Influence on AOA

63
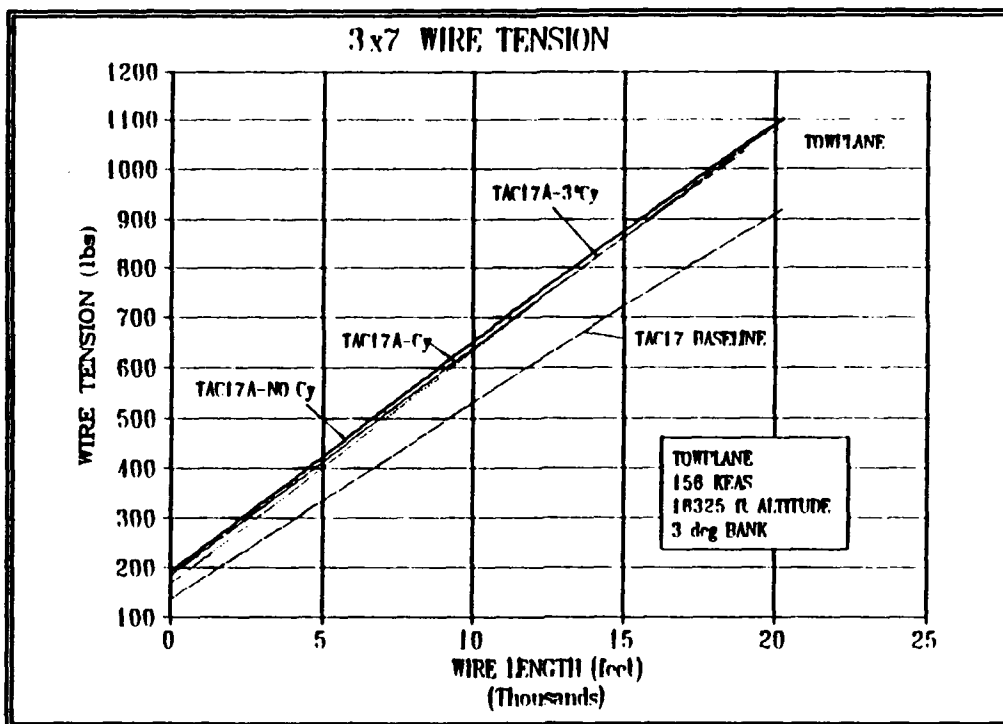
Figure 5.27 C_Y Influence on Wire Tension
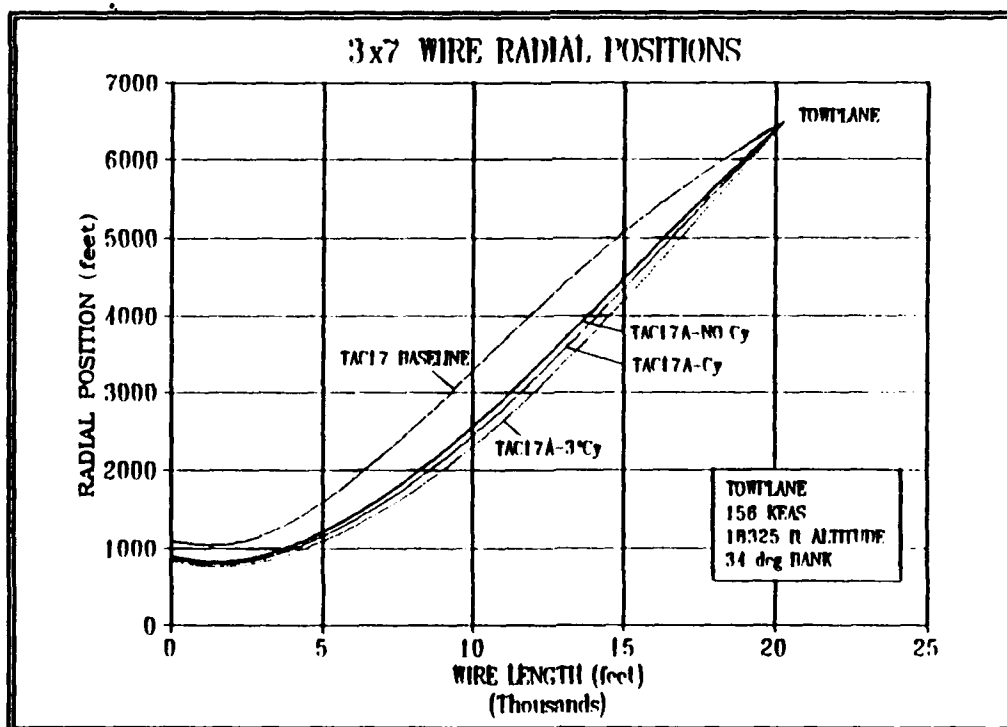
Figure 5.28 C_Y Influence on Radial Position, Operational

64

3x7 WIRE ANGLE OF ATTACK

ANGLE OF ATTACK (deg)

90
80
70
60
50
40
30
20
10

TAC17A-NO Cy

TAC17A-Cy

TAC17A-3*Cy

TAC17 BASELINE

TOWPLANE
156 KEAS
18325 ft ALTITUDE
34 deg BANK

TOWPLANE

TOWPLANE

0   5   10   15   20   25

WIRE LENGTH (feet)
(Thousands)
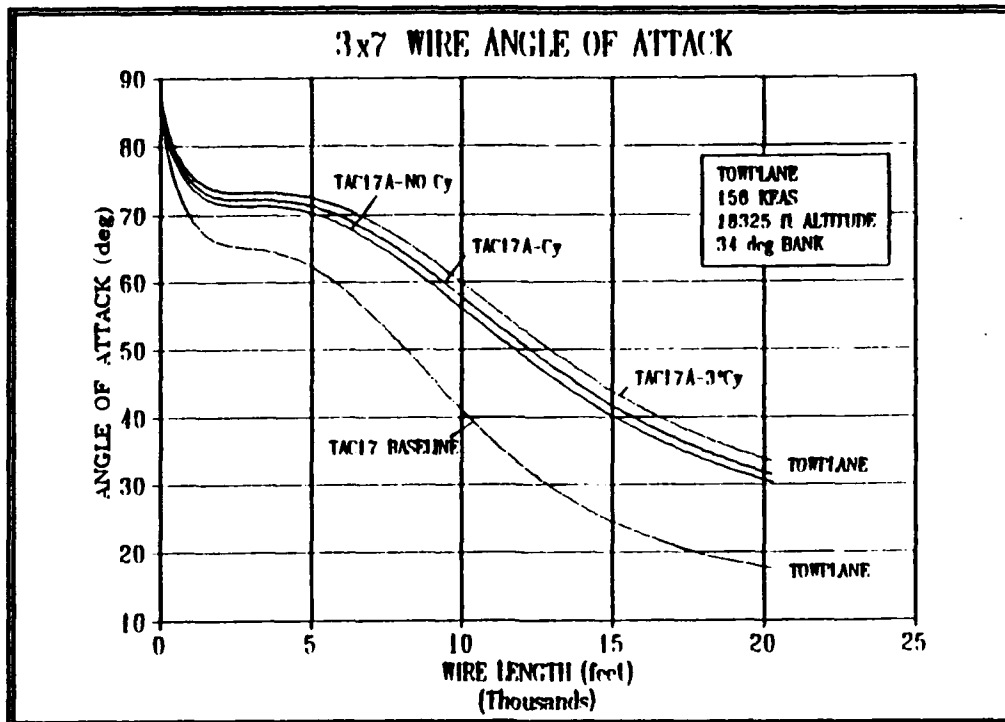
Figure 5.29 C_Y Influence on AOA, Operational

3x7 WIRE Z POSITIONS

Z COORDINATE POSITION (feet)
(Thousands)

20
18
16
14
12
10
8
6
4
2
0

TOWPLANE

TAC17 BASELINE

TAC17A-NO Cy

TAC17A-Cy

TAC17A-3*Cy

TOWPLANE
156 KEAS
18325 ft ALTITUDE
34 deg BANK

0   5   10   15   20   25

WIRE LENGTH (feet)
(Thousands)
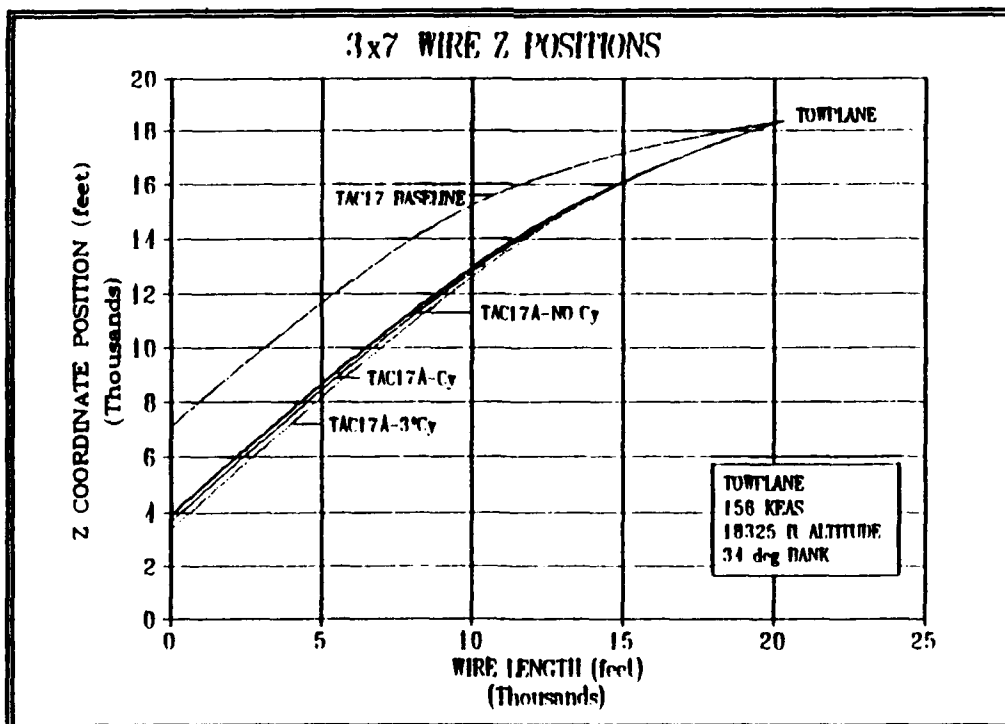
Figure 5.30 C_Y Influence on Wire Z Position, Operational

VI. CONCLUSIONS AND RECOMMENDATIONS

The experimentally derived force coefficients of a wire with a helical groove behaved similarly to historical relationships with respect to normal and axial forces. Specifically for the tested 3x7 wire

$$C_N(\alpha) = 1.09*\sin^2\alpha - 0.08*\sin^2(2\alpha) \qquad 0 \le \alpha \le 90°$$

$$C_A(\alpha) = \begin{cases} 0.017 & 0° \le \alpha \le 45° \\ 0.0 & 45° < \alpha \le 90° \end{cases}$$

Discovered in this experimentation was a side force coefficient, small in magnitude and present at lower angles of attack. Resulting from groove induced flow circulation and dependent on groove direction, the side force coefficient for the 3x7 wire was expressed as

$$C_Y(\alpha) = \begin{cases} -0.0148*\sin(3\alpha) & 0° \le \alpha \le 60° \\ 0.0 & 60° < \alpha \le 90° \end{cases}$$

For the system drogue, the experimental drag coefficient and the aerodynamic center, referenced to the apex, were found to be invariant with angle of attack as

$$C_{D_o} = 0.53, \qquad \left(\frac{X}{L}\right)_{ac} = 0.7558$$

Finally, the lift coefficient can be expressed as

66

$$C_L(\alpha) = \begin{cases} 0.61 * \alpha \ (rad) & 0.0 \le \alpha \le 0.785 \ rad \quad (0° \le \alpha \le 45°) \\ 0.42 & 0.785 < \alpha \le 1.05 \ rad \quad (45° < \alpha \le 60°) \\ 0.20 & 1.05 < \alpha \le 1.57 \ rad \quad (60° < \alpha \le 90°) \end{cases}$$

The wire force coefficients, coupled with the experimentally determined drogue coefficients, allowed for refinement of a previous static simulation model providing a closer relation between simulation prediction and flight test data. Additionally, inclusion of the experimental side force coefficient explained an observed phenomena, and revealed the impact the coefficient has over the "infinite" length of wire presented in this application.

Further research with helically grooved infinite cylinders at subcritical Reynolds numbers is recommended. Specific recommendations include:

- the use of more sensitive balances with expected forces at least 50% of balance resolution vice 2%,

- models with more helical revolutions,

- models with different helical angles,

- a detailed wake study, and

- quantification of wire trail angles through instrumented flight test.

Additionally, the computational challenge to represent the three dimensional forces on a wire should be undertaken to model generic helically grooved wires and reduce expensive flight test experimentation.

LIST OF REFERENCES

1.   Glauert, H., *The Form of a Heavy Flexible Cable Used for Towing a Heavy Body Below an Airplane*, R and M 1592, British Aeronautical Research Committee, England, Feb. 1934.

2.   Clifton, J., *Modeling and Control of a Trailing Wire Antenna Towed by an Orbiting Aircraft*, Doctoral Dissertation, U.S. Naval Postgraduate School, Monterey, CA, Sept. 1992.

3.   Bertin, J., Smith, M., *Aerodynamics for Engineers*, 2nd Edition, Prentice-Hall, Inc., 1989.

4.   Kuethe, A., Chow, C., *Foundations of Aerodynamics: Bases of Aerodynamic Design*, 3rd Edition, John Wiley & Sons, Inc., 1976.

5.   Relf, E., Powell, C., *Tests on Smooth and Stranded Wires Inclined to the Wind Direction, and a Comparison of Results on Stranded Wires in Air and Water*, R and M 307, British Aeronautical Research Committee, England, Jan. 1917.

6.   Hoerner, S., *Fluid-Dynamic Drag*, Published by the Author, 1958.

7.   Bootle, W., *Forces on an Inclined Circular Cylinder in Supercritical Flow*, AIAA Journal, Vol. 9, No. 3, p. 514-516, Mar. 1971.

8.   Almosnino, D., Rom, J., *Lateral Forces on a Slender Body and Their Alleviation at High Incidence*, Journal of Spacecraft, Vol. 18, No. 5, p. 393-400, Sept.-Oct. 1981.

9.   Reding, J., Ericsson, L., *Re-examination of the Maximum Normalized Vortex-Induced Side Force*, Journal of Spacecraft, Vol. 21, No. 5, p. 433-440, Sept.-Oct. 1984.

10.   Murthy, V., Rose, W., *Detailed Measurements on a Circular Cylinder in Cross Flow*, AIAA Journal, Vol. 16, No. 6, p. 549-550, Jun. 1978.

11.   *Laboratory Manual for Low-Speed Wind Tunnel Testing*, Department of Aeronautics and Astronautics, Naval Postgraduate School, Monterey, CA, Aug. 1989.

12.   Kersh, J., *Lift Enhancement using Close-Coupled Canard/Wing Vortex Interaction*, Master's Thesis, U.S. Naval Postgraduate School, Monterey, CA, Dec. 1990.

13.   *MC-MIO-16 User Manual*, National Instrument Corp., Jan. 1989.

14.   Yuan, Chih-Chung, *The Effects of Forebody Strakes on Asymmetric Vortices on a Vertically Launched Missile*, Master's Thesis, U.S. Naval Postgraduate School, Monterey, CA, Sept. 1990.

15.   Ericsson, L., Reding, J., *Asymmetric Flow Separation and Vortex Shedding on Bodies of Revolution*, Progress in Astronautics and Aeronautics, Vol. 141, Chap. 10, AIAA, 1992.

16.   Pacific Instruments, *Model 8255/6 Transducer Amplifier Operation and Maintenance Manual*, 860814-MAN1007, Concord, CA, 1986.

17.   Allen, H., *Estimation of the Forces and Moments acting on Inclined Bodies of Revolution of High Fineness Ratio*, NACA RM A 9I26, Nov. 1949.

18.   Anderson, W., *Dynamic Instability of a Cable in Incompressible Flow*, AIAA Paper No. 73-395, Mar. 1973.

19.   Roshko, A., *On Development of Turbulent Wakes from Vortex Streets*, NACA TN 2913, Mar. 1953.

APPENDIX A: WALL BALANCE CALIBRATION

An external, cylindrical, reflection-plane (wall) balance was used to measure forces and moments of the wire at the higher angles of attack. The flush mounted balance was designed with two pairs of strain gage bridges orthogonally mounted on flexure links separated vertically by 26.5 inches. Each bridge circuit had four active legs for automatic temperature compensation. The lower bridge A, and the upper bridge B, each output an axial and normal voltage (E_{aa}, E_{ba}, E_{an}, E_{bn}). The balance coordinate system consisted of the axial direction parallel with tunnel walls and flow, and normal direction perpendicular to the tunnel walls while at $0°$ angle of attack.

Calibration was conducted using the acquisition system with amplifier gain set at 1000, and MC-MIO-16L-9 board gain at 1, resulting in a 4.88 mV resolution. Calibration procedure consisted of loading a rig mounted on the aluminum plate in the normal and axial directions at two different heights. Figure A.1 and A.2 present the calibration rig loaded normally at a height equal to 7.75 inches above the tunnel floor. The pulley apparatus translated vertically to maintain level attitude of the cable. Prior to loading the rig, the amplifiers and signal conditioners were zeroed. The span control on the signal conditioner was set to 10 V_{DC} -0.05 V_{DC} for each channel. Amplifiers were shorted and output and input zeroed at an amplifier gain of 1 and 1000, respectively. Finally, the shorting plugs were removed, the channels zeroed, and the acquisition program started. Weights, measured to 0.001 lb_f

accuracy, were suspended from the rig. Measurements of E_{aa}, E_{ba}, E_{an}, E_{bn} were recorded as weights were incremented and decremented. Care was taken to relieve the load on the cable when changing the weights to prevent a displayed balance hysteresis.
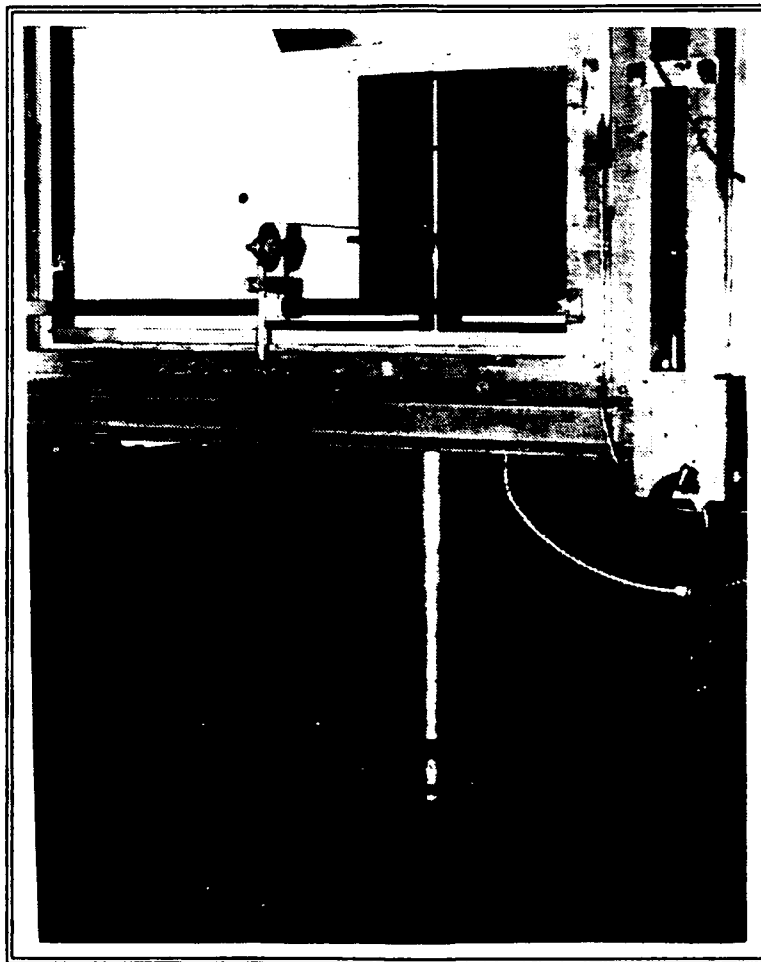
Figure A.1 Wall Balance Calibration Rig
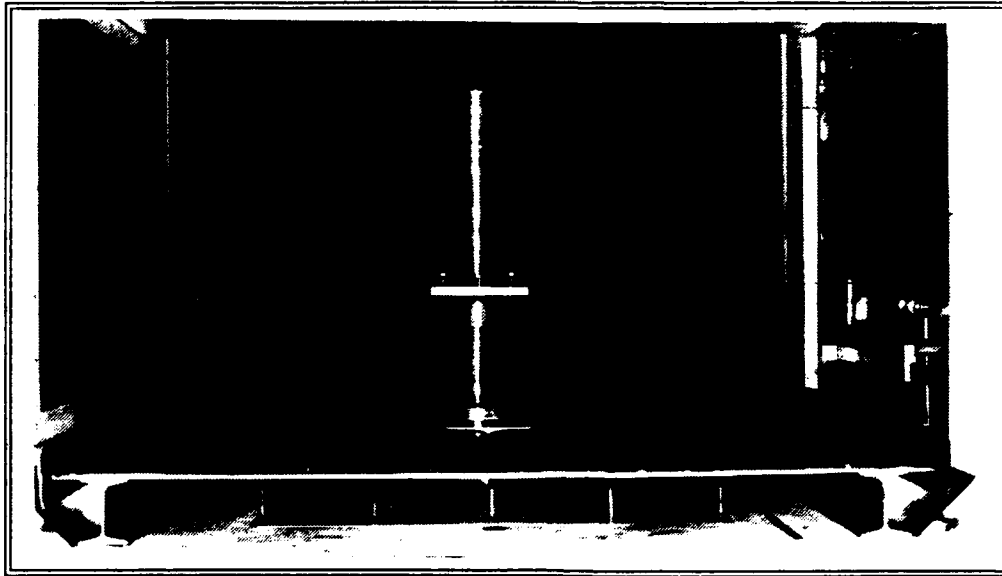
Figure A.2 Wall Balance Calibration Rig

Four calibration runs were conducted, two in the normal and two in the axial

direction, with the cable at 10.5625 and 7.75 inches of height referenced to the tunnel

floor. The data from the four runs were imported into QuattroPro 3.0 for analysis.

Plots of balance voltage versus calibration load are presented in Figures A.3. A.4,

A.5, and A.6. The figures reveal the linearity expected from elastic loading, and the

small interaction between channel bridges (cross-talk). Figures A.5 and A.6 also

reveal the reduced sensitivity in the E_{ba} channel due to replacing two legs of the

bridge circuit on a questionable flexure link (i.e. possibly buckled) by constant

reference resistance gages.   Linear regression was conducted in QuattroPro to

determine $d\Delta E/dload$ for each of the 16 conditions.   The maximum standard

deviation of the slopes was 1.5%.
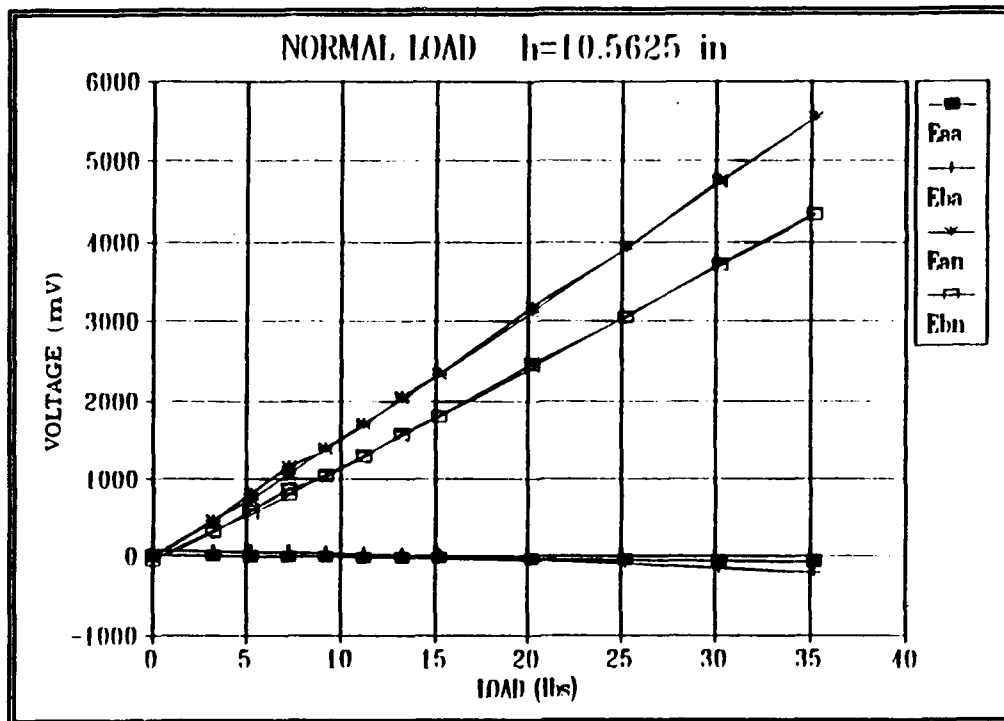
Figure A.3 Calibration Voltage vs Normal Load, h = 10.5625 inches
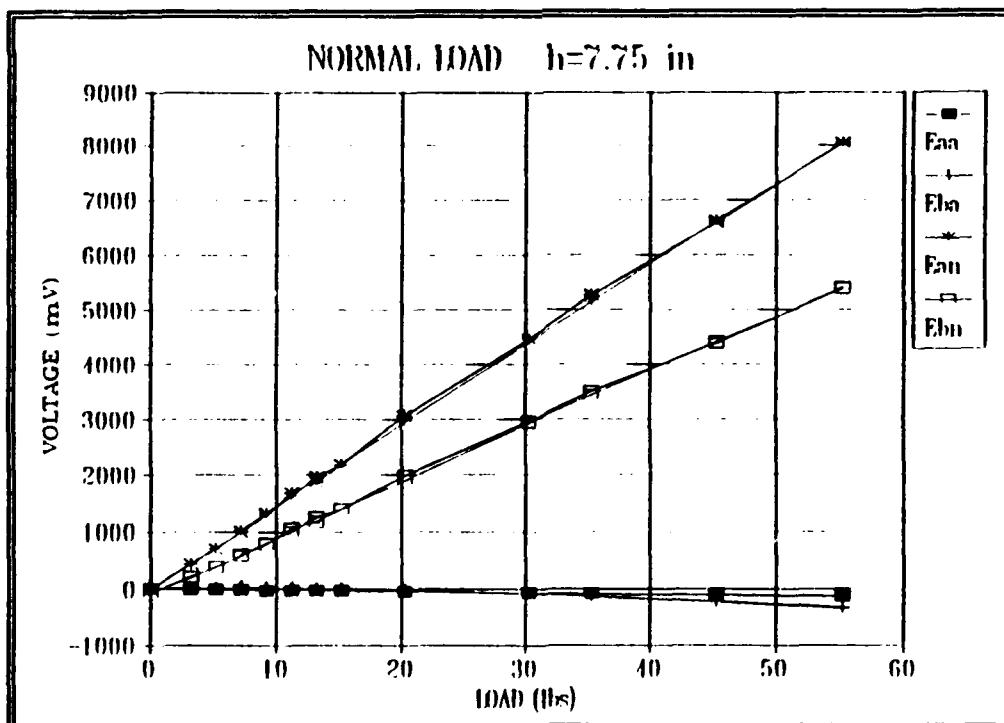
Figure A.4 Calibration Voltage vs Normal Load, h = 7.75 inches

73
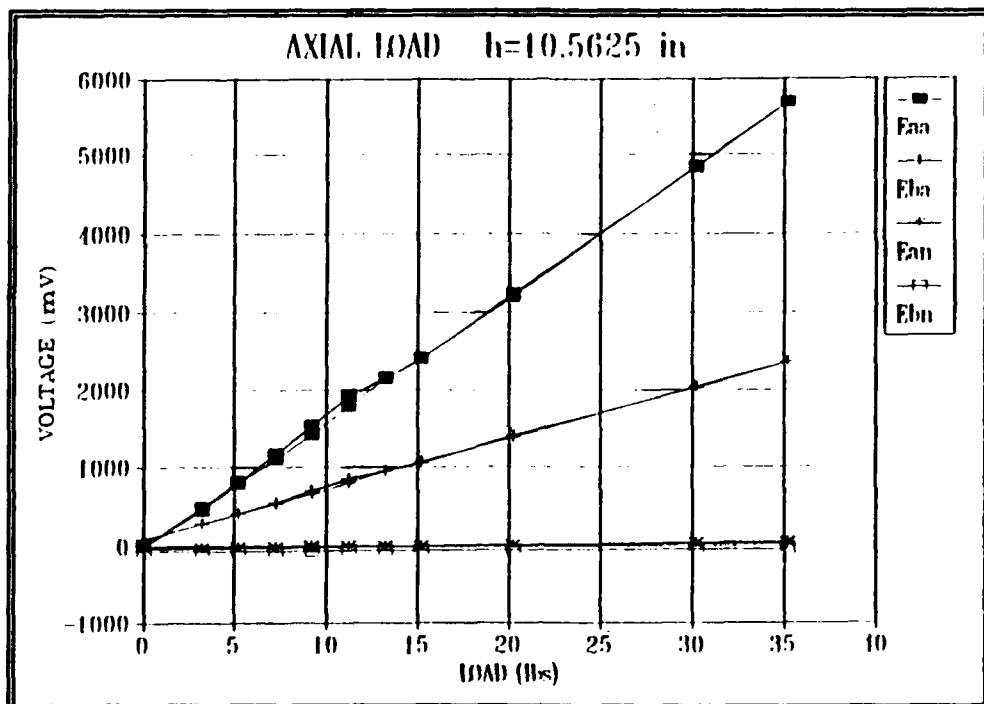
Figure A.5 Calibration Voltage vs Axial Load, h=10.5625 inches
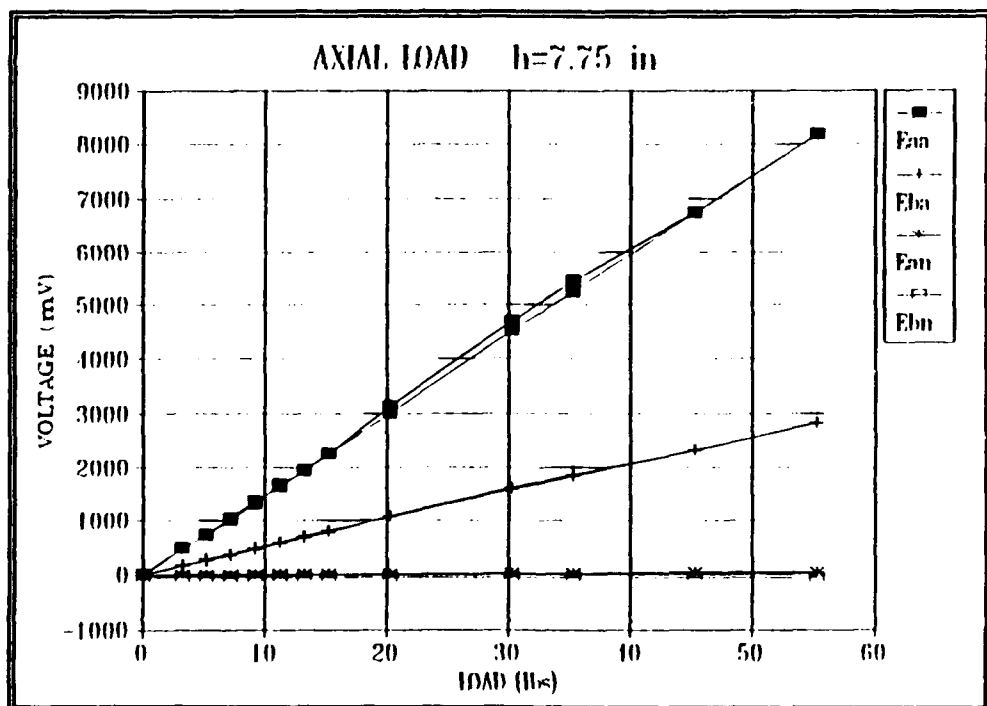
Figure A.6 Calibration Voltage vs Axial Load, h=7.75 inches

74

The goal of the calibration was the calculation of the 4x4 calibration matrix, [K]. When [K] is post-multiplied by balance output voltages, forces and moments are produced.

$$[K] * \begin{Bmatrix} E_{aa} \\ E_{ba} \\ E_{an} \\ E_{bn} \end{Bmatrix} = \begin{Bmatrix} AXIAL\ FORCE \\ AXIAL\ MOMENT \\ NORMAL\ FORCE \\ NORMAL\ MOMENT \end{Bmatrix} \tag{A.1}$$

Calculation of [K] came from inverting and post-multiplying the 4x4 $d\Delta E/dload$ matrix in

$$\begin{bmatrix} K_{11} & K_{12} & K_{13} & K_{14} \\ K_{21} & K_{22} & K_{23} & K_{24} \\ K_{31} & K_{32} & K_{33} & K_{34} \\ K_{41} & K_{42} & K_{43} & K_{44} \end{bmatrix} * \begin{bmatrix} d\Delta E_{aa}/dA & d\Delta E'_{aa}/dA & d\Delta E_{aa}/dN & d\Delta E'_{aa}/dN \\ d\Delta E_{ba}/dA & d\Delta E'_{ba}/dA & d\Delta E_{ba}/dN & d\Delta E'_{ba}/dN \\ d\Delta E_{an}/dA & d\Delta E'_{an}/dA & d\Delta E_{an}/dN & d\Delta E'_{an}/dN \\ d\Delta E_{bn}/dA & d\Delta E'_{bn}/dA & d\Delta E_{bn}/dN & d\Delta E'_{bn}/dN \end{bmatrix}$$

$$= \begin{bmatrix} 1 & 1 & 0 & 0 \\ (a-b) & (a-b)' & 0 & 0 \\ 0 & 0 & 1 & 1 \\ 0 & 0 & (a-b) & (a-b)' \end{bmatrix} \tag{A.2}$$

Where: (a-b)   ≡ height at upper position = 10.5625 inches
         (a-b)' ≡ height at lower position = 7.75 inches

The 4x4 $d\Delta E/dload$ matrix was defined as follows:

Column (1): slopes of voltages, axial load, h = 10.5625 inches
Column (2): slopes of voltages, axial load, h = 7.75 inches
Column (3): slopes of voltages, normal load, h = 10.5625 inches
Column (4): slopes of voltages, normal load, h = 7.75 inches

75

The calibration matrix can be defined by four (2x2) partitioned elements as

$$[K] = \begin{bmatrix} K1 & K2 \\ K3 & K4 \end{bmatrix} \qquad \text{(A.3)}$$

where K1 and K4 determine the direct axial and normal forces and moments, and K2 and K3 contribute the cross channel interaction terms. After three full calibrations, [K] was determined as

$$[K] = \begin{bmatrix} 0.009292 & -0.007686 & -0.000053 & -0.000209 \\ -0.033079 & 0.246046 & 0.007737 & 0.003644 \\ 0.000063 & -0.000417 & 0.009682 & -0.004241 \\ 0.002432 & -0.006519 & -0.033848 & 0.126897 \end{bmatrix} \qquad \text{(A.4)}$$

APPENDIX B: STING BALANCE CALIBRATION

A six degree of freedom, one inch diameter, Mark XIV, internal Task balance was used to measure forces and moments for models representing lower angles of attack of the wire, and for the drogue. The 4.9 inch long balance had eight 350Ω wheatstone bridges: two normal force (N1, N2), two side force (S1, S2), two axial force (A1, A2), and two rolling moment (l1, l2). The two axial force, and two rolling moment bridges were each connected in parallel to produce 175Ω circuits, and therefore six electrical outputs: N1, N2, S1, S2, A, l. Maximum balance loads were 400 lb_f in the normal channels, 200 lb_f in the side force channels, 100 lb_f axially, and 250 $inlb_f$ of rolling moment. On loan from NASA-Ames Research Center through the Navy-NASA Joint Institute of Aeronautics, the balance was calibrated to a 5 V_{DC} bridge excitation voltage by NASA-Ames personnel. Additional calibration was required to ensure proper force measurement, and moment focal point position prior to testing.

Local calibration consisted of setting the six bridge excitations at 5 V_{DC} and evaluating loads and moments. The two normal force bridges, located ±2.0 inches from the focal point, were loaded with an 11.2 lb_f load. Evaluation of N1, N2, and total normal force output was conducted while loaded at the N1 bridge (+2 inches), the focal point, and the N2 bridge (-2 inches). For example, when the balance was loaded on the N1 position, an accurate calibration would indicate 11.2 lb_f from the

N1 channel, 0 lb$_f$ from N2, and 11.2 lb$_f$ total. Similarly, if loaded at the focal point, N1 and N2 should both indicate 5.6 lb$_f$ with a total normal force, N = 11.2 lb$_f$. A reading high or low would indicate the direction of change required for the channel's bridge excitation. By conducting several experiments at all three positions, the N1 and N2 bridge excitation voltages were determined as 5.15 V$_{DC}$ and 5.75 V$_{DC}$ respectively to yield proper loadings.

The two side force bridges, 3.3 inches apart, were loaded in the same fashion with no change in excitation voltage required. Axial force was qualitatively assessed for magnitude and coordinate direction.

APPENDIX B, TAB I: STING BALANCE CALIBRATION CONSTANTS

BALANCE CALIBRATION
Start Date: 7-24-87   Completion Date: 7-28-87
NASA-Ames Calibration Laboratory

Invoice No.: 440517   Kind: Force
Pin No.: 3   Size: 1.0
Make: Task 14C   Rig No.:2

CH	Capacity (lb$_f$)	Max Load	Ω	X Gage	CAL Shunt	CAL ROG
N1	400.00	400.00	350	0.1667	100.K	4625
N2	400.00	400.00	350	0.1667	100.K	4626
A	100.00	100.00	175	-----	50.K	4618
S1	200.00	200.00	350	0.1375	100.K	4623
S2	200.00	200.00	350	0.1375	100.K	4597
1	21.0 ftlb	20.83 ftlb	175	-----	50.K	4623

CH	K POS(1)	K POS(2)	K NEG(1)	K NEG(2)	Dev	%AC
N1	5.0861E-02	-5.4826E-09	5.1591E-02	1.7157E-08	0.224	0.056
N2	4.7211E-02	-1.7015E-08	4.7763E-02	8.9153E-02	0.196	0.049
A	1.4309E-02	-7.1962E-10	1.4290E-02	-1.3322E-09	0.115	0.115
S1	3.1309E-02	-3.8153E-08	3.2073E-02	-8.9316E-09	0.263	0.132
S2	3.0366E-02	-3.8607E-08	3.1167E-02	-7.2517E-09	0.315	0.153
1	3.0885E-03	2.5672E-09	3.0908E-03	-2.4769E-09	0.042	0.204

Degree of Fit = 2   Accuracy = 15   Int. Degree of Fit = 2

INTERACTION COEFFICIENTS

Coefficient	Positive Value	Negative Value
N1/N2	-5.8036E-03	-1.0257E-02
N1/A	0.0000E-00	0.0000E-00
N1/S1	-4.1655E-03	4.5396E-03
N1/S2	0.0000E-00	0.0000E-00
N1/l	-5.8079E-02	4.4940E-02
N2/N1	-4.6218E-02	-5.1778E-02
N2/A	2.8393E-03	4.4056E-03
N2/S1	8.1694E-03	9.0385E-03
N2/S2	-4.1463E-03	0.0000E-00
N2/l	-7.7279E-02	6.1125E-02
A/N1	-8.6893E-04	2.1217E-03
A/N2	0.0000E-00	-9.1524E-04
A/S1	-6.0359E-04	0.0000E-00
A/S2	-7.7722E-05	0.0000E-00
A/l	1.1115E-01	9.7148E-02
S1/N1	6.3459E-04	7.1275E-03
S1/N2	0.0000E-00	0.0000E-00
S1/A	0.0000E-00	8.9235E-03
S1/S2	0.0000E-00	0.0000E-00
S1/l	1.1148E-01	5.2630E-02
S2/N1	2.4237E-03	3.7176E-03
S2/N2	0.0000E-00	5.2619E-03
S2/A	-2.2455E-03	-7.2915E-03
S2/S1	-606785E-03	-6.3560E-03
S2/l	2.6377E-01	6.2581E-02

Coefficient	Positive Value	Negative Value
1/N1	0.0000E-00	-3.5945E-04
1/N2	1.9928E-04	0.0000E-00
1/A	0.0000E-00	0.0000E-00
1/S1	0.0000E-00	0.0000E-00
1/S2	2.5893E-04	0.0000E-00
$N1/N2^2$	7.1926E-07	-7.9499E-07
$N1/A^2$	0.0000E-00	0.0000E-00
$N1/S1^2$	-4.0352E-06	1.9670E-06
$N1/S2^2$	0.0000E-00	0.0000E-00
$N1/l^2$	6.7860E-04	3.2320E-04
$N2/N1^2$	6.8577E-07	-5.2897E-06
$N2/A^2$	1.7755E-05	1.0467E-05
$N2/S1^2$	-2.1719E-06	4.8493E-07
$N2/S2^2$	-1.8585E-06	0.0000E-00
$N2/l^2$	1.9294E-03	1.1773E-03
$A/N1^2$	-4.4537E-07	4.2547E-06
$A/N2^2$	0.0000E-00	-4.5946E-06
$A/S1^2$	-4.7936E-06	0.0000E-00
$A/S2^2$	4.1033E-06	0.0000E-00
A/l^2	-2.0697E-04	7.5001E-04
$S1/N1^2$	-5.5350E-06	1.2923E-05
$S1/N2^2$	0.0000E-00	0.0000E-00
$S1/A^2$	0.0000E-00	4.0345E-05
$S1/S2^2$	0.0000E-00	0.0000E-00
$S1/l^2$	-2.4592E-03	9.3969E-04

Coefficient	Positive Values	Negative Values
$S2/N1^2$	-1.7099E-06	5.2110E-07
$S1/N2^2$	0.0000E-00	8.6265E-06
$S2/A^2$	-1.2072E-05	-3.7054E-05
$S2/S1^2$	2.7825E-06	-9.9830E-06
$S2/l^2$	-6.2217E-03	-8.0007E-04
$1/N1^2$	0.0000E-00	-1.5497E-07
$1/N2^2$	-1.1512E-07	0.0000E-00
$1/A^2$	0.0000E-00	0.0000E-00
$1/S1^2$	0.0000E-00	0.0000E-00
$1/S2^2$	5.1560E-08	0.0000E-00

APPENDIX C: ACQUISITION PROGRAMS

A. WALL BALANCE PROGRAM

```
'
'                           MULTI.BAS
'
'       This program was written and compiled using LabWindows and
'   QuickBasic 4.5.  (used "bc /o multi" to compile)  It's purpose
'   is to read and convert voltages from four channels connected to
'   the strain gauges on the tunnel wall balance.  The voltages are
'   converted to normal and axial forces and moments with respect to
'   the balance.  It was written and modified by LT Tom Stuart and
'   LT Dean C. Schmidt, 24 July 92.


'   Variables explained

'           eaa - Strain gauge voltage at point A in Axial direction.
'           eba - Strain gauge voltage at point B in Axial direction.
'           ean - Strain gauge voltage at point A in Normal direction.
'           ebn - Strain gauge voltage at point B in Normal direction.


'           AX  - Axial force
'           Max - Axial moment
'           NORM - Normal force
'           Mnorm - Normal moment


'****************************************************************************

REM     $INCLUDE: 'C:\LW\INCLUDE\LWSYSTEM.INC'
REM     $INCLUDE: 'C:\LW\INCLUDE\GPIB.INC'
REM     $INCLUDE: 'C:\LW\INCLUDE\FORMATIO.INC'
REM     $INCLUDE: 'C:\LW\INCLUDE\GRAPHICS.INC'
REM     $INCLUDE: 'C:\LW\INCLUDE\ANALYSIS.INC'
REM     $INCLUDE: 'C:\LW\INCLUDE\DATAACQ.INC'
REM     $INCLUDE: 'C:\LW\INCLUDE\RS232.INC'

DIM K#(4,4)
DIM ean.array#(1000),eaa.array#(1000),ebn.array#(1000),eba.array#(1000)
COMMON SHARED ean.array#(),eaa.array#(),ebn.array#(),eba.array#()

DECLARE SUB volt (ean#,eaa#,ebn#,eba#)

SCREEN 9, 0
COLOR 15, 1


'****************************************************************************
```

```
' CALIBRATION MATRIX INPUT (See thesis for explaination)

DATA  0.009292, -0.007686, -0.000053, -0.000209
DATA -0.033079,  0.246046,  0.007737,  0.003644
DATA  0.000063, -0.000417,  0.009682, -0.004241
DATA  0.002432, -0.006519, -0.033848,  0.126897

FOR L% = 1 TO 4: FOR M% = 1 TO 4
READ K#(L%,M%) : NEXT M%
NEXT L%


'**********************************************************************

LOCATE 10, 20: INPUT "Type the name of the voltage file"; VOL$
VOL$ = "C:\LW\INSTR\" + VOL$ + ".PRN"
OPEN VOL$ FOR APPEND AS #1

LOCATE 10, 20: INPUT "Type the name of the FORCE / MOMENT file"; FOR$
FOR$ = "C:\LW\INSTR\" + FOR$ + ".PRN"
OPEN FOR$ FOR APPEND AS #2

CLS: LOCATE 10, 20: PRINT "Make sure 'Caps Lock' is on now."
SLEEP 2


500
CLS: LOCATE 10, 20: INPUT "Input the Test AOA"; alpha#
alpha# = 90 - alpha#
CLS: LOCATE 5, 20: INPUT "Continue? (Y/N)"; A$

IF A$ = "Y" THEN CALL volt (eaa#,eba#,ean#,ebn#)
IF A$ <> "Y" THEN GOTO 5000
PRINT " "
PRINT "          AOA          EAA (mV)        EBA (mV)        EAN (mV)
EBN (mV)"
PRINT "        ********      **********      **********      **********
**********"

PRINT USING "  ######.######";  alpha#; eaa#; eba#; ean#; ebn#
PRINT #1, USING "######.######,"; alpha#; eaa#; eba#; ean#; ebn#

' FORCES AND MOMENTS CALCULATIONS (See thesis for explaination)

AX# = K#(1,1)*eaa# + K#(1,2)*eba# + K#(1,3)*ean# + K#(1,4)*ebn#
Max# = K#(2,1)*eaa# + K#(2,2)*eba# + K#(2,3)*ean# + K#(2,4)*ebn#
NORM# = K#(3,1)*eaa# + K#(3,2)*eba# + K#(3,3)*ean# + K#(3,4)*ebn#
Mnorm# = K#(4,1)*eaa# + K#(4,2)*eba# + K#(4,3)*ean# + K#(4,4)*ebn#

PRINT " "
PRINT "          AOA           AXIAL (lb)     MOMax (in-lb)  NORMAL (lb)
MOMnorm(in-lb)"
```

```
PRINT "         ********       *********      *************  ***********
**************"


PRINT USING "   #####.######";  alpha#; AX#; Max#; NORM#; Mnorm#
PRINT #2, USING "#####.######,"; alpha#; AX#; Max#; NORM#; Mnorm#


LOCATE 23, 15: INPUT "Do you want another reading?  (Y/N)"; ANS$
IF ANS$ = "Y" THEN GOTO 500
5000 CLOSE #1
CLOSE #2
END




'***********************************************************************
SUB volt (eaa#,eba#,ean#,ebn#)
'***********************************************************************
'
' S/R to read Channel 0,2,4,6 on MIO-16L-9 for Analog Voltage
'
'***********************************************************************


'  Setting Board code for MIO-16L-9
board.code%=0


'***********************************************************************

errl.num% = Init.DA.Brds(1, board.code%)
err2.num% = AI.Setup(1, 0, 1)
err3.num% = AI.Setup(1, 2, 1)
err4.num% = AI.Setup(1, 4, 1)
err5.num% = AI.Setup(1, 6, 1)

' Configure and set clock to 1 MHZ

err6.num% = CTR.Clock (1, 1, 1, 1)
err7.num% = CTR.Config (1, 1, 0, 0, 0, 0)

LWtotal! = 0

FOR i% = 1 TO 1000

err8.num% = CTR.EvCount (1, 1, 1, 0)
' CHAN 0 - eaa
        err9.num% = AI.Read(1, 0, 1, value0%)
        er10.num% = AI.Scale(1, 1, value0%, eaa.array#(i%))

' CHAN 2 - eba
```

85

```
        er11.num% = AI.Read(1, 2, 1, value2%)
        er12.num% = AI.Scale(1, 1, value2%, eba.array#(i%))


' CHAN 4 = ean
        er13.num% = AI.Read(1, 4, 1, value4%)
        er14.num% = AI.Scale(1, 1, value4%, ean.array#(i%))


' CHAN 6 = ebn
        er15.num% = AI.Read(1, 6, 1, value6%)
        er16.num% = AI.Scale(1, 1, value6%, ebn.array#(i%))

er17.num% = CTR.EvRead (1, 1, overflo%, tcount%)

LWtotal! = LWtotal! + tcount%

NEXT i%

CLS:LOCATE 5,15:PRINT "Total Time is " LWtotal!*1E-6" seconds."

CALL Mean (eaa.array#(), 1000, eaam#)
CALL Mean (eba.array#(), 1000, ebam#)
CALL Mean (ean.array#(), 1000, eanm#)
CALL Mean (ebn.array#(), 1000, ebnm#)
'*********************************************************************

' This multiplication (*1000) will make the voltages in mV
' This factor is required to work with the "K" cal matrix

eaa#=eaam#*1000
eba#=ebam#*1000
ean#=eanm#*1000
ebn#=ebnm#*1000


END SUB
```

B. STING BALANCE PROGRAM

```
'                                STING.BAS
'
'
'        This program was written and compiled using LabWindows and
'   QuickBasic 4.5.  (used "bc /o multi" to compile)  It's purpose
'   is to read and convert voltages from six sting balance channels
'   mounted in the Academic wind tunnel.  The voltages are converted
'   using NASA-AMES balance calibration constants and equations written
'   by Yuan.  The Labwindows program was written and modified by LT Tom
'   Stuart with assistance from LT Dean C. Schmidt.
'   Last date of modification: 10 Oct 92.


'   Variables explained


'        N1 - balance voltage at position 1 in the normal direction.
'        N2 - balance voltage at position 2 in the normal direction.
'        A - balance voltage in the axial direction.
'        S1 - balance voltage at position 1 in the side force direction.
'        S2 - balance voltage at position 2 in the side force direction.
'        RM - balance voltage from rolling moment gauge.


'*********************************************************************

REM     $INCLUDE:  'C:\LW\INCLUDE\LWSYSTEM.INC'
REM     $INCLUDE:  'C:\LW\INCLUDE\GPIB.INC'
REM     $INCLUDE:  'C:\LW\INCLUDE\FORMATIO.INC'
REM     $INCLUDE:  'C:\LW\INCLUDE\GRAPHICS.INC'
REM     $INCLUDE:  'C:\LW\INCLUDE\ANALYSIS.INC'
REM     $INCLUDE:  'C:\LW\INCLUDE\DATAACQ.INC'
REM     $INCLUDE:  'C:\LW\INCLUDE\RS232.INC'

D                               I                               M
none.array#(1000),ntwo.array#(1000),axial.array#(1000),sone.array#(1000)
DIM stwo.array#(1000),rm.array#(1000)
COMMON SHARED none.array#(),ntwo.array#(),axial.array#(),sone.array#()
COMMON SHARED stwo.array#(),rm.array#()

DECLARE SUB volt (none#,ntwo#,axial#,sone#,stwo#,rm#)

SCREEN 9, 0
COLOR 15, 1


'*********************************************************************


'  CALIBRATION CONSTANTS (See thesis for list of constants)
'   The calibration constants for the direct force nonlinear equations
'   and the force interaction equations are listed under separate appendix.
```

```
'*********************************************************************

LOCATE 10, 20: INPUT "Type the name of the raw data file"; VOL$
VOL$ = "C:\LW\INSTR\" + VOL$ + ".PRN"
OPEN VOL$ FOR APPEND AS #1

LOCATE 10, 20: INPUT "Type the name of the FORCE / MOMENT file"; FOR$
FOR$ = "C:\LW\INSTR\" + FOR$ + ".PRN"
OPEN FOR$ FOR APPEND AS #2

CLS: LOCATE 10, 20: PRINT "Make sure 'Caps Lock' is on now."
SLEEP 2

500
CLS: LOCATE 10, 20: INPUT "Input the Test AOA"; alpha#
alpha# = 90 - alpha#

CLS: LOCATE 5, 20: INPUT "Continue? (Y/N)"; A$
IF A$ <> "N" THEN CALL volt (none#,ntwo#,axial#,sone#,stwo#,rm#)
IF A$ = "N" THEN GOTO 5000

'PRINT #1, USING "######.######,"; alpha#; none#; ntwo#; axial#; sone#;
stwo#; rm#

'*********************************************************************
*****
'*********************************************************************
*****
' FORCES AND MOMENTS CALCULATIONS (Positive and Negative Equations)
'*********************************************************************
*****
'
VEX = 5!                 'Excitation voltage
N1 = none#*5000!/VEX
N2 = ntwo#*5000!/VEX
A = axial#*5000!/VEX
S1 = sone#*5000!/VEX
S2 = stwo#*5000!/VEX
R = rm#*416.67#/VEX
'
600 IF none#>=0 THEN GOTO 1000 ELSE GOTO 2000
620 IF ntwo#>=0 THEN GOTO 1100 ELSE GOTO 2100
640 IF axial#>=0 THEN GOTO 1200 ELSE GOTC 2200
660 IF sr   >=0 THEN GOTO 1300 ELSE GOTO 2300
680 IF stwo#>=0 THEN GOTO 1400 ELSE GOTO 2400
700 IF rm#>=0 THEN GOTO 1500 ELSE GOTO 2500
```

```
'******* POSITIVE EQUATIONS *******
'
1000 EN1 = 0.050861*N1-5.4826E-09*(N1^2)
GOTO 620
1100 EN2 = 0.047211*N2-1.7015E-08*(N2^2)
GOTO 640
1200 EA = 0.014309*A-7.1962E-10*(A^2)
GOTO 660
1300 ES1 = 0.031309*S1-3.8253E-08*(S1^2)
GOTO 680
1400 ES2 = 0.030366*S2-3.8607E-08*(S2^2)
GOTO 700
1500 ER = 0.0030885*R+2.5672E-09*(R^2)
GOTO 2600
'
'******* NEGATIVE EQUATIONS *******
'
2000 EN1 = 0.051591*N1+1.7157E-08*(N1^2)
GOTO 620
2100 EN2 = 0.047763*N2+8.915299E-09*(N2^2)
GOTO 640
2200 EA = 0.01429*A-1.3322E-09*(A^2)
GOTO 660
2300 ES1 = 0.032073*S1-8.931601E-09*(S1^2)
GOTO 680
2400 ES2 = 0.031167*S2-7.2517E-09*(S2^2)
GOTO 700
2500 ER = 0.0030908*R-2.4769E-09*(R^2)
'
'******* FORCE INTERACTION EQUATIONS *********************
'
2600
PRINT "  "
PRINT "              ******* FORCE INTERACTION CONVERGENCE *******
PRINT "    CYCLE    AOA       N1        N2        A        S1        S2
 R"
PRINT "      #      deg       lb        lb        lb       lb        lb
ftlb "
P              R              I              N              T
"***********************************************************************
***** "

'   Iteration to check for convergence
CYCLE = 0
FOR I = 1 TO 10
2800 IF none#>=0 THEN GOTO 3000 ELSE GOTO 4000
2820 IF ntwo#>=0 THEN GOTO 3100 ELSE GOTO 4100
2840 IF axial#>=0 THEN GOTO 3200 ELSE GOTO 4200
2860 IF sone#>=0 THEN GOTO 3300 ELSE GOTO 4300
```

```
2880 IF stwo#>=0 THEN GOTO 3400 ELSE GOTO 4400
2900 IF rm#>=0 THEN GOTO 3500 ELSE GOTO 4500


'******* POSITIVE EQUATIONS *******
'
3000 XN1 = EN1+0.0058036*N2+0.0041655*S1+0.058079*R-7.1926E-07*(N2^2)
     XN1=XN1+4.0352E-06*(S1^2)-0.0006786*(R^2)
GOTO 2820


3100 XN2 = EN2+0.046218*N1-0.0028393*A-0.0081694*S1+0.0041463*S2

XN2=XN2+0.077279*R-6.8577E-07*(N1^2)-1.7755E-05*(A^2)+2.1719E-06*(S1^2)
     XN2=XN2+1.8582E-06*(S2^2)-0.0019294*(R^2)
GOTO 2840


3200 XA = EA+8.6893E-04*N1+6.0359E-04*S1+7.7722E-05*S2-0.11115*R
     XA=XA+4.4537E-07*(N1^2)+4.7936E-06*(S1^2)-4.1033E-06*(S2^2)
     XA=XA+2.0967E-04*(R^2)
GOTO 2860


3300 XS1 = ES1-6.3459E-04*N1-0.11148*R+5.535E-06*(N1^2)+0.0024592*(R^2)
GOTO 2880


3400 XS2 = ES2-0.0024237*N1+0.0022455*A+0.0066785*S1-0.26377*R
     XS2=XS2+1.7099E-06*(N1^2)+1.2072E-05*(A^2)-2.7825E-06*(S1^2)
     XS2=XS2+0.0062217*(R^2)
GOTO 2900


3   5   0   0 X   R   =
ER-1.9928E-04*N2-2.5893E-04*S2+1.1512E-07*(N2^2)-5.156E-08*(S2^2)
GOTO 4600
'
'******** NEGATIVE EQUATIONS ********
'
4000 XN1 = EN1+0.010257*N2-0.0045396*S1-0.04494*R+7.9499E-07*(N2^2)
     XN1=XN1-1.967E-06*(S1^2)-0.0003232*(R^2)
GOTO 2820


4100 XN2 = EN2+0.051778*N1-0.0044056*A-9.038499E-03*S1-0.061125*R
     XN2=XN2+5.2897E-06*(N1^2)+1.0467E-05*(A^2)-4.8493E-07*(S1^2)
     XN2=XN2-0.0011773*(R^2)
GOTO 2840


4200 XA = EA-0.0021217*N1+9.1524E-04*N2-0.097148*R-4.2547E-06*(N1^2)
     XA=XA+4.5846E-06*(N2^2)-7.5001E-04*(R^2)
GOTO 2860


4300 XS1 = ES1-0.0071275*N1-0.0089235*A-0.05268*R-1.2923E-05*(N1^2)
     XS1=XS1-4.0345E-05*(A^2)-9.3969E-04*(R^2)
GOTO 2880
```

```
4400 XS2 = ES2-0.0037176*N1-0.0052619*N2+0.0072915*A+0.006856*S1
     XS2=XS2-0.062581*R-5.211E-07*(N1^2)-8.6265E-06*(N2^2)+3.7054E-05*(A^2)
     XS2=XS2+9.983001E-06*(S1^2)+8.0007E-04*(R^2)
GOTO 2900

4500 XR = ER+3.5945E-04*N1+1.5497E-07*(N2^2)


4600 '    Rename for next iteration
N1 = XN1
N2 = XN2
A = XA
S1 = XS1
S2 = XS2
R = XR
'
'    Counter for convergence iterations
CYCLE = CYCLE + 1

PRINT USING "####.####"; CYCLE; alpha#; N1; N2; A; S1; S2; R

NEXT I

PRINT #1, USING "####.######"; CYCLE; alpha#; N1; N2; A; S1; S2; R

LOCATE 21,15:INPUT "IS CONVERGENCE OK? (Y or N)";CONV$
IF CONV$ = "N" THEN GOTO 2600
'
NORMAL = N1 + N2
SIDE = S1 + S2
AXIAL = A
PITCH = (N1-N2)*0.1667
YAW = (S1-S2)*0.1375
ROLL = R/12.0
'
'****************************************************************
'******* TARE CALCULATIONS **************************************

LOCATE 23,15:INPUT "IS THIS A TARE READING? (Y or N)";TAR$
IF TAR$<>"Y" GOTO 4700

TNORM = NORMAL
TSIDE = SIDE
TAXIAL = AXIAL
TPITCH = PITCH
TYAW = YAW
TROLL = ROLL
```

```
CLS
PRINT " "
PRINT "                      ****** TARE CALCULATIONS ******"
PRINT "     NORMAL        SIDE        AXIAL        PITCH        YAW
    ROLL"
PRINT "       lb          lb          lb          ftlb         ftlb
    ftlb
P       R       I       N       T                                  "
******************************************************************
*****"
PRINT USING "#####.######,"; TNORM; TSIDE; TAXIAL; TPITCH; TYAW; TROLL
PRINT #2, USING "#####.######,"; alpha#; TNORM; TSIDE; TAXIAL; TPITCH;
TYAW; TROLL
GOTO 4800
'****************************************************************
*****************

4700 '
'******* FORCE CALCULATIONS ********
NORMF = NORMAL-TNORM
SIDEF = SIDE-TSIDE
AXIALF = AXIAL-TAXIAL
PITCHF = PITCH-TPITCH
YAWF = YAW-TYAW
ROLLF = ROLL-TROLL

CLS
PRINT " "
PRINT "                      ****** FORCE CALCULATIONS ******"
PRINT "    AOA=";alpha#
PRINT "   "
PRINT "     NORMAL        SIDE        AXIAL        PITCH        YAW
    ROLL"
PRINT "       lb          lb          lb          ftlb         ftlb
    ftlb
P       R       I       N       T                                  "
*******************************************************************
*******"
PRINT USING "#####.######,"; NORMF; SIDEF; AXIALF; PITCHF; YAWF; ROLLF
PRINT #2, USING "#####.######,"; alpha#; NORMF; SIDEF; AXIALF; PITCHF;
YAWF; ROLLF

4800 LOCATE 23, 15: INPUT "Do you want another reading?  (Y/N)"; ANS$
IF ANS$ <> "N" THEN GOTO 500
5000 CLOSE #1
CLOSE #2
END
```

```
'*********************************************************************
SUB volt (none#,ntwo#,axial#,sone#,stwo#,rm#)
'*********************************************************************
'
' S/R to read Channel 0,1,2,3,4,5 on MIO-16L-9 for Analog Voltage
'
'*********************************************************************

'   Setting Board code for MIO-16L-9
board.code%=0

'*********************************************************************

err1.num% = Init.DA.Brds(1, board.code%)
err2.num% = AI.Setup(1, 0, 1)
err3.num% = AI.Setup(1, 1, 1)
err4.num% = AI.Setup(1, 2, 1)
err5.num% = AI.Setup(1, 3, 1)
err6.num% = AI.Setup(1, 4, 1)
err7.num% = AI.Setup(1, 5, 1)



' Configure and set clock to 1 MHZ

err8.num% = CTR.Clock (1, 1, 1, 1)
err9.num% = CTR.Config (1, 1, 0, 0, 0, 0)

LWtotal! = 0

FOR i% = 1 TO 1000

er10.num% = CTR.EvCount (1, 1, 1, 0)

' CHAN 0 = none
        er11.num% = AI.Read(1, 0, 1, value0%)
        er12.num% = AI.Scale(1, 1, value0%, none.array#(i%))

' CHAN 1 = ntwo
        er13.num% = AI.Read(1, 1, 1, value1%)
        er14.num% = AI.Scale(1, 1, value1%, ntwo.array#(i%))

' CHAN 2 = axial
        er15.num% = AI.Read(1, 2, 1, value2%)
        er16.num% = AI.Scale(1, 1, value2%, axial.array#(i%))

' CHAN 3 = sone
        er17.num% = AI.Read(1, 3, 1, value3%)
        er18.num% = AI.Scale(1, 1, value3%, sone.array#(i%))
```

```
' CHAN 4 - stwo
        er19.num% - AI.Read(1, 4, 1, value4%)
        er20.num% - AI.Scale(1, 1, value4%, stwo.array#(i%))

' CHAN 5 - rolling moment
        er21.num% - AI.Read(1, 5, 1, value5%)
        er22.num% - AI.Scale(1, 1, value5%, rm.array#(i%))

er23.num% - CTR.EvRead (1, 1, overflo%, tcount%)

LWtotal! - LWtotal! + tcount%

NEXT i%

CLS:LOCATE 2,15:PRINT "Total Time is " LWtotal!*1E-6" seconds."

CALL Mean (none.array#(), 1000, none#)
CALL Mean (ntwo.array#(), 1000, ntwo#)
CALL Mean (axial.array#(), 1000, axial#)
CALL Mean (sone.array#(), 1000, sone#)
CALL Mean (stwo.array#(), 1000, stwo#)
CALL Mean (rm.array#(), 1000, rm#)
'*************************************************************************
END SUB
```

C. WALL BALANCE TARE CALCULATION PROGRAM

```
'                    TARE CONVERSION CALCULATION

'        The purpose of this program is to calculate the time varing
'windoff tare readings given the four channel tare values immediately
'prior to tunnel operation, and immediately after shutdown.
'Assumptions include: linear drift, samples taken at equal time
'intervals.  This program is designed to run in Quickbasic 4.5.

DIM A(4, 4), B(4), C(35, 4)
TARE$ = "C:\QPRO\XXX.PRN"
OPEN TARE$ FOR OUTPUT AS #1

P = 31      'Total number of data points taken
T = .4      'Total run time
delT = T / (P - 1)'Incremented time step per point

DATA  -0.722499,  16.772749,  0.475904, -9.318065
DATA  -1.436443,  39.308192,  0.403325, -5.661456

FOR L = 1 TO 2
  FOR M = 1 TO 4
READ A(L, M)
  NEXT M
NEXT L

FOR N = 1 TO 4
  B(N) = (A(2, N) - A(1, N)) / T   'Calculates the slope
NEXT N

AOA = 105

FOR X = 1 TO P - 1

   FOR K = 1 TO 4
      C(X, K) = A(1, K) + B(K) * delT * X 'THE Calculation
   NEXT K
   FOR S = 1 TO 3
      PRINT #1, USING "#####.######,"; AOA; C(X, 1); C(X, 2); C(X, 3);
C(X, 4)
   NEXT S    'The values are printed three times to match the three
             'samples taken at each AOA during the runs
   AOA = AOA - 5      'Decrement AOA

NEXT X
CLOSE #1
END
```
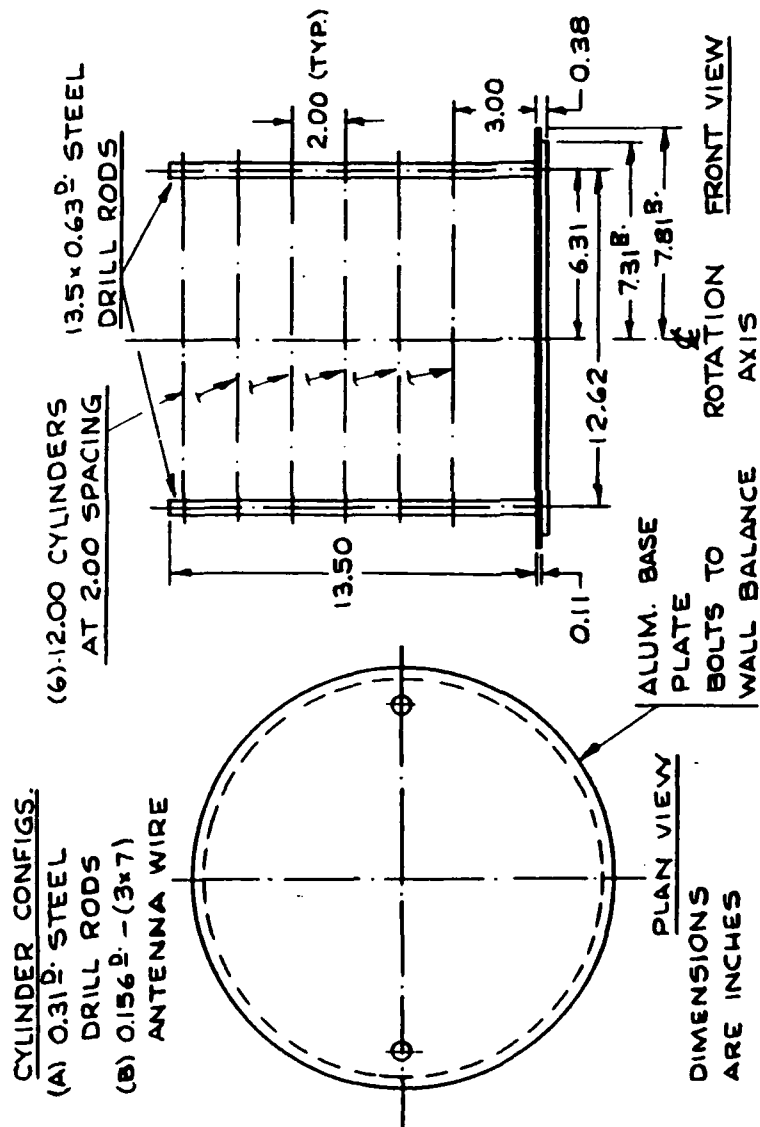
Figure D.1 Wall Balance Model Sketches
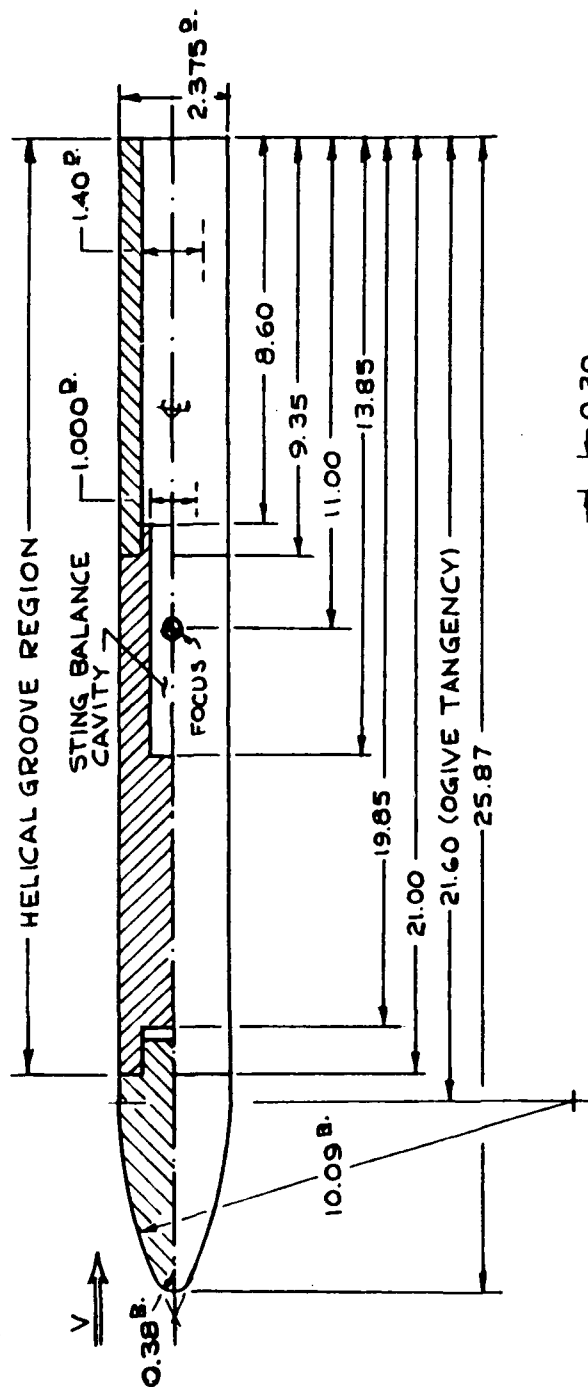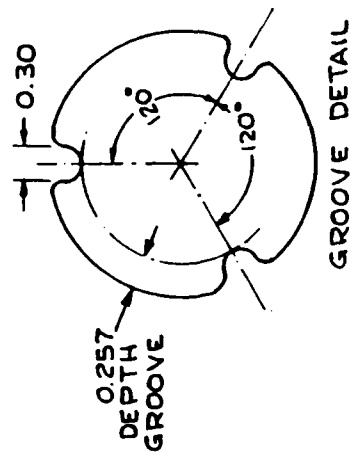
Figure D.2 Cylinder Sting Balance Model Sketches

97
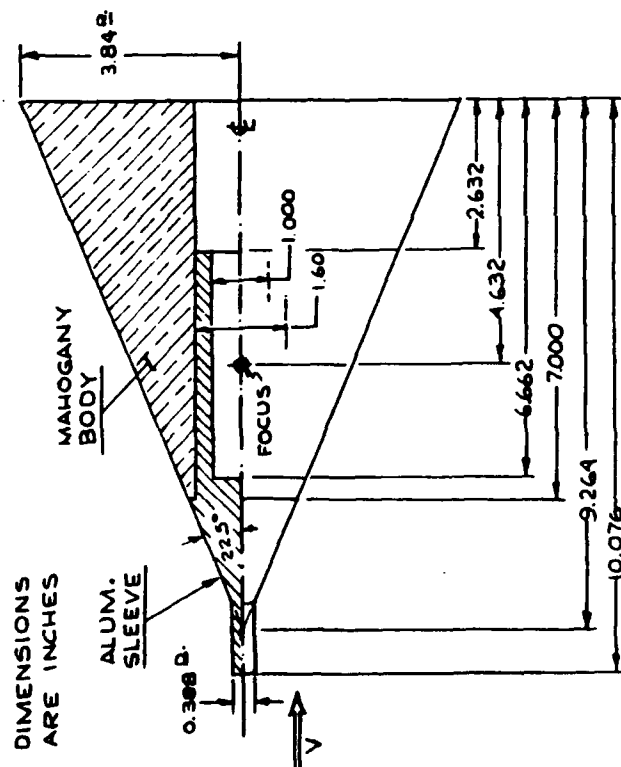
Figure D.4 Sting Balance Apparatus

Figure D.3 Drogue Sting Balance Model

98

APPENDIX E: STATIC CONDITIONS SIMULATION MODEL

```
          PROGRAM TAC17A
C         THIS PROGRAM IS AN ITERATIVE SOLUTION TO THE STEADY
C         STATE TACAMO WIRE PROBLEM.
C         THE COEFFICIENTS AND DIMENSIONS REFLECT THE NEW 3X7 RATTAIL
C         WIRE.
C***************************************************************************
C         DECLARE AND DIMENSION VARIABLES.
C
C         SCALARS FIRST.
C
C         A1, B1, C1, A2, B2, C2 ARE THE TENSION TIMES THE SLOPE AT
C         THE HALF STEP POINTS USED IN THE ITERATIVE SOLUTION.
          REAL A1,B1,C1
          REAL A2,B2,C2
C         A22, B22, C22 ARE PLACEHOLDERS USED DURING THE ITERATIONS.
          REAL A22,B22,C22
C         A2A2, B2B2, C2C2 ARE SUMMERS USED IN AVERAGING.
          REAL A2A2,B2B2,C2C2
C         AC IS THE AERODYNAMIC CENTER OF THE DROGUE MEASURED FROM THE LE.
          REAL AC
C         ALFAD IS THE DROGUE ANGLE OF ATTACK.
          REAL ALFAD
C         ALTTP IS THE TOWPLANE ALTITUDE IN FEET.
          REAL ALTTP
C         ASFD IS THE AERODYNAMIC SIDEFORCE OF THE DROGUE DUE TO THE
C         SIDESLIP ANGLE BETA.
          REAL ASFD
C         BETA IS THE SIDESLIP ANGLE OF THE DROGUE.
          REAL BETA
C         CDD IS THE CD FOR THE DROGUE.
          REAL CDD
C         CA IS THE WIRE AXIAL AERODYNAMIC FORCE COEFFICIENT.
          REAL CA
C         CN IS THE WIRE NORMAL AERODYNAMIC FORCE COEFFICIENT.
          REAL CN
C         CG IS THE CENTER OF GRAVITY OF THE DROGUE, MEASURED AFT OF THE
C         TIP.
          REAL CG
C         CLALD IS THE LIFT COEFFICIENT CURVE SLOPE FOR THE DROGUE.
          REAL CLALD
C         CLALDM IS THE MAXIMUM LIFT CURVE SLOPE FOR THE DROGUE.
          REAL CLALDM
C         CMACD IS THE COEFFICIENT OF MOMENT AROUND THE AERODYNAMIC
C         CENTER FOR THE DROGUE.
          REAL CMACD
```

```
C       CY IS THE WIRE SIDEFORCE COEFFICIENT.
        REAL CY
C       D IS THE WIRE DIAMETER.
        REAL D
C       DELTAS IS THE INCREMENT OF WIRE LENGTH AT THE N'TH GRIDPOINT.
        REAL DELTAS
C       G IS THE ACCELERATION DUE TO GRAVITY.
        REAL G
C       LEND IS THE LENGTH OF THE DROGUE.
        REAL LEND
C       LD IS THE LIFT PRODUCED BY THE DROGUE.
        REAL LD
C       MHU IS THE MASS OF THE WIRE PER UNIT LENGTH.
        REAL MHU
C       PHI IS THE ANGLE OF BANK OF THE TOWPLANE.
        REAL PHI
C       Q IS THE LOCAL DYNAMIC PRESSURE.
        REAL Q
C       RADTP IS THE ORBIT RADIUS OF THE TOWPLANE.
        REAL RADTP
C       RHO IS THE LOCAL AIR DENSITY.
        REAL RHO
C       RNEW IS A PLACEHOLDER FOR R(1) WHILE AN UPDATE IS CALCULATED
C       ON THE OUTER LOOP.
        REAL RNEW
C       STUFF1,2,3,4,5,6,7 ARE DUMMY VARIABLES FOR INTERIM CALCULATIONS.
        REAL STUFF1, STUFF2, STUFF3
        REAL STUFF4, STUFF5, STUFF6
        REAL STUFF7
C       THEDOT IS THE ORBIT RATE IN RADIANS PER SECOND.
        REAL THEDOT
C       RR IS A CONSTANT USED TO START THE RADIAL COORDINATE
C       CALCULATIONS AT THE DROGUE.
        REAL RR
C       SD IS THE MAXIMUM CROSS SECTIONAL AREA OF THE DROGUE.
        REAL SD
C       THTH IS A CONSTANT USED TO START THE THETA COORDINATE
C       CALCULATIONS AT THE DROGUE.
        REAL THTH
C       VEAS IS THE TOWPLANE EQUIVALENT AIRSPEED.
        REAL VEAS
C       VTRUE IS THE TOWPLANE TRUE AIRSPEED.
        REAL VTRUE
C       WD IS THE WEIGHT OF THE DROGUE.
        REAL WD
C       ZNEW IS A PLACEHOLDER FOR Z(1) WHILE AN UPDATE IS
C       CALCULATED ON THE OUTER LOOP.
        REAL ZNEW
C
C       NOW INTEGERS.
```

```fortran
C
C       N IS THE MAIN LOOP GRIDPOINT COUNTER.
        INTEGER N
C       COUNT AND COUNT1 ARE COUNTERS USED DURING AN AVERAGING PROCESS.
        INTEGER COUNT, COUNT1
C       INDEX CORRELATES THE GRIDPOINT ALTITUDE WITH THE INDEX OF THE
C       CORRECT DENSITY VALUE.
        INTEGER INDEX
C       TICK COUNTS THE NUMBER OF OUTER LOOPS PERFORMED TO CONVERGENCE.
        INTEGER TICK
C
C       FINALLY ARRAYS.
C
C       DENSITY(S) IS THE DENSITY MEASURED AT 1000 FEET INTERVALS.
        REAL DENSTY(30)
C       R(N) IS THE GRIDPOINT RADIAL POSITION IN FEET.
        REAL R(200)
C       T(N) IS THE GRIDPOINT TENSION. THE ACTUAL GRIDPOINT LOCATION
C       IS AT N-1/2.
        REAL T(200)
C       THETA(N) IS THE GRIDPOINT ANGULAR POSITION IN FEET.
        REAL THETA(200)
C       Z(N) IS THE GRIDPOINT HEIGHT IN FEET.
        REAL Z(200)
C*******************************************************************
C       SHAKE HANDS WITH THE OPERATOR.
        WRITE(6,*)'         '
        WRITE(6,*)'          '
        WRITE(6,*)'          '
        WRITE(6,*)'            NAVAL POSTGRADUATE SCHOOL        '
        WRITE(6,*)'                 CLASS OF 1992               '
        WRITE(6,*)'                                             '
        WRITE(6,*)'                         \\                  '
        WRITE(6,*)'                        \\- - > >            '
        WRITE(6,*)'                         * //                '
        WRITE(6,*)'                       *                     '
        WRITE(6,*)'                     *                       '
        WRITE(6,*)'                    *                        '
        WRITE(6,*)'                    *                        '
        WRITE(6,*)'                     *                       '
        WRITE(6,*)'                       *  *<                 '
        WRITE(6,*)'       '
        WRITE(6,*)' TAC17A IS THE STEADY STEADY STATE SOLUTION TO THE'
        WRITE(6,*)'           TACAMO WIRE PROBLEM.  '
        WRITE(6,*)'       '
        PAUSE
C*******************************************************************
C       OPEN THE DATA FILES.
C
        OPEN (UNIT=11,FILE='DATA01.MAT')
```

```
        OPEN (UNIT=12,FILE='DATA02.MAT')
        OPEN (UNIT=13,FILE='DATA03.MAT')
        OPEN (UNIT=14,FILE='DATA04.MAT')
        OPEN (UNIT=15,FILE='DATA05.MAT')
        OPEN (UNIT=16,FILE='DATA06.MAT')
        OPEN (UNIT=17,FILE='DATA07.MAT')
        OPEN (UNIT=18,FILE='DATA08.MAT')
        OPEN (UNIT=19,FILE='DATA09.MAT')
        OPEN (UNIT=20,FILE='DATA00.MAT')
C***********************************************************************
C       FORMAT THE DATA FILES.
C       DATA01.MAT IS UNFORMATTED.
C
1       FORMAT(F12.6)
2       FORMAT(F5.1)
C***********************************************************************
C       INITIALIZE CONSTANTS.
C
C       DROGUE CONSTANTS.
C
        AC=23.97/12.0
        CG=13.80/12.0
        CDD=0.53
        CMACD=0.0
        CLALDM=0.61
        LEND=31.71/12.0
        SD=3.14159
        WD=81.95
C
C       GENERAL CONSTANTS.
C
        G=32.174
        PI=3.1415926535879
        COUNT=1
        TICK=1
C
C       WIRE CONSTANTS.
C
        D=0.1582/12
        DELTAS=101.96
        MHU=0.062107/G
C
C       RR AND THTH ARE CONSTANTS USED TO START THE CALCULATIONS
C       AT THE DROGUE.
C
        RR=1.0
        THTH=0.001
C
C       READ THE DENSITY DATA FILE.
C
```

```
        OPEN (31,FILE-'DENSTY.MAT',STATUS-'OLD',FORM-'FORMATTED',
      : ACCESS-'SEQUENTIAL',RECL=5)
5       READ (31,2,END=6)DENSTY
        GOTO 5
6       CLOSE(31)
C**************************************************************
C       CALCULATE THE RADIUS OF THE TOWPLANE FLIGHT PATH AND THE THEDOT.
C       THE PROGRAM WILL WORK AT ALL AIRSPEEDS AND ALTITUDES OF
C       INTEREST AND FOR BANK ANGLES OF BETWEEN 5 AND 50 DEGREES.  FOR
C       BANK ANGLES ABOVE 45 DEGREES, AND AT TIMES AROUND THE LOCATION
C       OF THE JUMP PHENOMENON, A SMALL ADJUSTMENT TO THE PROGRAM
C       MAY BE REQUIRED.  DOCUMENTATION WILL PRINT ON THE SCREEN IF
C       THIS SITUATION OCCURS THAT WILL EXPLAIN HOW TO MAKE THE
C       ADJUSTMENT.
C
        WRITE(6,*)'INPUT AIRCRAFT KEAS, ALT IN FT, BANK ANGLE IN DEG'
C
        READ(5,*) VEAS,ALTTP,PHI
C
C       CONVERT KNOTS TO FEET PER SECOND.
C
        VEAS=VEAS*6076.1/3600.0
C
C       CONVERT TO RADIANS.
C
        PHI=PHI*2.0*PI/360.0
C
C       LOCAL GRIDPOINT DENSITY.  A FILE OF MEASURED DATA MAY BE USED
C       OR STANDARD ATMOSPHERE DATA MAY BE CALCULATED.  COMMENT OUT THE
C       METHOD NOT CHOSEN.
C
        INDEX-INT(ALTTP/1000.0)+1
        RHO-DENSTY(INDEX)*0.0023769/1013.0
C
C       RHO-0.0023769*(((518.69-0.0035662*ALTTP)/518.69)**
C     : ((-1.0)*(1.0/(-0.0035662*53.3))+1.0))
C
C       RHO-0.002378*(1-0.006875*Z(N)/1000.0)**4.256
C
C       TRUE AIRSPEED FROM EQUIVALENT AIRSPEED.
C
        VTRUE-VEAS/SQRT(RHO/0.0023769)
C
C       CALCULATE TOWPLANE ORBIT RADIUS.
C
        RADTP-VTRUE**2/(G*SQRT(1/(COS(PHI))**2-1))
C
C       ORBIT RATE CALCULATION.
C
        THEDOT-VTRUE/RADTP
```

```
C*********************************************************************
C*********************************************************************
C*********************************************************************
C          THE INITIAL POSITION AT GRIDPOINT 1.
C          THIS IS AN INITIAL GUESS AT THE BOTTOM POSITION.  THIS VALUE IS
C          ITERATED TO MATCH THE BOUNDARY CONDITION POSITION AT THE
C          TOWPLANE. THESE VALUES MAY ALSO BE ADJUSTED TO FORCE THE
C          MULTIPLE SOLUTIONS.  TO FORCE MULTIPLE SOLUTIONS THE INITIAL
C          POSITION MAY BE CHOSEN AT OR OUTSIDE THE TOWPLANE RADIUS OF
C          ORBIT.
C
           THETA(1)=0.0
           IF (PHI .GT. 32.0*2.0*PI/360.0) THEN
           Z(1)=0.3*ALTTP
C            Z(1)=0.4*ALTTP
           R(1)=0.2*RADTP
C            R(1)=1.6*RADTP
           ELSE
           Z(1)=0.6*ALTTP
C            Z(1)=0.2*ALTTP
           R(1)=0.6*RADTP
C            R(1)=1.2*RADTP
           ENDIF
C*********************************************************************
20         CONTINUE
C
C          AT THE DROGUE.
C
C          GUESS AT THE POSITION USING THE FORCING FACTORS.
C
           R(2)=R(1)+RR
           THETA(2)=THETA(1)+THTH
           Z(2)=Z(1)+SQRT(DELTAS**2-R(2)**2-R(1)**2+
          : 2*R(2)*R(1)*COS(THETA(2)-THETA(1)))
C
C          DENSITY AT GRIDPOINT 1.  AGAIN, CHOOSE TABLE LOOKUP
C          OR STANDARD ATMOSPHERE.
C
           INDEX=INT(Z(1)/1000.0)+1
           RHO=DENSTY(INDEX)*0.0023769/1013.0
C
C          RHO=0.0023769*(((518.69-0.0035662*Z(1))/518.69)**
C         : ((-1.0)*(1.0/(-0.0035662*53.3))+1.0))
C
C           RHO=0.002378*(1-0.006875*Z(N)/1000.0)**4.256
C
C          LOCAL DYNAMIC PRESSURE.
C
           Q=0.5*RHO*(R(1)*THEDOT)**2
C
```

```
C        CALCULATE THE AOA AND SIDESLIP ANGLE OF THE DROGUE BY CALCU-
C        LATING THE MOMENT EQUATION RESIDUES AND CHOOSING THE AOA AND
C        SIDESLIP ANGLE AT WHICH THE RESIDUE COMES CLOSEST TO VANISHING.
C        ONE DEGREE INCREMENTS ARE CONSIDERED SUFFICIENT.
C
C        INITIALIZE THE RESIDUE HOLDERS SINCE THEY ARE REUSED AT EACH
C        NEW BOUNDARY SHOT.
C
         STUFF2=1000.0
         STUFF5=1000.0
C
C        LOOP THROUGH EACH ANGLE FROM 0 TO 90 DEGREES.
C        NEGLECT ALL OTHER ANGLES THROUGH PHYSICAL REASONING.
C
         DO 50 N=1,90
C
C        USE INDEX TO GET ANGLE IN RADIANS.
C
         ALFAD=N*2.0*PI/360.0
         BETA=ALFAD
C
C        CALCULATE THE LIFT CURVE SLOPE AT THIS ANGLE.
C
         CLALD=CLALDM
C        NOW THE RESIDUES AT THIS ANGLE.
C
C        FOR THE ANGLE OF ATTACK.
C
C        FIRST CALCULATE THE PRODUCT OF CLALD AND ALFAD ACCOUNTING
C         FOR THE EFFECTS OF STALL.
C
         STUFF7=CLALD*ALFAD
         IF (ABS(ALFAD) .GT. 0.786)THEN
         STUFF7=0.42*(ALFAD)/(ABS(ALFAD))
         ELSE
         ENDIF
         IF (ABS(ALFAD) .GT. 1.05) THEN
         STUFF7=0.2*(ALFAD)/(ABS(ALFAD))
         ELSE
         ENDIF
C
         STUFF1=-STUFF7*Q*SD*AC*COS(ALFAD)-CDD*Q*SD*AC*SIN(ALFAD)+
       : WD*CG*COS(ALFAD)+CMACD*Q*SD*LEND-CDD*SIN(BETA)*AC*Q*SD
C
C        FOR THE SIDESLIP ANGLE.
C
C        AGAIN CALCULATE THE PRODUCT OF CLALD AND BETA ACCOUNTING FOR
C        THE EFFECTS OF STALL.
C
         STUFF7=CLALD*BETA
```

105

```fortran
      IF (ABS(BETA) .GT. 0.786)THEN
      STUFF7-0.42*(BETA)/(ABS(BETA))
      ELSE
      ENDIF
      IF (ABS(BETA) .GT. 1.05) THEN
      STUFF7-0.2*(BETA)/(ABS(BETA))
      ELSE
      ENDIF
C
      STUFF4-WD*THEDOT**2*R(1)*CG*COS(BETA)/G-STUFF7*Q*SD*AC*
     : COS(BETA)+CMACD*Q*SD
C
C     SAVE RESIDUE AND ANGLE IF IT IS LESS THAN THE LAST.
C
C     FOR THE ANGLE OF ATTACK.
C
      IF (ABS(STUFF1) .LT. ABS(STUFF2)) THEN
      STUFF2-STUFF1
      STUFF3-ALFAD
      ENDIF
C
C     FOR THE SIDESLIP ANGLE.
C
C     ELIMINATE THE POSSIBILITY OF MULTIPLE SOLUTIONS BEYOND 45
C     DEGREES.
C
      IF (BETA .GT. PI/4.0) THEN
      GOTO 50
      ENDIF
      IF (ABS(STUFF4) .LT. ABS(STUFF5)) THEN
      STUFF5-STUFF4
      STUFF6-BETA
      ENDIF
50    CONTINUE
C
C     SELECT THE MINIMUM RESIDUE ANGLE OF ATTACK AS THE DESIRED VALUE.
C
      ALFAD-STUFF3
      BETA-STUFF6
C
C     CALCULATE THE LIFT FORCE OF THE DROGUE DEFINED PERPENDICULAR TO
C     THE RELATIVE FLOW AND CALCULATE THE LIFT AND SIDEFORCE OF THE
C     DROGUE.
C
      CLALD-CLALDM*(PI-2.0*ALFAD)/PI
      LD-CLALD*ALFAD*Q*SD
      CLALD-CLALDM*(PI-2.0*BETA)/PI
      ASFD-CLALD*BETA*Q*SD
C
C     CALCULATE THE DRAG FORCE OF THE DROGUE DEFINED PARALLEL TO
```

```
C        THE RELATIVE FLOW.
C
         DD=CDD*Q*SD
C*********************************************************************
C        NOW GET TENSION AT 1 AND POSITION AT 2 BY ASSUMING THE
C        AERODYNMIC AND INERTIAL FORCES ON THE FIRST SEGMENT OF WIRE
C        ARE SMALL COMPARED TO THE DROGUE FORCES.
C
C        THE TENSION AT GRIDPOINT 1 MUST BALANCE THE VECTOR SUM OF THE
C        FORCES UPON THE DROGUE IN ORDER TO SATISFY STATIC EQUILIBRIUM.
C
         STUFF1=WD*THEDOT**2*R(1)/G
         T(1)=SQRT((STUFF1-ASFD)**2+DD**2+(LD-WD)**2)
C
C        ASSUME THAT THE FORCES ON THE FIRST SEGMENT OF THE WIRE ARE
C        SMALL COMPARED TO THE FORCES ON THE DROGUE.
C
         T(2)=T(1)
C
C        THE RESULTANT FORCE MUST ALSO BE IN THE RECIPROCAL DIRECTION
C        TO MAINTAIN STATIC EQUILIBRIUM.
C
         R(2)=R(1)-(STUFF1-ASFD)*DELTAS/T(1)
         THETA(2)=THETA(1)+DD*DELTAS/(T(1)*((R(1)+R(2))/2))
C
C        USE THE TWO POINT SEGMENT LENGTH CONSTRAINT TO GET THE Z AT
C        GRIDPOINT 2.
C
         Z(2)=Z(1)+SQRT(DELTAS**2-R(2)**2-R(1)**2+
       : 2*R(2)*R(1)*COS(THETA(2)-THETA(1)))
C
C*********************************************************************
C*********************************************************************
C        ITERATE TO THE TOP.
C
C        MAKE INITIAL GUESSES AT THE ITERATION VALUES FOR GRIDPOINT TWO.
C
         A1=T(1)*(R(2)-R(1))/DELTAS
         B1=T(1)*(R(2)+R(1))*(THETA(2)-THETA(1))/(2*DELTAS)
         C1=T(1)*(Z(2)-Z(1))/DELTAS
C
         DO 3500 N=3,200
C
C        GUESS AT NEXT POINT. USE THE THREE POINT UNIT TANGENT VECTOR
C        CONSTRAINT TO GET THE Z AT GRIDPOINT N.
C
         R(N)=R(N-1)+R(N-1)-R(N-2)
         THETA(N)=THETA(N-1)+THETA(N-1)-THETA(N-2)
         Z(N)=4*DELTAS**2-(R(N)-R(N-2))**2-R(N-1)**2*
       : (THETA(N)-THETA(N-2))**2
```

```
C
C         PROTECT AGAINST A NEGATIVE RADICAND DURING THE ITERATIONS.
C
          IF (Z(N) .LT. 0.0) THEN
          Z(N)-0.000001
          ELSE
          ENDIF
          Z(N)-Z(N-2)+SQRT(Z(N))
C
          T(N)-T(N-1)+MHU*DELTAS*G/(R(N-1)*(THETA(N-1)-THETA(N-2))/DELTAS)
C*****************************************************************************
C         THE INNER LOOP FOR MOVING FROM ONE GRID POINT TO THE NEXT.
C
C         INITIALIZE COUNTERS FOR LATER USE.
C
          COUNT-1
          COUNT1-1
C
C         INITIALIZE SUMMERS FOR USE IN AVERAGING LATER.
C
          A2A2-0.0
          B2B2-0.0
          C2C2-0.0
C
1000      CONTINUE
C
C         CALCULATE DENSITY.
C
          INDEX-INT(Z(N)/1000.0)+1
          RHO-DENSTY(INDEX)*0.0023769/1013.0
C
C         RHO-0.0023769*(((518.69-0.0035662*Z(N))/518.69)**
C       : ((-1.0)*(1.0/(-0.0035662*53.3))+1.0))
C
C          RHO-0.002378*(1-0.006875*Z(N)/1000.0)**4.256
C
C         INCREMENT COUNTER.
C
          COUNT-COUNT+1
C
C         NOW THE ITERATIONS.
C
C         CALCULATE SOME TRANSCENDENTALS USED IN LATER CALCULATIONS.
C
          STUFF1-R(N-1)*(THETA(N)-THETA(N-2))/(2*DELTAS)
          STUFF2-(1-STUFF1**2)
          STUFF3-3*SQRT(STUFF2)-4*(SQRT(STUFF2))**3
C
C         CALCULATE CN, CA AND CY.
C
```

```fortran
      CN=1.09*STUFF2-0.08*4.0*STUFF2*STUFF1**2
      IF (STUFF1 .LT. 0.707) THEN
      CA=0.0
      ELSE
      CA=0.017
      ENDIF
      IF (STUFF1 .LT. 0.5) THEN
      CY=0.0
      ELSE
      CY=0.0148*STUFF3*3
      ENDIF
C      CY=0.0
C
C      THE ITERATIVE EQUATIONS.
C
      STUFF1=(T(N)+T(N-1))*R(N-1)*(THETA(N)-THETA(N-2))**2
     : /(8*DELTAS**2)
      STUFF2=CN*R(N-1)*(THETA(N)-THETA(N-2))*(R(N)-R(N-2))/
     : (4*DELTAS**2)
      STUFF3=CA*R(N-1)*(THETA(N)-THETA(N-2))*(R(N)-R(N-2))/
     : (4*DELTAS**2)
      STUFF5=(R(N)-R(N-2))**2+R(N-1)**2*(THETA(N)-THETA(N-2))**2
      STUFF5=SQRT(STUFF5)
      STUFF4=R(N-1)*(THETA(N)-THETA(N-2))*0.5*RHO*(R(N-1)*THEDOT)**2
     : *D*CY/STUFF5
      A2=A1+(STUFF1-0.5*RHO*(R(N-1)*THEDOT)**2*D*(STUFF2-STUFF3)
     : -MHU*THEDOT**2*R(N-1)+STUFF4)*DELTAS
C
      STUFF1=(T(N)+T(N-1))*(R(N)-R(N-2))*(THETA(N)-THETA(N-2))
     : /(8*DELTAS**2)
      STUFF2=CN*((R(N-1)**2*(THETA(N)-THETA(N-2))**2/
     : (4*DELTAS**2))-1)
      STUFF3=CA*R(N-1)*(THETA(N)-THETA(N-2))/(2*DELTAS)
      STUFF4=(R(N)-R(N-1))*0.5*RHO*(R(N-1)*THEDOT)**2*D*CY/STUFF5
      B2=B1-(STUFF1+0.5*RHO*(R(N-1)*THEDOT)**2*D*(STUFF2-STUFF3)
     : +STUFF4)*DELTAS
C
      STUFF1=CN*R(N-1)*(THETA(N)-THETA(N-2))*(Z(N)-Z(N-2))
     : /(4*DELTAS**2)
      STUFF2=CA*(Z(N)-Z(N-2))/(2*DELTAS)
      C2=C1+(-0.5*RHO*(R(N-1)*THEDOT)**2*D*(STUFF1-STUFF2)
     : +MHU*G)*DELTAS
C
      T(N)=SQRT(A2**2+B2**2+C2**2)
      R(N)=R(N-1)+A2*DELTAS/T(N)
      THETA(N)=THETA(N-1)+B2*2*DELTAS/(T(N)*(R(N)+R(N-1)))
      Z(N)=Z(N-1)+C2*DELTAS/T(N)
C
C      HERE, AGAIN APPLY A LITTLE TRICK.  FOR 8088 SYSTEMS AND
C      ON VERY RARE OCASSIONS FOR 16 BIT SYSTEMS, THE PROGRAM TENDS TO
```

```
C          ENTER A LIMIT CYCLE LIKE BEHAVIOR IN TENSION AFTER 100-200
C          ITERATIONS WHICH CYCLES EVERY 2-3 STEPS.
C          IT IS SOLVED BY SIMPLY AVERAGING THE VALUES OVER 20
C          STEPS ANY TIME 400 ITERATIONS ARE EXCEEDED.  THIS SIMPLE
C          SOLUTION HAS BEEN FOUND TO WORK FOR ALL CASES CHECKED.
C          AGAIN, USING THE 16 BIT 486 TYPE MACHINE TO RUN THE SOFTWARE
C          PRETTY MUCH PRECLUDES THE PROBLEM EXCEPT IN THE RAREST OF
C          CIRCUMSTANCES.
C
           IF (COUNT .LT. 400) THEN
           GOTO 1200
           ELSEIF (COUNT1 .LT. 21) THEN
           COUNT1=COUNT1+1
           A2A2=A2A2+A2
           B2B2=B2B2+B2
           C2C2=C2C2+C2
           GO TO 1200
           ELSE
           A2=A2A2/20.0
           B2=B2B2/20.0
           C2=C2C2/20.0
           GOTO 3000
           ENDIF
1200       CONTINUE
C
C          COMPARE TO THE CONVERGENCE CRITERIA.
C
           IF (ABS((A2-A22)/A2) .GT. 0.0001) THEN
           GOTO 2000
           ELSEIF (ABS((B2-B22)/B2) .GT. 0.0001) THEN
           GOTO 2000
           ELSEIF (ABS((C2-C22)/C2) .GT. 0.0001)THEN
           GOTO 2000
           ELSE
           GOTO 3000
           ENDIF
C
2000       CONTINUE
           A22=A2
           B22=B2
           C22=C2
           GOTO 1000
C
3000       CONTINUE
C
C          MOVE THE ITERATION VALUES FORWARD ONE TIME STEP.
C
           A1=A2
           B1=B2
           C1=C2
```

```
C
C         UPDATE THE POSITION VALUES AND THE TENSION USING ALL THE
C         LATEST INFORMATION.
C
          T(N)=SQRT(A2**2+B2**2+C2**2)
          R(N)=R(N-1)+A2*DELTAS/T(N)
          THETA(N)=THETA(N-1)+B2*2*DELTAS/(T(N)*(R(N)+R(N-1)))
          Z(N)=Z(N-1)+C2*DELTAS/T(N)
C
C         RESET THE SUMMERS FOR THE NEXT LOOP.
C
          A2A2=0.0
          B2B2=0.0
          C2C2=0.0
3500      CONTINUE
C
C*********************************************************************
C         MATCH THE BOUNDARY CONDITION AT THE TOP.  THAT IS, MATCH THE
C         TOP POSITION OF THE WIRE TO THAT OF THE TAIL OF THE TOWPLANE.
C         THE ERROR AT THE TOP IS INTERPOLATED AND USED AS A FACTOR TO
C         ADJUST THE BOTTOM POINT.  ON OCCASSION, THE MULTIPLICATIVE
C         FACTORS BELOW MUST BE ADJUSTED TO ENSURE CONVERGENCE OF THE
C         BOUNDARY CONDITION SHOOTING ROUTINE.  WHEN THIS IS REQUIRED,
C         THE PROGRAM PROVIDES GUIDANCE ON HOW TO PERFORM THE ADJUSTMENTS.
C
C         MATCH THE Z AT EACH CHOSEN RADIUS.
C
          IF (ABS(Z(200)-ALTTP) .GT. 50.0) THEN
C
          IF (R(1) .LT. 700.0) THEN
          ZNEW=Z(1)+0.1*(ALTTP-Z(200))
          GOTO 3550
          ELSEIF (R(1) .LT. 1000.0) THEN
          ZNEW=Z(1)+0.2*(ALTTP-Z(200))
          GOTO 3550
          ELSEIF (R(1) .LT. 1700.0) THEN
          ZNEW=Z(1)+0.25*(ALTTP-Z(200))
          GOTO 3550
          ELSE
          ZNEW=Z(1)+0.3*(ALTTP-Z(200))
          ENDIF
C
3550      CONTINUE
C
C         NOW ADJUST TO A NEW RADIUS.
C
          Z(1)=ZNEW
          RNEW=R(1)
          GOTO 3600
C
```

```
            ELSEIF (ABS(R(200)-RADTP) .GT. 10.0) THEN
C

            IF (R(1) .LT. 800.0) THEN
            RNEW=R(1)+0.07*(RADTP-R(200))
            GOTO 3560
            ELSEIF (R(1) .LT. 1000.0) THEN
            RNEW=R(1)+0.15*(RADTP-R(200))
            GOTO 3560
            ELSEIF (R(1) .LT. 2000.0) THEN
            RNEW=R(1)+0.15*(RADTP-R(200))
            GOTO 3560
            ELSE
            RNEW=R(1)+0.3*(RADTP-R(200))
            ENDIF
C
3560     CONTINUE
C
            R(1)=RNEW
            ZNEW=Z(1)
            GOTO 3600
            ELSE
            GOTO 3700
            ENDIF
C
3600     CONTINUE
C
            R(1)=RNEW
            Z(1)=ZNEW
C
3640     CONTINUE
C
C         PRINT SOME OUTPUTS USEFUL IN KEEPING UP WITH HOW THE BOUNDARY
C         CONDITION SHOOTING ITERATIONS ARE PROGRESSING.
C
            WRITE(6,*) 'R(1),Z(1)=',R(1),Z(1)
            WRITE(6,*) 'R(200),Z(200),T(200)=',R(200),Z(200),T(200)
            WRITE(6,*) 'RADTP,ALTTP=',RADTP,ALTTP
            WRITE(6,*)'*****************************************'
C
C         JUST BOOKKEEPING HERE FOR THE NEXT LOOP.
C
            DO 3650 N=2,200
            R(N)=0.0
            THETA(N)=0.0
            Z(N)=0.0
            T(N)=0.0
C
3650     CONTINUE
            TICK=TICK+1
C
```

```
C          CHECK TO SEE IF THE UPDATE MULTIPLIERS ABOVE HAVE PLACED THE
C          BOUNDARY SHOOTING PROCESS INTO AN "INFINITE LOOP" AND IF SO
C          STOP THE PROCESS AND TELL THE OPERATOR HOW TO FIX THE PROBLEM.
C
          IF (TICK .GT. 400) THEN
          WRITE(6,*)'YOU HAVE EXCEEDED 400 ATTEMPTS TO SHOOT THE BOUNDARY'
          WRITE(6,*)'CONDITION AT THE TOP.  TO MAKE THE PROGRAM RUN '
          WRITE(6,*)'CORRECTLY YOU MUST ADJUST THE MULTIPLIER'
          WRITE(6,*)'COEFFICIENTS IN THE PROGRAM BETWEEN LINES 3500 AND'
          WRITE(6,*)'3560.  NOTE THE PRINTOUT OF R(1) AND Z(1) ABOVE AS'
          WRITE(6,*)'THEY FLOP BACK AND FORTH ON EITHER SIDE OF THE '
          WRITE(6,*)'CORRECT VALUE.  FIRST TRY TO HALVE THE COEFFICIENT'
          WRITE(6,*)'ASSOCIATED WITH THE R(1) VALUES YOU SEE (NOTE THE'
          WRITE(6,*)'R(1) .LT. STATEMENT).  IF YOU ARE STILL NOT '
          WRITE(6,*)'CONVERGING, TRY THE Z(1) COEFFICIENT.  YOU WILL HAVE'
          WRITE(6,*)'TO RE-COMPILE AFTER EACH FIX.  I RECOMMEND THAT'
          WRITE(6,*)'YOU WRITE DOWN THE ORIGINAL VALUES AND RETURN THEM'
          WRITE(6,*)'WHEN YOU ARE DONE.  THESE MULTIPLIERS GIVE YOU THE'
          WRITE(6,*)'QUICKEST CONVERGENCE FOR THE MAJORITY OF CASES OF'
          WRITE(6,*)'INTEREST.'
C
          GOTO 6000
          ELSE
          ENDIF
C
          GOTO 20
C***********************************************************************
C***********************************************************************
3700      CONTINUE
          WRITE(6,*)'NUMBER OF OUTER LOOPS-',TICK
C***********************************************************************
C         WRITE OUTPUT TO THE THREE DATA FILES.
C         FIRST, CONVERT SOME BACK TO MORE RECOGNIZABLE FORMS.
C
          VEAS=VEAS*3600.0/6076.0
          PHI=PHI*360.0/(2.0*PI)
C
C         NOW, WRITE SOME OF THE CONSTANTS TO FILES.
C
          WRITE(11,*) 'TOWPLANE KEAS-',VEAS,'KTS'
          WRITE(11,*) 'TOWPLANE ALTITUDE-',ALTTP,'FEET'
          WRITE(11,*) 'TOWPLANE BANK ANGLE-',PHI,'DEGREES'
          WRITE(11,*) 'TOWPLANE ORBIT RADIUS-',RADTP,'FEET'
          WRITE(11,*) 'TOWPLANE ORBIT RATE-',THEDOT,'RAD/SEC'
          WRITE(11,*) 'DROGUE ANGLE OF ATTACK-',ALFAD,'RAD'
          WRITE(11,*) 'DROGUE SIDESLIP ANGLE-',BETA,'RAD'
          WRITE(11,*) 'DROGUE ORBIT RADIUS-',R(1),'FEET'
          WRITE(11,*) 'DROGUE AIRSPEED-',THEDOT*R(1),'FT/SEC'
          WRITE(11,*) 'VERTICALITY-',(ALTTP-Z(1))/(200.0*DELTAS)
          WRITE(11,*) 'DROGUE/TOWPLANE SEPARATION-',ALTTP-Z(1),'FEET'
```

```
            STUFF1=ASIN((R(199)-R(200))/DELTAS)
            STUFF1=STUFF1*57.3
            WRITE(11,*) 'WIRE TRAIL ANGLE=', STUFF1
            WRITE(16,1) THEDOT
            WRITE(17,1) CLALD*ALFAD
            WRITE(19,1) VTRUE
            WRITE(20,1) PHI*2.0*PI/360.0
C
C       WRITE THE POSITION AND TENSION TO DATA FILES.
C
            DO 4000 I=1,200
            WRITE(12,1) R(I)
            WRITE(13,1) THETA(I)
            WRITE(14,1) Z(I)
            WRITE(15,1) T(I)
4000        CONTINUE
C**********************************************************************
C       BUILD A FILE THAT CONTAINS THE ANGLE OF ATTACK OF EACH WIRE
C       GRIDPOINT.  NOTE THAT THIS DOES NOT INCUDE THE FIRST OR LAST
C       POINTS.
C
            DO 5000 I=2,199
            STUFF1=ACOS(R(I)*(THETA(I+1)-THETA(I-1))/(2*DELTAS))
            STUFF1=STUFF1*360/(2*PI)
            WRITE(18,1)STUFF1
5000        CONTINUE
C**********************************************************************
C       THESE FILES CONTAIN THE REYNOLDS NUMBER AND TRUE AIRSPEED AT
C       EACH GRIDPOINT.
C
            OPEN (UNIT=70,FILE='VTRUE.MAT')
            OPEN (UNIT=71,FILE='RE.MAT')
            DO 5100 I=1,200
            INDEX=INT(Z(I)/1000.0)+1
            RHO=DENSTY(INDEX)*0.0023769/1013.0
C          RHO=0.002378*(1-0.006875*Z(N)/1000.0)**4.256
C          RHO=0.0023769*(((518.69-0.0035662*Z(N))/518.69)**
C        : ((-1.0)*(1.0/(-0.0035662*53.3))+1.0))
            VTRUE=R(I)*THEDOT
            STUFF1=RHO*VTRUE*D/.00000038
            WRITE(70,1)VTRUE
            WRITE(71,1)STUFF1
5100        CONTINUE
            CLOSE(70)
            CLOSE(71)
C**********************************************************************
            WRITE(6,*)'          '
            WRITE(6,*)'RUN COMPLETE!!!'
            WRITE(6,*)'          '
            WRITE(6,*)'THE OUTPUT IS INCLUDED IN THE FOLLOWING:'
```

```fortran
      WRITE(6,*)'DATA01.MAT CONTAINS MISCELLANOUS VALUES OF INTEREST.'
      WRITE(6,*)'DATA02.MAT CONTAINS EACH GRIDPOINT RADIAL COORD.'
      WRITE(6,*)'DATA03.MAT CONTAINS EACH GRIDPOINT THETA COORD.'
      WRITE(6,*)'DATA04.MAT CONTAINS EACH GRIDPOINT Z COORD.'
      WRITE(6,*)'DATA05.MAT CONTAINS EACH GRIDPOINT TENSION VALUE.'
      WRITE(6,*)'DATA06.MAT, DATA07.MAT AND DATA00.MAT CONTAIN VALUES'
      WRITE(6,*)'REQUIRED BY THE DYNAMIC SOLUTION PROGRAM.'
      WRITE(6,*)'DATA08.MAT CONTAINS THE TRUE ANGLE OF ATTACK OF'
      WRITE(6,*)'GRIDPOINTS 2 THROUGH 199.  VTRUE .MAT CONTAINS THE'
      WRITE(6,*)'TRUE AIRSPEED AT EACH GRIDPOINT AND RE.MAT CONTAINS'
      WRITE(6,*)'THE REYNOLDS NUMBER AT EACH GRIDPOINT.'
C****************************************************************
6000  CONTINUE
      END
```

INITIAL DISTRIBUTION LIST

1. Defense Technical Information Center   2
   Cameron Station
   Alexandria, VA 22304-6145

2. Library, Code 52   2
   Naval Postgraduate School
   Monterey, CA 93940-5002

3. Professor L.V. Schmidt, AA/Sc   2
   Naval Postgraduate School
   Monterey, CA 93940-5002

4. Professor R.M. Howard, AA/Ho   1
   Naval Postgraduate School
   Monterey, CA 93940-5002

5. Professor D.J. Collins, AA/Co   1
   Naval Postgraduate School
   Monterey, CA 93940-5002

6. Naval Air Systems Command (PMA-271)   1
   Naval Air Systems Command Headquarters
   Washington, D.C. 20361-1271

7. LCDR Thomas D. Stuart, USN   3
   21 Sawyer Avenue
   Atkinson, N.H. 03811